



Effects of glucoprivation on the adrenal medulla: a time course study using shotgun proteomics

By
Roshana Vander Wall
(41217128)

Australian School of Advanced Medicine

A thesis submitted for the partial fulfillment of the requirements for
the degree of Master of Research in Neuroscience

Supervisors

Associate Professor Ann Goodchild¹

Dr. Mehdi Mirzaei²

¹. Australian School of Advanced Medicine, Faculty of Human Sciences, Macquarie University, Sydney, NSW, Australia

². Department of Chemistry and Biomolecular Sciences, Faculty of Science, Macquarie University, Sydney, NSW, Australia

Key words: adrenal medulla, hypoglycemia, protein profile, proteomics, 2-deoxyglucose, time course

Abstract character count: 249

Word count: 17,121

Number of figures: 13

Contents

Conflict of interest statement	i
Declaration of Originality	ii
Publications arising from this work.....	iii
Acknowledgements	iv
Abstract.....	v
Abbreviations	vi
1.0 Introduction	1
2.0 Experimental Procedures	5
2.1 Ethics	5
2.2 Glucoprivation induction and sample preparation	5
2.3 Protein extraction and SDS-PAGE fractionation.....	6
2.4 Trypsin in-gel digestion.....	6
2.5 Peptide extraction.....	7
2.6 Nanoflow liquid chromatography-tandem mass spectrometry	7
2.7 Protein identification	8
2.8 Data processing and quantitation	8
2.9 Statistical analysis of differentially expressed proteins	9
2.10 Functional annotation	9
2.11 Western blot analysis.....	10
2.12 Immunohistochemistry	10
3.0 Results.....	12
3.1 Experimental protocol	12
3.2 Mass spectrometry data quality	13
3.3 Profile of the adrenal medulla proteome	14
3.4 The response of the adrenomedullary proteome to 2DG.....	14
3.5 The response of the adrenomedullary proteome to 2DG.....	14
3.6 Animal weights affect protein clustering between time points.....	16
3.7 Changes in the proteome of the adrenal medulla at 20min, 4hr and 24hours following 2DG	18
3.7.1 Processes changed at 20min	19
3.7.2 Processes changed at 4hr.....	19
3.7.3 Processes changed at 24hr.....	20

3.8 Time dependent changes in the proteome of the adrenal medulla.....	24
3.9 Western blot analysis	26
3.10 Localisation using Immunohistochemistry.....	31
3.11 Localisation following activation of the adrenal medulla	31
4.0 Discussion	33
4.1 Major findings and implications	33
4.2 Protein profile of the adrenal medulla.....	33
4.3 Differentially expressed proteins	34
4.4 Methodological considerations.....	34
4.4.1 The effects of 2DG	34
4.4.2 Impact of animal age on protein expression	36
4.4.3 Protein profiling	37
4.4.4 Western blot and IHC validation.....	38
4.5 Cellular processes and changes in response to 2DG.....	40
4.5.1 Metabolic processes.....	40
4.5.2 Signalling	42
4.5.3 Cytoskeletal changes	44
4.5.4 Transport	45
4.5.5 Stress response	47
4.5.6 Protein synthesis.....	49
4.5.7 Proteolysis	50
4.5.8 Summary of processes changed	52
4.6 Future directions	53
4.7 Conclusion.....	54
5.0 References.....	54
6.0 Appendix.....	66

Conflict of interest statement

The research was conducted in the absence of any commercial or financial relationships that could be construed as a potential conflict of interest.

Declaration of Originality

I certify that the work in this thesis entitled “Effects of glucoprivation on the adrenal medulla: a time course study using shotgun proteomics” has not previously been submitted for a degree nor has it been submitted as part of requirements for a degree to any other university or institution other than Macquarie University.

I also certify that the thesis is an original piece of research and it has been written by me. Any help and assistance that I have received in my research work and the preparation of the thesis itself have been appropriately acknowledged.

In addition, I certify that all information sources and literature used are indicated in the thesis.

The research presented in this thesis was approved by Macquarie University Ethics Review Committee, reference number: 2014/018 on 24/03/2014



Roshana Vander Wall

MQ student number: 41217128

10/10/2014

Publications arising from this work

Changes to the proteome of the adrenal medulla evoked 20 min to 24 h after a single episode
of glucoprivation

A. K. GOODCHILD¹, P. BOKINIEC¹, S. F. HASSAN¹, L. M. PARKER¹, R. VANDER
WALL¹, P. HAYNES², M. Z. MOGHADDAM³, M. MIRZAEI¹;

¹The Australian Sch. of Advanced Medicine, Macquarie Univ., Sydney, Australia; ²CBMS,
Macquarie Univ., Sydney, Australia; ³Texas Tech. Univ., Lubbock, TX
Abstract for presentation at Society for Neuroscience Nanosymposia 2014

Acknowledgements

I would like to acknowledge the hard work and patience of my supervisor, Ann Goodchild for guiding me through this learning process. I would also like to thank her for her support. The encouragement and direction she provided was invaluable in navigating this endeavour.

I would also like to acknowledge Dr. Mehdi Mirzaei, for sharing his immense knowledge in the field of proteomics and without whom the mass spectrometry work could not have been completed.

I would also like to thank all those in the Goodchild group for teaching me, assisting me and supporting me.

Finally I would like to express my gratitude to my friends and family who shared this journey with me.

Abstract

The adrenal medulla is the sole endocrine gland responsible for catecholamine release in response to stress. While a time course of stress response has been described for rate-limiting enzyme in catecholamine synthesis; tyrosine hydroxylase (TH), none have yet described any other metabolic changes in this gland. Therefore the aims of this study are to map the proteome of the adrenal medulla and determine any changes over time following an acute episode of glucopenia, a potent stimulus thereof. In addition, the final aim is to determine whether or not Western blot analysis reflects the findings shown using mass spectrometry (MS). A single IP injection of 2-deoxyglucose was used to induce glucopenia in Sprague Dawley rats. The adrenal glands were harvested over at 0min, 20min, 50min, 4h, 8h and 24h after the stimulus (n=6 for each timepoint). Label-free LC-MS/MS was then performed on the samples (n=3) for each timepoint to obtain the proteomic profile. Profiles were quantitatively compared to the control (0min/unstimulated). Western blotting was then used in order to validate the MS data using specifically selected proteins. The protein profile was determined and comprises 973 proteins, with marked changes at each time point; 20min=78, 50min=138, 4h=163, 8h=136 and 24h=107. Western blot analysis regarding TH corresponded with MS data, however other proteins showed differing expression levels. From this we understand that cellular metabolic changes occur rapidly in response to stress and last longer than 24h. It is also apparent that Western blot analysis does not always correspond with the MS output.

Abbreviations

Protein symbol abbreviations found in Table A1.

2DG	2-deoxyglucose
Actr3	Actin-related protein 3
ATP	Adenosine triphosphate
BG	Blood glucose
GAPDH	Glyceraldehyde 3-phosphate dehydrogenase
Ide	Insulin degrading enzyme
LC	Liquid chromatography
MS	Mass spectrometry
MS/MS	Tandem mass spectrometry
NADH	Nicotinamide adenine dinucleotide
Nsf	N-ethylmaleimide sensitive fusion protein
PACAP	Pituitary adenylate cyclase activating polypeptide
PNMT	phenylethanolamine N-methyltransferase
Rmdn3	Regulator of microtubule dynamics 3
TCA	Tricarboxylic acid
Th	Tyrosine hydroxylase
Vapb	Vesicle-associated membrane protein-associated protein B
Vat1	Vesicle amine transport 1

1.0 Introduction

The survival of a biological system, whether it is a whole animal or a single cell, is influenced by the way in which it responds to stress. The molecular changes that occur in response to psychological and physiological stressors have been intensively investigated. It is the response to physiological stress that is the topic of this thesis. Such stressors include, but are not limited to, changes in blood glucose levels, blood pressure, cold stress, hypoxia and starvation. Although there are fundamentally conserved counteractive measures mobilised in response to these stresses there may be multiple pathways available to mitigate any potential damage (Kültz, 2005). One such stressor with a very well described counter regulatory response (CRR) is hypoglycemia (low blood glucose) which is activated in order to restore glucose homeostasis (Cryer and Gerich, 1985; Cryer, 1997; Sprague and Arbeláez, 2011; Verberne et al., 2014).

In healthy adult humans the normal blood glucose (BG) range is considered between 4.0–8.0mmol/L. A small decrease within this range will lower the insulin secretion from the β -cells in the pancreas, slowing glucose uptake (Sprague and Arbeláez, 2011). When BG falls below 3.3mmol/L insulin production is completely ceased, halting glucose absorption and α -cell glucagon production rises (Cryer, 1997). Glucagon acts at the liver to induce glycogenolysis and gluconeogenesis (Cryer, 2005; 2013), enabling the release of glucose into the bloodstream for uptake by other cells. The hormonal response continues with adrenaline release from chromaffin cells of the adrenal medulla, a key glucose regulatory substance as this is the major system that counteracts hypoglycaemia in diabetic patients (Marty et al., 2007). Adrenaline also acts to stimulate glycogenolysis and can therefore be released as a compensatory mechanism in the absence of glucagon.

Other CRRs are activated over prolonged periods/levels of hypoglycemia/glucoprivation (BG < 3.2 mmol/L) including cortisol secretion from the adrenal cortex (Wurtman and Axelrod, 1966). Through paracrine action, the adrenal cortex secretes cortisol to act directly at the adrenal medulla, stimulating adrenaline synthesis and promotes the upregulation of the phenylethanolamine N-methyltransferase (PNMT) (Wurtman and Axelrod, 1966) which methylates noradrenalin to form adrenaline, adrenaline thus catalysing the last step catecholamine biosynthesis (Martins et al., 2004). Release of adrenaline also induces changes

in metabolic processes such as lipolysis in adipose tissue and ketogenesis and gluconeogenesis in the liver (Tesfaye and Seaquist, 2010). When BG drops to 2.8–3.0 mmol/L cholinergic neurogenic symptoms such as dizziness, hunger and sweating occur. These are mediated by the sympathetic and parasympathetic systems (DeRosa and Cryer, 2004; Sprague and Arbeláez, 2011). Sympathetic activation of the adrenal gland via the preganglionic cholinergic adrenal nerve evokes adrenaline release important in a number of the counterregulatory responses described above (Parker et al., 1993).

The adrenal medulla consists of a few ganglion cells and mostly chromaffin cells, 80% of which contain adrenaline with the remaining 20% containing noradrenaline. The chromaffin cells are innervated specific chemically distinct groups of cholinergic sympathetic preganglionic neurons (Parker et al., 1993; Morrison and Cao, 2000). During prolonged hypoglycemic episodes activation by acetylcholine cannot be sustained for longer than 2hr, so pituitary adenylate cyclase activating polypeptide (PACAP) is released (Watanabe et al., 1995; Hamelink et al., 2002). Peppered with PACAP receptors, the chromaffin cells are depolarised causing exocytosis (Vaudry et al., 2009; Hill et al., 2011). Much is known about the effects of acetylcholine, PACAP and other activators on the function of chromaffin cells (Dun et al., 1996; Hamelink et al., 2002; Eiden et al., 2004), however, few studies have tracked the resultant proteomic changes. Furthermore, little is known about the time course of cellular responses to a hypoglycemic/glucoprivic stress. The time at which a particular pathway is activated or inactivated after a stimulus and the duration these changes endure will enable us to understand how the response is executed at the molecular level.

Some studies have focussed on the time course of change to a single protein in the pathway (Bobrovskaya et al., 2010; Damanhuri et al., 2012). However, this is insufficient to understand the possible changes to an entire pathway or process over time. The most widely studied protein of the adrenal medulla is the enzyme tyrosine hydroxylase (Th), the rate limiting enzyme in the synthesis of catecholamines (Dunkley et al., 2004; Bobrovskaya et al., 2010). Such studies highlight the importance of investigating a single protein as significant regulation in both the short and longer term have been identified. Following a stimulus, adrenaline is released but the level of adrenaline present in the adrenal gland does not change as a selection of phosphorylation steps of Th occur which increases the activity of the enzyme promoting the synthesis of adrenaline. Some investigation of the complex array of kinases and phosphatases responsible has also been conducted (Dunkley et al., 2004). These responses

have been investigated at the *in vivo*, *in situ* and cell culture levels (Haycock, 1993;Bobrovskaya et al., 1998;Eisenhofer et al., 2008;Damanhuri et al., 2012).

Following glucoprivation achieved using 2-deoxyglucose significant changes in Th phosphorylation were measured over 2 hours however the level of Th protein was found to be increased at 24 hours but not 2 hours after the stimulus (Bobrovskaya et al., 2010). This process represents the longer term phase of Th regulation showing changes in transcription and translation in response to the stimulus. It should be pointed out that the precise changes that occur between 2 and 24 hours and what happens to other proteins even in the catecholamine synthetic pathway are unknown.

Another major focus of study has been of adrenaline release from the chromaffin cell cultures in response to stress however the focus has been on single pathways involved (Thomas et al., 1997;Egea et al., 2007). Such pathways include in intracellular signalling post stimulation (Neher, 2006), vesicle trafficking (Maucort et al., 2014) or cytoskeletal proteins in regulating vesicle release (Vitale et al., 1995). Furthermore the protein profile of large dense core vesicles, the main secretory vesicle in chromaffin cells has been detailed (Wegrzyn et al., 2007;Wegrzyn et al., 2010). However, no studies to date have endeavoured to catalogue protein expression in the adrenal medulla and compared both normal and stimulated conditions.

This raises the question whether an entire systems response to a stressor can indeed be investigated. Several elegant studies have been performed to elucidate the changes of yeast proteomes under stressful conditions, including oxidative stress and nitrogen starvation (Vogel et al., 2011;Breker et al., 2013). These studies tracked changes in time in both protein abundance and their intracellular location, and also identified potential regulatory mechanisms for proteins that were “changed”. As demonstrated by Berghoff et al. (2013), mRNA changes in response to a stimulus were often not reflective of the protein changes. This is most likely due to alternate splicing, protein degradation and post-translational modification. As proteins are the functional products of genes, tracking proteomic changes provides greater understanding of cellular processes and metabolism. However, these studies have been performed in single cell organisms and therefore the translation of this information to the stress response in animals is difficult. Balfoussia et al. (2014) tracked the proteomic changes in human plasma before and after extreme physical stress, identifying a sharp

increase in circulating stress-related proteins compared to baseline particularly those relating to inflammation and protection against oxidative stress. Together these studies suggest that investigation of the proteome will best describe changes evoked by the stressor. These studies also highlight the importance of investigating changes in response to stress over time. Vogel et al. (2011) observed, in yeast at least, distinct patterns of protein expression over the two hour time period monitored.

Hypoglycemia is a naturally occurring stressor, particularly in type I diabetes where maintaining a normal blood glucose level using exogenously applied insulin often results in hypoglycemic episodes (McCrimmon and Sherwin, 2010). Many methods are available for experimentally inducing low effective glucose concentrations. A structural analogue of glucose, 2DG competitively inhibits glucose phosphorylation (Wick et al., 1957). 2DG strongly activates the adrenal medulla inducing phosphorylation of Th and expression of c-Fos protein (Damanhuri et al., 2012; Parker et al., 2013) more so than other stressors (Ong et al., 2014) and protein changes can be easily tracked over time (Bobrovskaya et al., 2010).

Using glucoprivation induced by 2-deoxyglucose (2DG) as the stressor, the objective of this study was to track changes in the proteome of the rat adrenal medulla over time in response to a single episode of glucopenia. To achieve this, the first aim was to profile the proteome of the adrenal medulla utilizing liquid chromatography tandem mass spectrometry (LC/MS-MS). This protein profile would serve as the control. The second aim was to determine the protein profiles at 20min, 50min, 4h, 8h and 24hr after 2DG stimulus and compare each of these profiles to the control. We also determined proteins and/or pathways that change over the timecourse. Finally, controversy abounds as to whether there is a need to validate protein changes identified LC/MS-MS by utilising genomic or other proteomic methods (Aebersold et al., 2013). Therefore we will determine the efficacy of Western blotting validation of MS output regarding protein identification and quantitation.

2.0 Experimental Procedures

2.1 Ethics

All procedures described in this paper were approved by the Macquarie University Animal Ethics Committee (reference number ARA 2014-018) and adhered to the regulations outlined in the Australian code of practice for the care and use of animals for scientific purposes (National Health & Medical Research Council 8th Edition).

2.2 Glucoprivation induction and sample preparation

Experiments were conducted on male Sprague Dawley rats (n=44) obtained from the Animal Resource Centre in Perth, WA and housed in the Macquarie University central animal facility (CAF). Rats were housed 3-4 to a cage and had ad libitum access to standard rat chow and water prior to treatment. To minimise stress due to handling and moving, rats were weighed and relocated to the laboratory for 12 hours to acclimatise prior to any experimentation. All experiments were begun at 10 am.

The initial data collection utilised 18 rats. Two groups of rats were available. Cohort 1 (age 14-15 weeks) with average weights of 496.3 ± 17.85 g were allocated to 4 time points (0, 20 min, 4hr and 24 hr) and Cohort 2 (age 7-8 weeks) with average weights 247.7 ± 8.91 g were allocated the remaining two time points (50min and 8hr). To induce glucopenia, each animal received an intraperitoneal (ip.) injection of 2-deoxy-D-glucose (2DG; 400 mg/kg). This high dose of 2DG was used as almost all adrenergic chromaffin cells expressed c-Fos protein indicative of activation (Parker et al., 2013). At selected time points following 2DG (0 min; 20-30 min; 50-60 min; 4 hr; 8 hr; 24 hr) animals (n= 3 for each time point) were anesthetized with sodium pentobarbital (100 mg/kg; ip.).

Selection of the time points were based on previous time course studies involving 2DG, tyrosine hydroxylase or the time course of stress (Haycock, 1993; Dunkley et al., 2004; Bobrovskaya et al., 2010).

All animals housed together in their home cage (n=3) were randomly selected as representatives for each time point in order to minimize variability within groups.

Food and water were removed from all cages following 2DG administration for accurate blood glucose testing. By preventing the animals from feeding, there will be no additional

glucose present except that which is unable to be metabolised. This is to assess whether 2DG has been correctly administered. Food was returned at 4hr as this is the approximate length of time until feeding response has returned to normal post 2DG administration (Wu et al., 2010). The 0 min time point was selected as the control, with simultaneous administration of 2DG and sodium pentobarbital.

Upon the cessation of the pinch withdrawal reflex and the corneal reflex both whole adrenal glands were rapidly removed (1-2 min) from each animal and snap frozen on dry ice prior to storage at -80°C. The adrenal medulla was dissected from the surrounding cortex on dry ice and refrozen ready for analysis. Samples were stored at -80°C. Blood glucose levels were measured using a glucometer (Roche Accu-Chek Performa glucometer, Germany) from a drop of blood obtained a heart puncture. This first series of samples were utilised for mass spectrometry analysis.

A second set of samples were collected in order to perform Western blot analysis of proteins identified using mass spectrometry. Animals were carefully selected to match the weights of those utilised for the first study. Adrenal medullas were obtained from male Sprague Dawley rats (n=20) using the method described above at time points: 0 min (n=4), 20-30 min (n=4), 50 min (n=2), 4 hr (n=4), 8 hr (n=2), 24 hr (n=4).

2.3 Protein extraction and SDS-PAGE fractionation

Adrenal medulla samples were homogenized in lysis buffer (0.32mM sucrose, 2mM EDTA, 4mM HEPES, 1% SDS) with a FastPrep homogenizer. The solutions were centrifuged at 14,000 rpm for 15 minutes at 4 C°, supernatants were transferred to new tubes and then a bicinchronic acid assay (BCA) protein assay was carried out. 100ug protein from each sample were combined with 15µl of a 5x SDS sample buffer containing 200mM DTT and then separated using a Bio-Rad 10% Tris-HCl SDS-PAGE gel. Gels were stained overnight by Coomassie Brilliant Blue G 250 (Bio-Rad). A solution of 50% H₂O, 40% Methanol and 10% Acetic Acid and was used to destain the gel for 2 hours prior to in-gel digestion.

2.4 Trypsin in-gel digestion

Each SDS-PAGE gel lane was cut and diced into 10 equal pieces, with each piece further divided into smaller pieces before being transferred to a 96-well plate. Gel pieces were briefly washed with 100mM NH₄HCO₃ and then 3 times with 200µl of ACN (50%)/100mM

NH₄HCO₃ (50%), each for 10 mins. Fractions were then dehydrated with 100% ACN for 5 minutes, air dried, and then reduced using 50µl of 10mM DTT/NH₄HCO₃ (50mM) at 37°C for 1 hr. Samples were cooled at room temperature before being alkylated with 50µl of 50mM iodoacetamide/NH₄HCO₃ (50%) for 45 mins in dark, then they were washed with 100mM NH₄HCO₃ for 5 minutes and further de-stained with 200µl of ACN (50%)/100mM NH₄HCO₃ (50%). each for 10 minutes. Gel pieces were then dehydrated with 100% ACN and air-dried. Finally, samples were placed on ice and digested with 20µl of trypsin (12.5ng/ml 50mM NH₄HCO₃) for 30 minutes before digestion overnight at 37°C.

2.5 Peptide extraction

Tryptic peptide digests were transferred to individual Eppendorf tubes. 50µl of ACN (50%)/formic acid (2%) was added to remaining gels and incubated for 30 mins. Extraction was repeated 3 times. Extracts were then dried using a vacuum centrifuge and reconstituted with 20µl with 2% formic acid.

2.6 Nanoflow liquid chromatography-tandem mass spectrometry

In collaboration with Dr. Mehdi Mirzaei from Macquarie University, samples underwent MS analysis at the Centre for Biotechnology and Genomics, Texas Tech University, Lubbock, TX. The following describes the process that was carried out.

The peptides from the tryptic digests were analysed by nanoflow liquid chromatography tandem mass spectrometry (LC-MS/MS) using an LTQ-XL ion-trap mass spectrometer (Thermo, San Jose, CA) as in similar procedures (Gammulla et al., 2011; Mirzaei et al., 2012a). Chromatographic separation of the peptides was performed using a Dionex nano-HPLC (Ultimate 3000) with a reverse phase column (Zorbax C18, 2µm, 100 Å, 75µm × 15cm; Agilent Technologies, CA, USA) in a fused silica capillary with an integrated electrospray tip. Peptides were first injected onto the trapping column and equilibrated with 1% ACN, 0.1% formic acid in water before a 10min wash with the same solvent at a flow rate of 300 nl/min. The trapping column was then switched to the reverse phase column and the bound peptides were eluted with buffers A (5% v/v formic acid) and B (95% (v/v) ACN, 0.1% (v/v) formic acid). The gradient was maintained for 10min at 4% buffer B followed by a linear increase to 30% for 20 min. Buffer B was further increased to 60% for 40 min and then a rapid increase up to 90% over 5min. Eluted peptides were finally guided into the nanospray ionisation source and a voltage of 2kV was applied through a gold-electrode liquid

junction upstream of the C18 column. The collected spectra were scanned over the mass/charge (m/z) range of 300–2000 atomic mass units (amu) (Xcalibur version 2.1). After automated peak recognition, data dependent scan settings were refined to select the six most intense ions with dynamic exclusion list size of 100, exclusion duration of 30 (s), a repeat count of 2 and a repeat duration of 15 (s). MS/MS spectra were generated by collision-induced dissociation of the peptide ions at normalized collision energy of 35%.

2.7 Protein identification

Proteins were identified using the Global Proteome Machine (GPM) software (2.1.1 version of the X!Tandem algorithm) by searching data from converted raw MS files (mzXML format, ReAdW.exe program) against National Centre for Biotechnology Information *Rattus Norvegicus* Reference Sequence database (94699 proteins, April 2013). For each replicate the 10 gel fractions were processed consecutively with an output file generated for each fraction. Then, a combined, nonredundant output file was created for protein identifications with log (e) values <-1 . Search parameters for proteins included MS/MS tolerances of +2 Da and +0.2 Da respectively, fixed modifications; carbamidomethylation of cysteine, variable modifications; oxidation of methionine and tolerance of K/R-P cleavage and two missed tryptic cleavages. The database also incorporated common human and trypsin peptide contaminants, and additional searching was performed against a reversed sequence database in order to assess the false discovery rate (FDR).

2.8 Data processing and quantitation

The output files of three replicates from GPM were combined using the Scrappy software (Neilson et al., 2013). Only proteins that were present in all three replicates with a total spectral count of at least 5 for at least one condition in each comparison test were retained for quantitation. The relative standard deviation (RSD%) values for each data set of the three biological replicates was calculated as per Francis et al. (2013) and the peptide FDR and protein FDR were calculated as described in Voelckel et al. (2010) and Mirzaei et al. (2012a). The normalised spectral abundance factor (NSAF) for each protein was calculated according to Neilson et al. (2011) and used to determine protein abundance as described previously (Zybailov et al., 2006). For each protein in each sample, the number of spectral counts identifying the protein was divided by the estimated length of the protein (spectral counts/peptide length). The protein length was determined as the protein molecular weight divided by the average amino acid molecular weight. The resulting values were normalized to

the total by dividing by the sum of spectral counts/peptide length over total number of proteins, yielding the NSAF values for each sample. When plotting or summarizing overall protein abundance for a particular condition the average of the NSAF values for all replicates was used as a measure of protein abundance. A spectral fraction of 0.5 was added to all spectral counts initially, to compensate for null values and allow for log transformation of the NSAF data prior to statistical analysis. The mean NSAF value across triplicates was used when summarizing protein abundance for each time point (Mirzaei et al., 2012b).

2.9 Statistical analysis of differentially expressed proteins

The log transformed NSAF data was used for series of 2-sample unpaired t-test to identify differentially expressed proteins between the control (0 min) and other time points (20min, 50min, 4hr, 8hr, 24hr). Proteins with a p-value < 0.05 were considered to be significantly differentially expressed. In order to assess protein changes across time, a second analysis was performed on log transformed NSAF comparing all time points between each other using a one-way ANOVA. Proteins with a p-value < 0.05 and were changed compared to more than one time point (including 0min) were considered to be significantly differentially expressed with respect to time. All statistical analyses were performed using the Scrappy program (Neilson et al., 2013).

2.10 Functional annotation

Functional annotations were obtained manually as gene ontology annotations from Uniprot database (The UniProt Consortium, 2014), Genecards database and Pubmed BLAST database (Altschul et al., 1990). The subcellular localization and biological processes were chosen based on the best known function of the proteins in neurons, adrenal gland cells and response to glucoprivation and general cellular stress, for which evidence exists as defined using Pubmed and Google Scholar searches. Evidence was also acquired from STRING searches however this evidence usually replicated what was found using data bases previously mentioned. Additional databases used to assign functions and understand pathway analysis included the enzyme database BRENDA and the KEGG pathway database.

Although INGENUITY was also used for pathway analysis this did not provide functionally significant pathways with respect to what is known regarding the functions of the adrenal medulla. For example, the first 3 pathways contain no more than 2 proteins each and pertained to nucleotide salvage and the pyruvate dehydrogenase complex. While the latter is

pertinent to cellular metabolism, the pathways gleaned from this program only revealed protein relationships with strict direct involvement and did not show linkages between pathways. Therefore, it was not frequently relied upon.

2.11 Western blot analysis

Western blotting was performed for validation of a selection of differentially expressed proteins identified by MS; tyrosine hydroxylase (Th), actin-related protein 3 (Actr3), Calpain 2 (Capn2), dopamine beta-hydroxylase (Dbh), insulin degrading enzyme (Ide), membrane-associated progesterone receptor component 1 (Pgrmc1), phosphatidylinositol transfer protein alpha isoform (Pitpna), N-ethylmaleimide-sensitive factor (Nsf), regulator of microtubule dynamics protein 3 (Rmdn3) and vesicle-associated membrane protein b (Vapb), synaptic vesicle membrane protein (Vat1). Proteins were selected based on a fold change ≥ 2 , functional relevance and peptide abundance (which differed for the chosen proteins). β -actin (Actb) and Glyceraldehyde 3-phosphate dehydrogenase (GAPDH) were used as loading controls based on NSAF values in the samples analysed, ensuring these proteins did not significantly change over time. The use of each loading control depended upon the molecular weight of the target protein to minimise interference.

A bicinchoninic acid assay (BCA) was performed to determine protein concentration in each sample using a Pherastar FS plate reader (BMGLabtech, Germany). The amount of sample for loading was based on protein concentrations gained from the BCA assay. Equal volumes of sample homogenate and sample buffer (β -mercaptoethanol, 2x Laemmli; 1:20, Biorad) were combined. Three biological replicates of 4 time points (0, 20min, 4hr, 24hr) were loaded into 15 lane gels (Biorad 10% Mini-PROTEAN TGX Stain Free) and run at 120V to separate. Proteins were then transferred from the gel to a nitrocellulose membrane (Biorad) using a trans-blot electrophoresis transfer cell (Biorad). Membranes were blocked with 5% skim milk in tris-buffered saline and 1% Tween (TBST) for 1hr at room temperature. For selected proteins this procedure was repeated with 3 biological replicates of the remaining 2 time points (50min, 8hr) on a 10 lane gel (Biorad 10% Mini-PROTEAN TGX Stain Free).

2.12 Immunohistochemistry

Intact perfused and paraformaldehyde (4%) fixed adrenal glands from adult male Sprague Dawley rats collected 120 min following 2DG (n=3) or saline (n=3) were also collected as c-Fos protein has previously been used to demonstrate activation of adrenal chromaffin cells.

Bilateral whole adrenal glands from each animal were embedded in OCT™ (Tissue-Tek®) and cryosectioned at 40µm free-floating into ice cold TPBS. Sections were incubated in a 50% ethanol solution for 30 min at room temperature, washed in TPBS 3x 10 min and blocked with 10% normal horse serum (in TPBS-m). Samples were then incubated in primary antibodies overnight at 4°C followed by 6 hr at room temperature and a further 12 hrs at 4°C. The following antibodies were used in several combinations and under conditions of different titrations: Th (1:4000, Sigma Aldrich, USA), Dbh (1:100, Sigma Aldrich, USA), Vapb (1:100, Abcam, USA), Vat1 (1:500, Abcam, USA), Actr3 (1:500, Abcam, USA), Rmdn3 (1:500, Proteintech, Aus), c-Fos (1:1000, Santa Cruz Biotech, USA), Ide (1:500, Abcam, USA) and VaChT (1:400, Millipore, USA). Time did not permit completion of all titrations and antibody retrieval steps required.

Sections were then washed in TPBS 3x 30 min followed by overnight incubation in secondary antibodies in 4% normal horse serum and TPBS-m at 4°C. Secondary antibodies used were: Alexa Fluor® 555 Donkey Anti-Rabbit IgG (H+L) (1:250, Invitrogen, USA), Alexa Fluor® 488 Donkey Anti-Goat IgG (H+L) (Invitrogen, USA; 1:250) and Alexa Fluor® 647-AffiniPure Donkey Anti-Mouse IgG (H+L) (1:250, Jackson ImmunoResearch, USA). Following secondary antibodies, adrenal sections were washed 3x 30min in TPBS, mounted on glass slides and coverslipped for viewing (Dako Fluorescent mounting medium, Denmark). Sections were photographed under epifluorescence on a Zeiss Axioimager Z2 microscope using Zen 2012 Pro software (Zeiss, Germany).

3.0 Results

3.1 Experimental protocol

Adrenal samples for MS analysis were collected first. The experimental design originally only included four time points (0min, 20min, 4hr and 24hr) in order to determine changes in the short, medium and longer term. However, time course analysis in yeast showed significant changes throughout the first 60 min following a stimulus (Vogel et al., 2011) therefore additional time points (50min, 8hr) were added close to the time of sample collection. Rats of similar weight were not available for all time points so an additional cohort of smaller animals was used. These were used for the newly selected time points (50min and 8hr) (Fig 1A).

All rats were then subjected to 2DG (400mg/kg ip) and the blood glucose responses are shown in Fig 1B. At 0min the blood glucose reading was 10.03 ± 0.41 mmol/L, a value considered normal for Sprague Dawley rat (Damanhuri et al., 2012). 2DG induced a 2.1 fold increase in blood glucose at 20min as described previously (Bobrovskaya et al., 2010;Damanhuri et al., 2012) which remained elevated at least for 50 min (one-way ANOVA, compared to 0min). The adrenal medullas were isolated and sent for processing to the Centre for Biotechnology and Genomics at Texas Tech University for MS analysis.

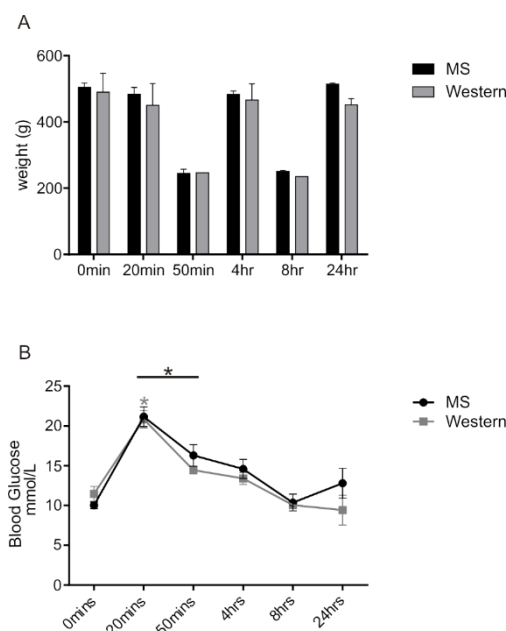


Figure 1. Comparison of animal weights and blood glucose levels between mass spectrometry (MS) and Western blot groups. A) Weights of animals for MS and Western blot groups were matched. B) Changes in blood glucose levels over time (mmol/L), time 0min as control. MS; n=18, n=3 per time point. Western blot; n=20, n=4 per group (0min, 20min, 4hr, 24hr), n=2 per time point (50min, 8hr). Values are means \pm SEM, *p < 0.05; unpaired Student's t-test.

3.2 Mass spectrometry data quality

A Kernel density plot of the log normalised spectral abundance factor (NSAF) data distribution (Fig. 2) was constructed in Scrappy. This shows that the data distribution was consistent between biological replicates and under differing experimental conditions and provides data to indicate consistency between runs on the MS. The overlay indicates that the log NSAF data distribution is close to normal hence the data is suitable for subsequent statistical analysis by methods such as ANOVA. False discovery rates (FDR) of both peptides and proteins were calculated after combining the data acquired from 3 biological replicates at their respective time points (Table 1). These indicate that the data is of high quality and suggest that few false positives will be identified.

Table 1. Protein and peptide false discovery rates (FDR)

Time point	Protein FDR	Peptide FDR
0min	0.006	0.001238
20min	0.005988	0.001045
50min	0.006105	0.001724
4hr	0.00502	0.000948
8hr	0.004994	0.001023
24hr	0.006536	0.001481

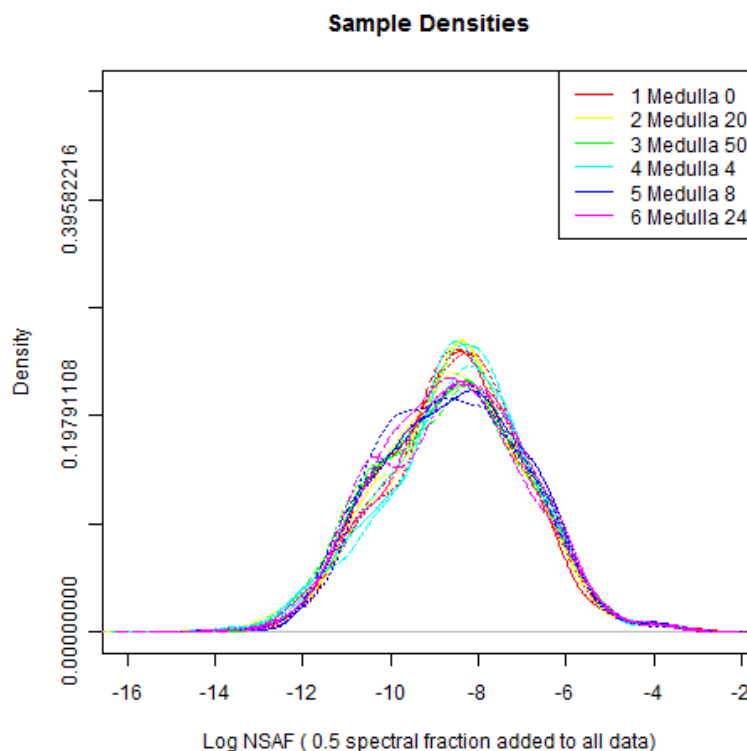


Figure 2. Kernel density plot. Replicates of time points (0min, 20min, 50min, 4hr, 8hr and 24hr) are represented by colour. All 18 samples overlap with no significant disparity between them.

3.3 Profile of the adrenal medulla proteome

A list of 2217 ± 40.04 (mean value, \pm SEM) proteins were identified from the 3 biological replicates of the control (0min). From this list only proteins that appeared in all 3 replicates with a total peptide count ≥ 5 were accepted. This produced a list of 972 non-redundant proteins at 0min (Table. A1) and this list was considered to comprise the proteome of the adrenal medulla.

3.4 The response of the adrenomedullary proteome to 2DG

To determine the proteome at each time point a similar analysis was performed. Of the total proteins identified at their respective time points (Table 2), those found in all three replicates but not differentially expressed were termed the ‘unchanged proteins’. The greatest number of unchanged proteins is at 20min (1034) (Table 2). Non-redundant proteins at 0min (Table. A1) served to act as baseline from which the differentially expressed proteins could be calculated. Two sets of analysis were then performed; the first and major analysis was to assess the proteome at each time point following 2DG and compare these to control, this analysis defined the proteins that were differentially expressed at each time point. The mean NSAF value across triplicates was used to estimate peptide abundances. These were then compared to those at 0min using Student’s t-test, proteins with p-value < 0.05 were considered differentially expressed (Table 1). Figure 3 (gray bars) shows the number of differentially expressed proteins at each time point. The lowest number of differentially expressed proteins was found at 20min (78) with the greatest number (163) found at 4hr. The total number of differentially expressed proteins compared to 0min when all time points were considered is 433 individual proteins (Table A2).

The second analysis performed was to assess changes to the proteome over time. One way ANOVA was conducted and 107 proteins were identified. Details of this second analysis will be described later.

3.5 The response of the adrenomedullary proteome to 2DG

To determine the proteome at each time point a similar analysis was performed. Of the total proteins identified at their respective time points (Table 2), those found in all three replicates but not differentially expressed were termed the ‘unchanged proteins’. The greatest number of unchanged proteins is at 20min (1034) (Table 2). Non-redundant proteins at 0min (Table.

A1) served to act as baseline from which the differentially expressed proteins could be calculated. Two sets of analysis were then performed; the first and major analysis was to assess the proteome at each time point following 2DG and compare these to control, this analysis defined the proteins that were differentially expressed at each time point. The peptide abundances were compared to those at 0min using Student's t-test and proteins with p-value <0.05 were considered differentially expressed (Table 1). Figure 3 (gray bars) shows the number of differentially expressed proteins at each time point. The lowest number of differentially expressed proteins was found at 20min (78) with the greatest number (163) found at 4hr. The total number of differentially expressed proteins compared to 0min when all time points were considered is 433 individual proteins (Table A2).

Table 2. Mass spectrometry data - Protein Numbers at Each Time Point

	20mins	50mins	4hrs	8hrs	24hrs
Total proteins identified ⁺	2133± 30.3	2068 ± 38.0	2168 ± 25.8	2175 ± 13.5	2153 ± 66.0
Unchanged proteins*	1034	926	953	913	982
Differentially expressed [‡]	78	138	163	136	107

+Values are means of proteins identified in 3 biological replicates ± SEM.

*Of the total identified, those unchanged compared to total identified at 0min. P > 0.05; unpaired Student's t-test.

‡When compared to the list of 972 proteins at 0min. P ≤ 0.05; unpaired Student's t-test.

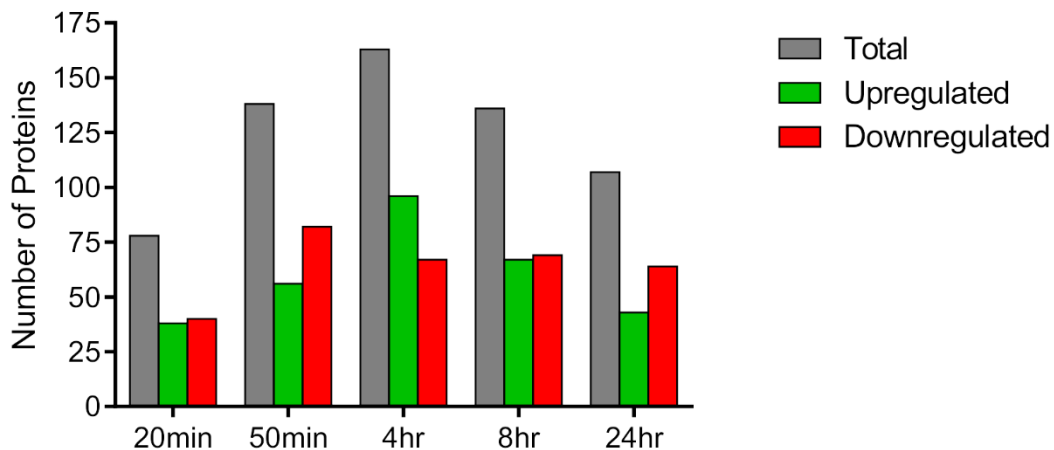


Figure 3. Number of differentially expressed proteins across time points. Proteins considered differentially expressed when logNSAF values were compared to those in the list of 972 proteins at 0min.

The second analysis performed was to assess changes to the proteome over time. One way ANOVA was conducted and 107 proteins were identified. Details of this second analysis will be described later.

3.6 Animal weights affect protein clustering between time points

Using Pearson distance correlation a heat map was generated of the 433 differentially expressed proteins using the Scrappy program (Fig. 4). The purpose of the heat map was to reveal protein expression patterns between the time points. This revealed an unexpected clustering of data which isolated 50min and 8hr time points from the other time points (x-axis, Fig. 4). We suspect that this clustering resulted from the differences in weight and/or age of the animals selected. From this point the data were separated and considered as two separate groups, Cohort 1 (0min, 20min, 4hr and 24hr) consisting of 289 differentially expressed proteins and Cohort 2 (50min and 8hr). Heat maps were generated for both cohorts; 0min, 20min, 4hr and 24hr which demonstrate a graded trend of changes in expression patterns and clustering (Fig. 5). Similarly, distinct differences were seen in proteins abundance at 50min and 8hr (Fig. 6). Some analysis was also performed on this cohort (see below).

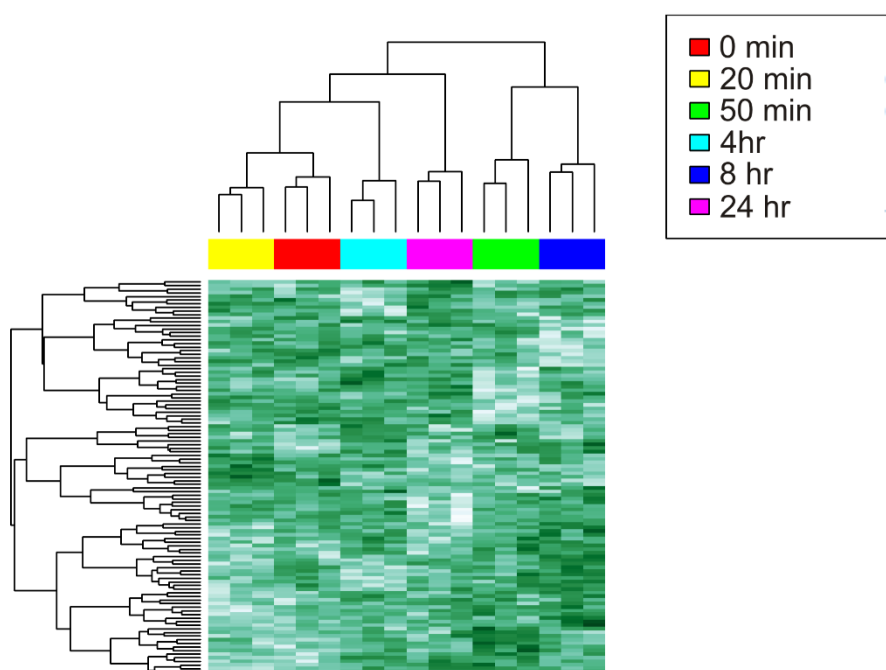


Figure 4. Heat map of all samples. Protein expression patterned of time points 50min and 8hr deviate from the clustering pattern of the other time points. Each column represents one sample, each row represents an individual protein. X-axis shows replicates of groups/time points (n=3 per group represented by the colour box) and the protein expression pattern between groups (measured by Pearson distance correlation) is shown by the matrix tree plot. Y-axis matrix tree plot shows protein clusters by genomic based protein-protein interaction (measured by Pearson distance correlation). White represents high spectral counts, while the darkest green represents the lowest number of spectra.

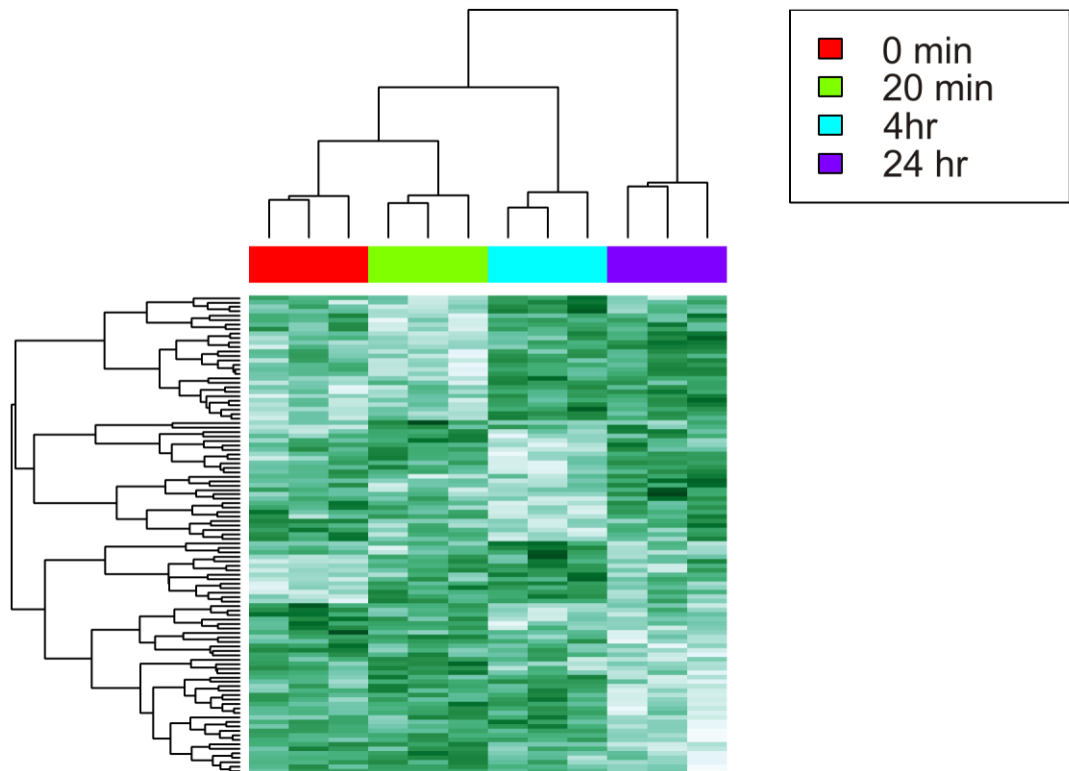


Figure 5. Heat map of samples 0min, 20min, 4hr and 24hr. The heat map is similar to that defined in Figure 4 however shows data acquired at only 4 time points. A distinct pattern of change in protein abundance is evident across time.

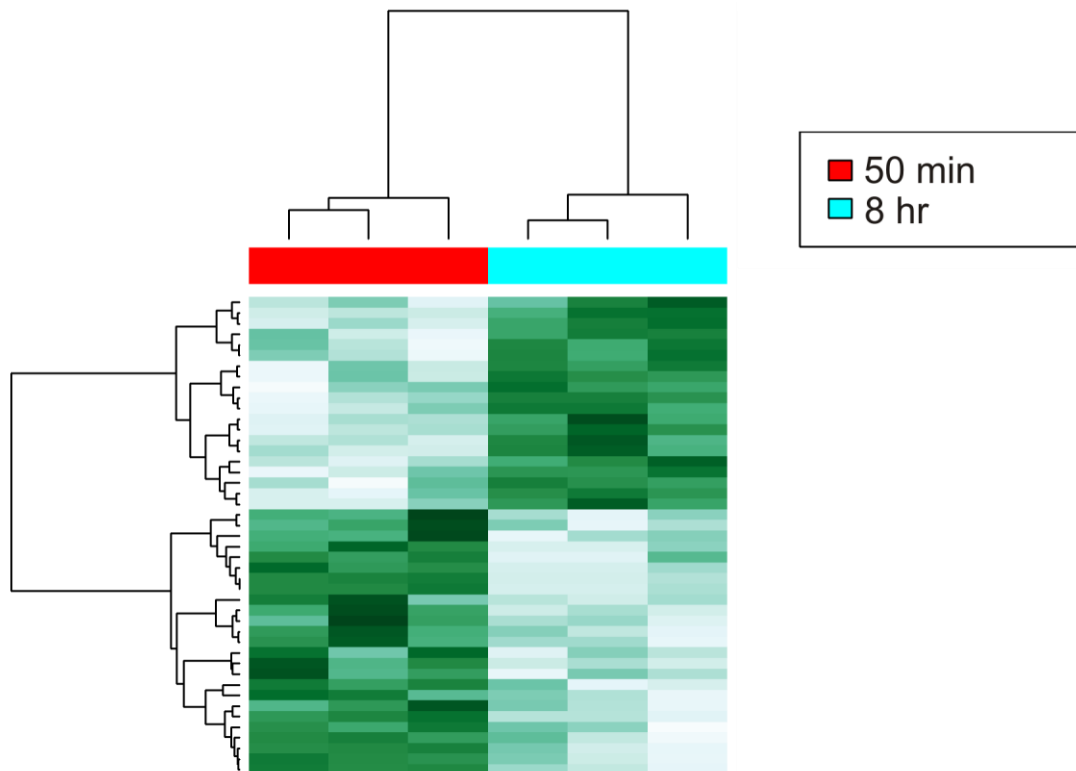


Figure 6. Heat map of samples 50min and 8hr. The heat map is similar to that defined in Figure 4 however shows data acquired at only 2 time points. Only proteins differentially expressed in the two time points are shown. Evidence of both up and down regulated proteins is evident.

3.7 Changes in the proteome of the adrenal medulla at 20min, 4hr and 24hours following 2DG

The primary data set analysed for this thesis was Cohort 1 which compared 0min with each other time point 20min, 4hr and 24hr. Figure 3 shows that when compared to 0 min proteins were both up (green) or down (red) regulated at each time point. At 4 hr post 2DG the large number of both up and down regulated proteins was detected. In total 296 proteins were differentially expressed in Cohort 1. These protein were identified and sorted. Figure 7 shows the number of proteins that were changed at each time point and the number of proteins changed at multiple time points. Only two proteins (Ambp and Ncl) were upregulated and one protein (Scp2) were down regulated at all three time points. These data indicate that independent processes occur over time following the stimulus.

All differentially expressed proteins were manually sorted and categorised using information from a range of databases (see Methods) to identify the proteins function or potential function and cellular location taking into the account that the protein was identified in the adult male adrenal medulla. This information was used to identify the biological pathways and molecular processes changing in response to 2DG. Tables 3-9 show 245 of the 289 proteins could be allocated to 7 major processes: Signalling, cellular remodelling, transport, mitochondrial function, response to stress and protein synthesis and degradation. Table 10 shows that a number of proteins (10) were not able to be categorised due to lack of any available information with respect to function or their known function was not related to those defined above (34). Tables 3-9 also show the proteins that are significantly changed at each time

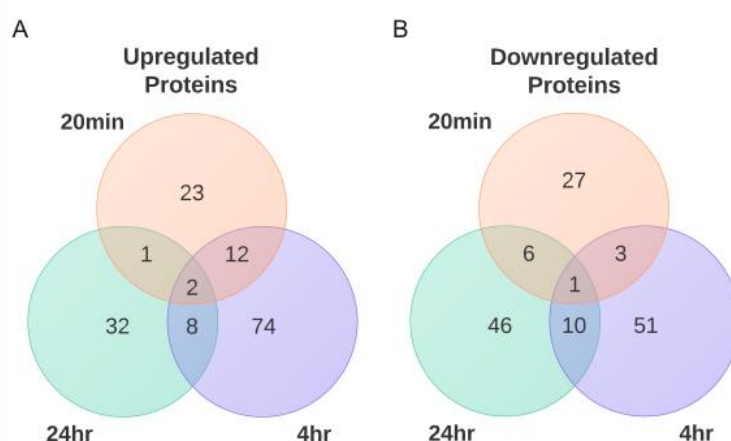


Figure 7. Differentially expressed proteins at single and multiple time points. Numbers of proteins upregulated A) and downregulated B) compared to 0min that are expressed at one or more time points. Areas of overlap indicate proteins expressed at both/all those time points.

3.7.1 Processes changed at 20min

Significant protein changes were seen as early as 20min following 2DG administration. Of the 78 proteins changed at 20min, 38 were upregulated and 40 were down regulated (Fig 3). Changes in steroidal signalling are indicated. Regulatory proteins involved in the GTPase Rho signalling pathway, a pathway involved in actin polymerisation and endocytosis, are downregulated (Table 3). There was significant upregulation of proteins involved in cytoskeletal remodelling, particularly related to actin polymerisation (Table 4). There are slight changes in favour of intracellular movement (microtubules), including the downregulation of cell matrix-adhesion molecule Lgals1, also known to inhibit microtubule formation (Table 4). Changes in cellular transport were not evident at this time (Table 5). Many proteins involved in oxidative phosphorylation and tricarboxylic acid (TCA) cycle in mitochondria were downregulated, though the processing of lipids were upregulated (Table 6). As well as fatty acid beta oxidation, pyruvate synthesis was up 20min. *De novo* purine synthesis was downregulated (Atic) but the purine nucleotide synthesis salvage pathway was upregulated (Hprt1). At 20min, constituents of the glutathione pathway were downregulated (Table 7). Early transcription factors such as Supt16h were upregulated despite the majority of transcription and translation related proteins being downregulated (Table 8). Protein degradation through proteolytic proteins was upregulated at 20min (Table 9).

3.7.2 Processes changed at 4hr

At 4hr 163 proteins were found changed with 96 upregulated and 67 downregulated (Figure 3), which provided a clear indication of the progression of changes in molecular processes. For instance, more proteins involved in the GTPase Rho signalling pathway were changed, the majority upregulated (Table 3). There was a downward trend in steroid signalling/regulatory proteins and changes to proteins in the complement cascade (Table 3). Cytoskeletal remodelling continued to change and increases in microtubule related proteins involved in intracellular trafficking were evident (Table 4). Transport proteins were changed; production of vesicle related transport proteins were upregulated, particularly those functioning in exocytosis (Table 5). However, intracellular vesicle transport to and from the Golgi apparatus were downregulated. The TCA cycle related proteins remain downregulated, however some involved in mitochondrial oxidative phosphorylation were now upregulated (Table 6). Proteins involved in lipid processing for TCA cycle are upregulated. Evidence of alternate pathways of glucose production such as the uronate cycle and anaerobic glycolysis, as well as gluconeogenesis utilising pyruvate is increasing (Table 6). The glutathione

oxidative stress pathway is upregulated in conjunction with the pentosephosphate pathway and peroxisome (Table 7). Although only a single protein is upregulated from the pentose phosphate pathway (Taldo1), it is the rate limiting enzyme for this pathway. Transcription factors are upregulated, some >2 fold, as are translation initiation and elongation factors (Table 8). Protein degradation appears to have slowed; ubiquitination proteins are downregulated and protease inhibitors upregulated (Table 9).

3.7.3 Processes changed at 24hr

At the final time point, the rate limiting protein in catecholamine synthesis, Th is upregulated >2 fold. Steroid related proteins continue to be changed, though significantly fewer are down regulated compared to 4hr (Table 3). There is a fall in the number of actin polymerisation proteins down regulated but some required for cytoskeletal stabilisation are maintained. Proteins involved in microfilament intracellular transport were also down regulated (Table 4). Vesicular transport proteins remain unregulated and the trans-golgi transport proteins down regulated (Table 5). TCA cycle proteins are still down regulated and oxidative phosphorylation proteins altered diminished in number with the majority downregulated (Table 6). Lipid processing proteins are also downregulated. The pyruvate metabolism is still changed. Stress related proteins are downregulated together with some in the glutathione pathway and the peroxisome (Table 7). Additionally, a key enzyme in the pentose phosphate pathway is downregulated (Tkd). There are fewer transcriptional proteins upregulated at 24hr, though several translational proteins are upregulated (Table 8). Protein degradation is diminished (Table 9).

Some proteins were unable to be categorised as functional annotations could not be clearly identified or were unavailable (Table 10). Time point 20min had only one protein of unknown function with respect to the adrenal medulla. At 4hr, the time point showing the greatest number of differentially expressed proteins, 7 proteins with unknown functions were identified with one protein (LOC100364062) ascribed as both up and downregulated. It is possible that although this protein had 2 different gene identifiers that this represents both type M and type K pyruvate kinase like proteins as found in the adrenal gland (Millaruelo et al., 1986). This also occurs with Tpm3 at 20min (Table 4), for which two distinct protein identifiers were coded. However Uniprot identifies 7 isoforms produced by alternative splicing that likely account for the proteins.

Table 3. Signalling

	20min	4hr	24hr	ANOVA
Catecholamine		Ppp1cc, Pebp1 , Th Spr		
Steroid	Akr1b7*, Cyp21a1	Cp*, Akr1a1, Pgrmc1*, Hsd17b8, Hsd3b1, Fdx1, Akr1b7*, Akr1b10*, Fdxr*	Cp*, Pgrmc1*, Akr1b10*, Fxdx*, Mtus1	Star
GTPase pathway	Nme1, Nme2	Rab5c, Rab3b , Ces1c , C11orf54 , Farp1	Plxnb2	Rab2a
Complement	Pafah1b2*	Pafah1b2*, C9, Cfh, Anxa5*, Prkcsh , Fetub	Anxa5*	Cd81

Table 4. Cellular remodelling

	20min	4hr	24hr
Cytoskeletal remodelling	Tpm3*, Tpm3[#] Actr2 , Actr3* , Syne3	Actr3* , Arpc5l , Pfn1, Tpm3*, Plg, Fgb , Svep1 , Sptan1 , Sptbn1 , Bst2 , Myof	Myl12a, Map1b
Intracellular movement	Myh11, Rmdn2	Capza2, Nudc, Tubb4b, Tubb5, LOC100911313 , Mgarp, Htt , Rmdn3*	LOC100911313 , Myo1c , Rmdn3*
Cell-cell adhesion	Lgals1	Fgb , Tjp1*	Dpp4 , Tjp1*

Table 5. Transport

	20min	4hr	24hr	ANOVA
General		Alb		Hba1
Transmembrane		Timm23*	Timm23*, Abcc5	
Internuclear	Tpr*	Lrrc59 , Lrrc58 , Ipo9 , Kpnb1, Tpr*		
SNARE/ Vesicular	Nsf*	Uso1 Ykt6 Vat1* Vat1l , Lman2 , Vapb, Ashg Hook3 , Ank1 , Npc1 Vps13a , Vps35*, Bcap31	Vcp, STX8 , Vat1* Ap1s1 Vps35* , Myo18a , Nsf* , Clint1	Vapa , Copb1 , Cltc ,
Solute carriers	Slc41a3*		Slc41a3*	

Table 6. Mitochondrial metabolism

	20min	4hr	24hr	ANOVA
TCA cycle	Mdh1, Dcakd	Dhtkd1	Aco1, Sdha	Idh1
Oxidative phosphorylation	Sfxn3, Atp5h*, Ndufa9*, Ndufa8*	Atp5h*, Slc25a5, Slc25a11*, Vdac2, Vdac3, Sfxn3*, Slc25a24, Atp5g1, Ndufa8*, Hspd1, Nfu1	Cyc1, Aars, Ndufa9*, RGD1309586, Slc25a30	LOC684270, LOC687295, Gbas, Cox4i1, Atp5f1, Por, Gpd1, Gpd1l
Glucose		Ldha, Cryl1, Got1,	Rbp4, Dmp1	
Pyruvate	Me2*	Me2*, Hoga1		
Inositol	Impa1*, Pi4ka		Isyna1, Impa1*	
Lipids	Acaa1a*, Mut, Acot2, Scp2*	Acads, Decr1, Apoal*, Acaa1a*, Pitpna, Fxdr*, Cpt1a, Scp2*	Apoal*, Cpt1a, Timm44, Fxdr*, Scp2*, Apob	Dbt, Gesh
Other metabolic processes	Hprt1, Atic, Hint3	LOC100911034, LOC100912917, Abhd3	Mccc1	Aldh9a1, Dpyd, Aprt

Table 7. Stress response

	20min	4hr	24hr
Pentose phosphate		Taldo1	Tkd
Glutathione	Gpx1, Gpx4, LOC100360601*, Hagh	Glo1, Gsst2, Gsst3, Txnl1, Adh5, Gsta3,	LOC100360601*, Txnrd1,
Peroxisome		Prdx3, Prdx5*	Prdx5*
Stress related proteins		Stoml2, Ak3	Hyou1, Mthfd2, RGD1304982, Pyroxd2

Table 8. Protein synthesis

	20min	4hr	24hr	ANOVA
Transcription	Hist1h2ba*, Hspa8, Ncl*, Phb2, Creg1, H1f0*, Supt16h*, Nme2*,	Abhd14b, Ncl*, Pcnal, Hcfc1, U2af1*, Lsm3, Zfp361l, Phb	Ncl*, Supt16h*, Cbx1, Tardbp, Hist1h1b	

	Npm3,			
Spliceosome	Hspa8, Fus*, Snrpd1	Hnrnpa1 Hnrnp3 Ptbp1, H1f0, POLR2	Ptbp1, Fus*, Hnrnp2, Snrpd2, POLR2*	Ybx1, Eftud2
Ribosome	Rpl3, Rpl23*, Rplp2*, LOC100362830	Rps15a2, Rpl26, Rplp1*	Rpl19, Rpl24, Rplp2*, Rplp1*, LOC100362830*	Rps15
Translation	Eef1g*, Eif5a, Tars, Tars2*, Eif2b1,	Eef1g*, Eif4h, Eprs, Sec61a1, Get4, Eif2b5*, Eif5a	Eef1b2, Eef1d, LOC100364427, Lars, Eif2b5*	
Posttranslational modifications	Uba2, Ppia, Aga	Fkbp2, Unc45a, Phpt1	Pdia3	Rpn1, Calr

Table 9. Protein degradation

	20min	4hr	24hr	ANOVA
General	Ide, Ermp1, Htra2 and Pepd, Aga		Cops8, Ece1, Lta4h, Dnpep, Pitrm,1 Pmpca, Pmpcb, Psmb10	
Ubiquitination		Skp1, Ubr4, Spg20		
Proteasome	Psma5	Psmd6, Psmd1, Psmd13	Psmb5	Psma4
Inhibitors	Ambp*	Pzp, Ambp*, Serpina1	Ambp*	

Table 10. Unknown function

	20min	4hr	24hr
	Efr3a	LOC100363439, LOC100364062[#], LOC681544, LOC685179, YPN, LOC100364062[#], RGD1303003*	UPF0587, LOC100911515, LOC101552443, RGD1303003*

Symbols in green and red represent upregulated and downregulated proteins respectively.

Those in bold font have a fold change >2. Symbols in blue represent from the second (ANOVA) analysis proteins differentially expressed over time

*Differentially expressed at multiple time points.

[#]Proteins with different gene identifiers, search resulting in the same protein

3.8 Time dependent changes in the proteome of the adrenal medulla

The second analysis of the proteins was performed to assess proteomic changes over time, as opposed to the first analysis which compared all time points only to the control (0 min). Using the Scrappy program, an ANOVA was conducted on all proteins in the adrenomedullary proteome list (Table A1.) to compare mean logNSAF (log normalised spectral abundance factor) of each protein at each time point to all the other time points, including 0min.

Of the 972 proteins 107 proteins were significantly altered with respect to time, 79 of which were differentially expressed (at individual time points) with the remaining 28 identified only when all time points were taken into account (Table. A3). These 28 proteins are also shown in Tables 3-9 (blue text) describing the key cellular processes with which they are associated. A key steroidogenic protein was found to be changed in the signalling pathway (Table 3). The majority of these “ANOVA” proteins (8) contributed to the mitochondrial oxidative phosphorylation process (Table 6). Another interesting change was to the protein isocitrate dehydrogenase, a key enzyme in the TCA cycle. The criteria for selection was that proteins had to have a total peptide count ≥ 5 in all time points, and be changed compared to at least 2 time points; eg. 0min vs. 20min and 20min vs. 4hr or 20min vs. 8hr and 20min vs. 50min.

The analysis shows that there is a time dependence in the response and the multiple time point comparisons provides an indication of when these changes are occurring. One of the proteins was Th, upregulated at 24hr compared to both control as well as 20min time points (Fig. 8A, Table 3). Vat1, a protein involved in cholinergic vesicle transport (Eiden et al., 2004), was upregulated at both 4hr and 24hr compared to the control (Fig. 8B, Table 5). A key protein in actin polymerisation for exocytosis (Trifaró et al., 2008), Actr3 was upregulated at both 20min and 4hr compared to the control (Fig. 8C, Table 4). Nsf, a protein responsible for multiple steps in exocytotic and endocytic pathways was downregulated both at 20min and 24hr compared to control and was downregulated at 24hr when compared to 4hr (Fig. 8D, Table 5).

For proteins not shown changed with respect to 0min (control) isocitrate dehydrogenase, as previously mentioned is an important enzyme in the TCA cycle that is considered rate limiting (Stueland et al., 1988), was upregulated at 20min compared to 4hr and 24hr (Fig 9 A, Table 6) . P450 oxoreductase is a protein involved in mitochondrial oxidative phosphorylation

is downregulated at 24hr compared to 20min and 4hr, as is vesicular transport protein, Vapa. Several proteins from this list were selected for Western blot analysis including Th, Actr3, Nsf and Vat1 (see below).

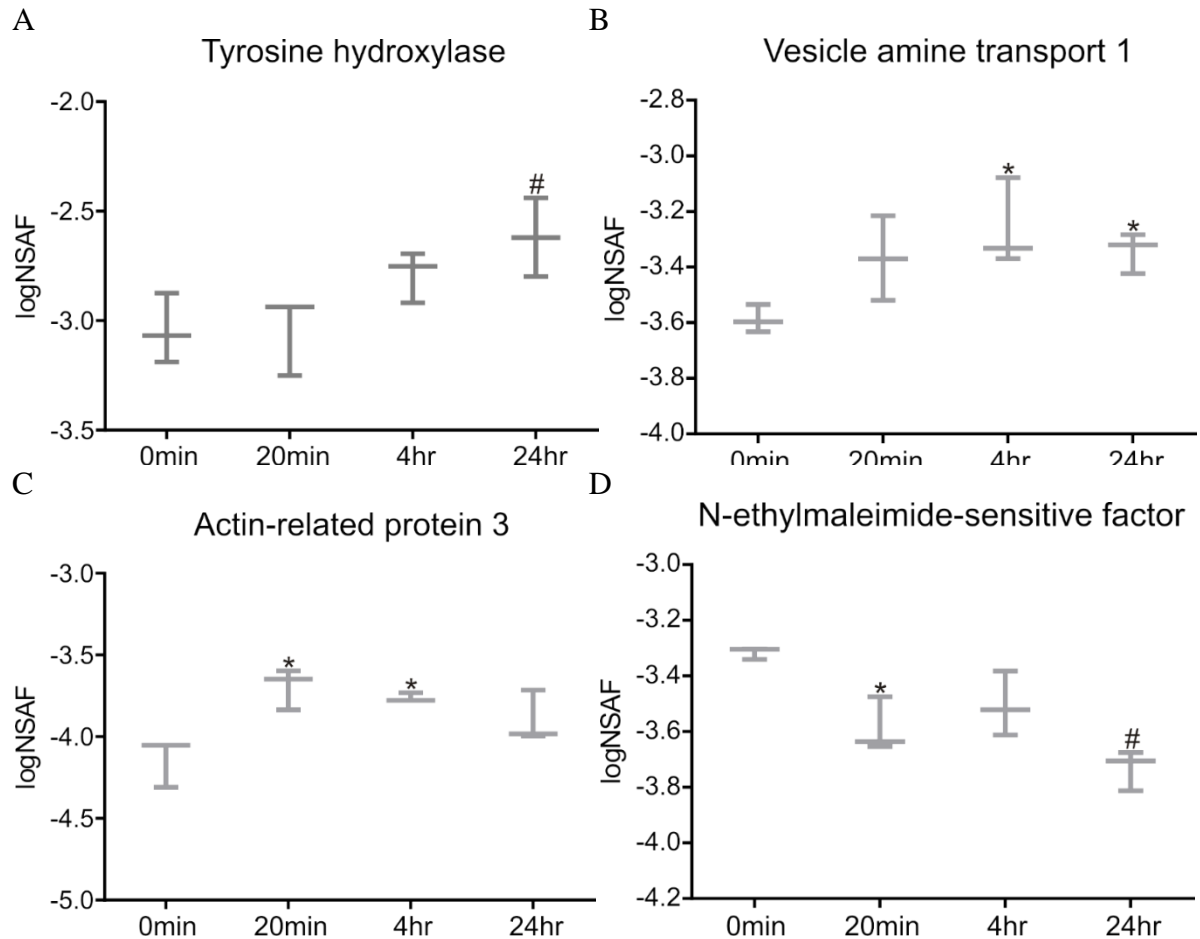


Figure 8. Time dependent changes in protein abundance. A) Tyrosine hydroxylase is upregulated at 24hr compared to both 0min and 20min. B) Vesicle amine transport 1 is upregulated at 4hrs and 24hrs compared to 0min. C) Actin-related protein 3 is upregulated at 20min and 4hrs compared to 0min. D) N-ethylmaleimide-sensitive factor is downregulated at 20min compared to 0min and at 24hr compared to 0min and 4hr.

* Differentially expressed compared to 0min; $p < 0.05$, one-way ANOVA

Differentially expressed compared to multiple time points; $p < 0.05$, one-way ANOVA

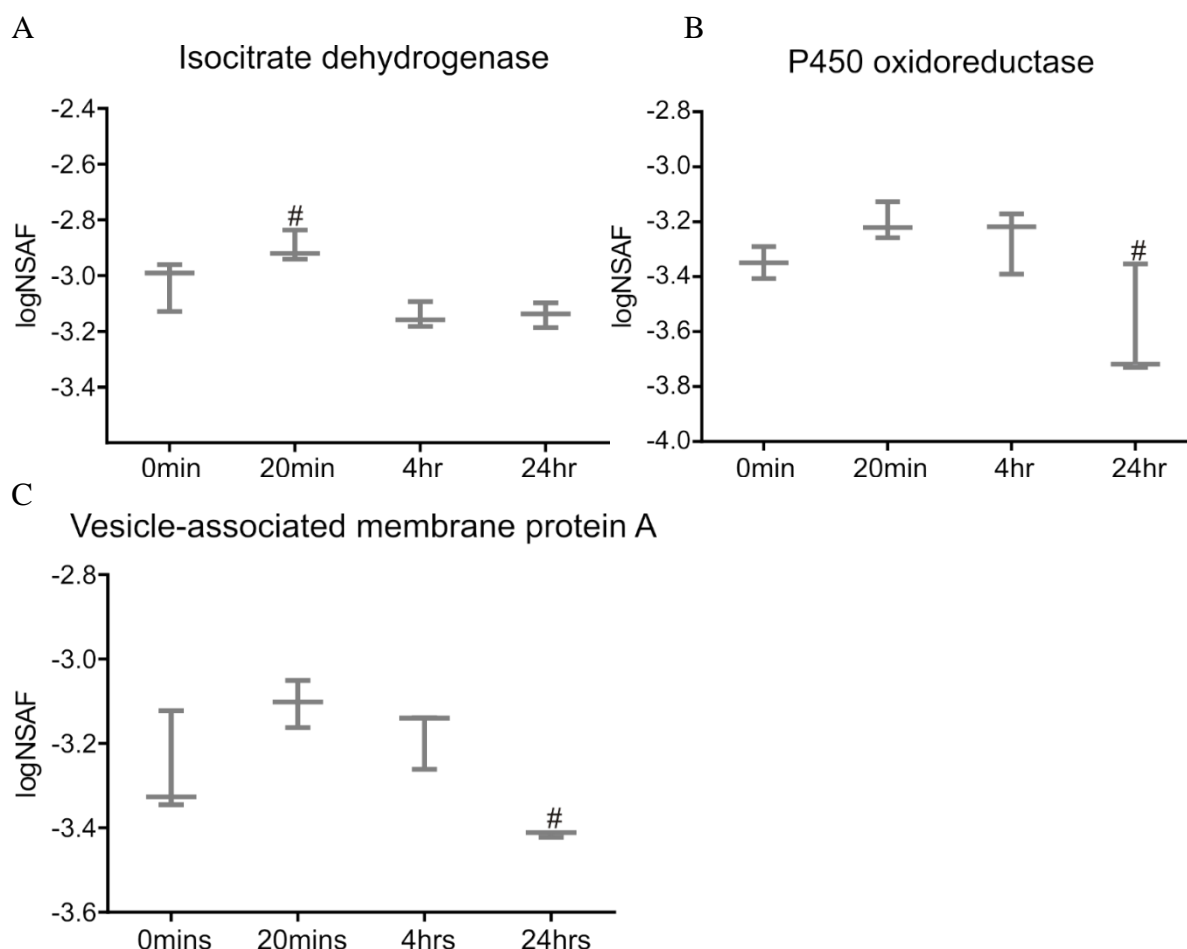


Figure 9. Time dependent changes in protein abundance that were not detected when protein abundances at each time point were compared only to time 0min (control).

A) Isocitrate dehydrogenase, B) P450 oxidoreductase and C) Vesicle associated membrane protein A are all downregulated at 20min compared to both 20min and 4hr.

Differentially expressed compared to multiple time points; $p < 0.05$, one-way ANOVA

3.9 Western blot analysis

The next step in the study was to determine if some of the protein changes detected using MS could be validated using Western blot analysis. In order to maintain consistency in data acquisition, animals used for Western blot analysis were weight and age matched with those used for LC-MS/MS analysis (Fig. 1A). No significant differences between groups at each time point were seen (Student's t-test), with the exception of time points 8hr and 24hr in which the animals used for Western blot analysis weighed less than those used for MS. However, animals in each of these groups were of similar ages (9-10 and 13-15 weeks respectively). The samples for the Western blot group were collected after MS analysis had been completed however all samples for each analysis were collected on the same day and at the same time of day. For the Western blot group blood glucose levels at 0min were 11.48 ± 0.92 mmol/L (Fig. 1B). No significant differences in blood glucose were observed between

corresponding time points between the groups (Student's t-test, $p < 0.05$). Blood glucose levels in the Western blot group as for the MS group showed a significant increase at 20min (one-way ANOVA, compared to 0min).

These findings indicate the valid use of these data for comparative analysis. It should also be noted where possible one sample (remains) from the MS analysis was used in each Western analysis to further ensure that the samples were similar.

Ten proteins were selected for Western blot analysis based on fold change detected using MS: Th, Ide, Rmdn3, Actr3, Nsf, Pitpna, Capn2, Vapb, Vat1 and Dbh. Successful Western blots showing single bands were not achieved for all proteins (in the time frame allowed) so description is restricted to a selection shown below: Th, Ide, Nsf, Rmdn3 and Dbh. The antibodies that were not successfully visualised by Western blot were mainly those with low molecular weights. This was due to an unidentified band of approximately 30kDa that recurred in almost all blots. Therefore, proteins such as Vapb (30kDa) and Pitpna (32kDa) were indistinguishable from this recurring band. The use of beta actin as a normalising protein was used in some instances as the band occasionally obscured GAPDH if the gel was not run for a longer time. Other antibodies such as Actr3, Capn2 and Vat1 were unsuccessful due to poor quality did not show well defined bands, therefore these were not used in analysis.

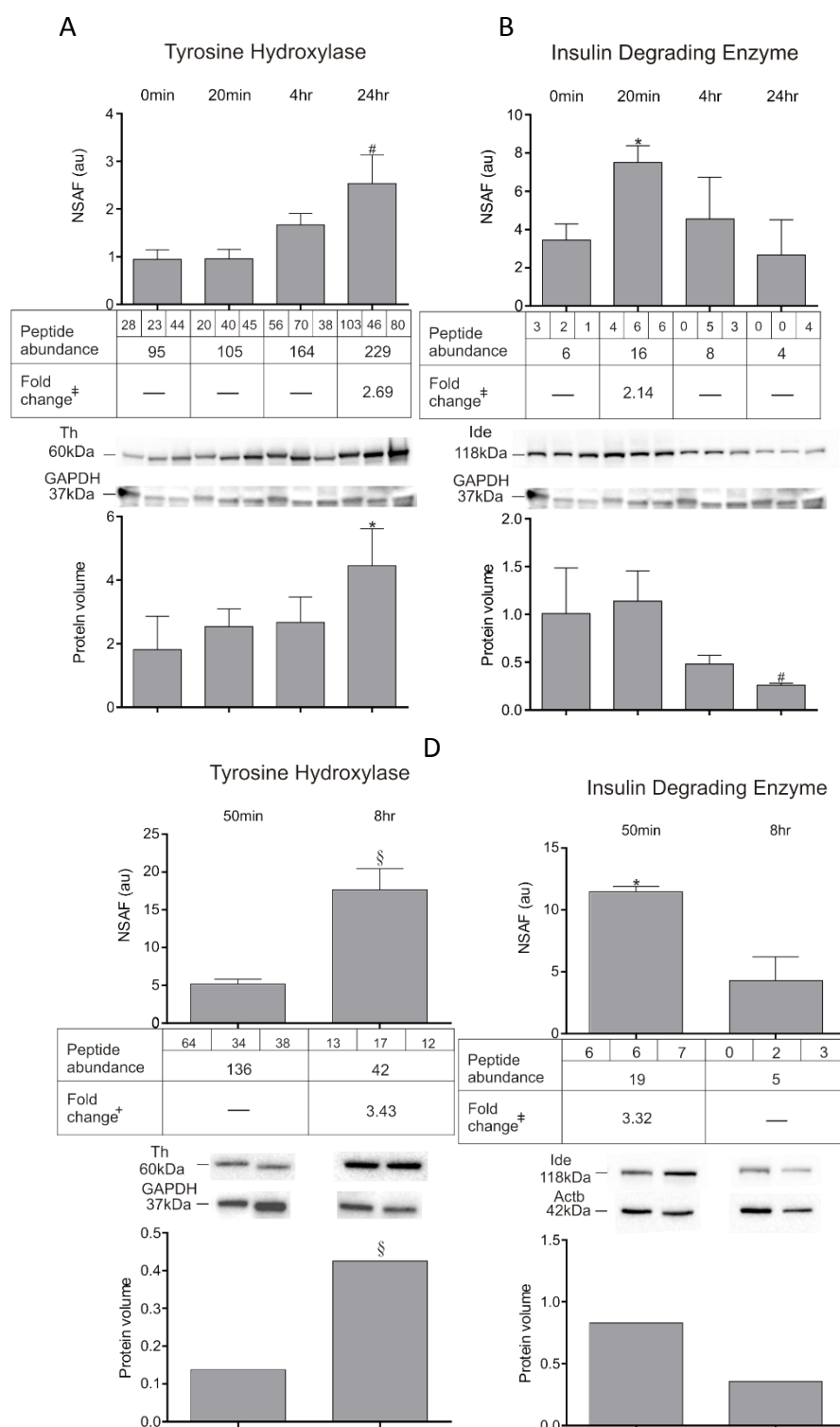


Figure 10. Comparison of MS data and Western blot data. normalised spectral abundance factor (NSAF) values, protein abundances and Western blot analysis of individual proteins. A), B) tyrosine hydroxylase (Th) and insulin degrading enzyme (Ide) expression at 0min, 20min, 4hr and 24hr respectively. Each time point in biological triplicate; first 3 bands =0min etc. C) Th expression at 50min and 8hr, logNSAF significantly changed between 50min and 8hr. D) Ide expression at 50min and 8hr, logNSAF 50min compared to 0min. C and D Western blots done in biological duplicate.

* Differentially expressed compared to 0min; $p < 0.05$, Student's t-test (with the exception of C)

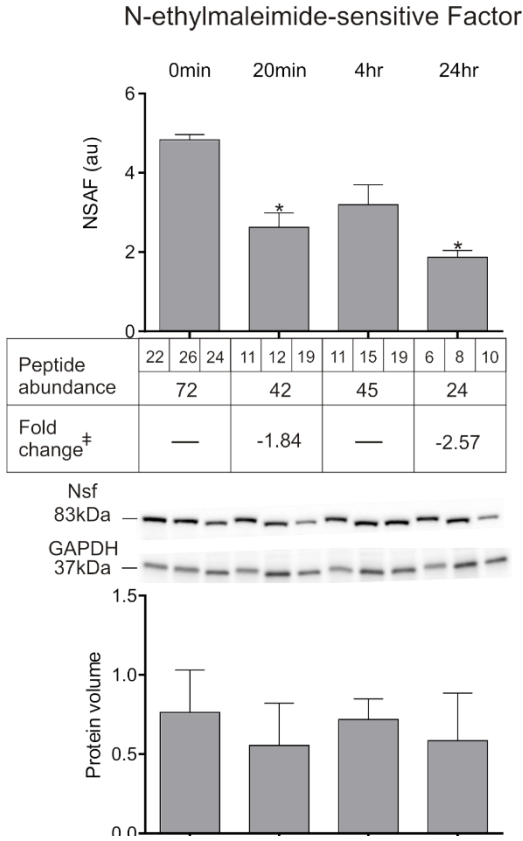
Differentially expressed compared to multiple time points; $p < 0.05$, Student's t-test

\$ Differentially expressed compared to 50min; $p < 0.05$, Student's t-test

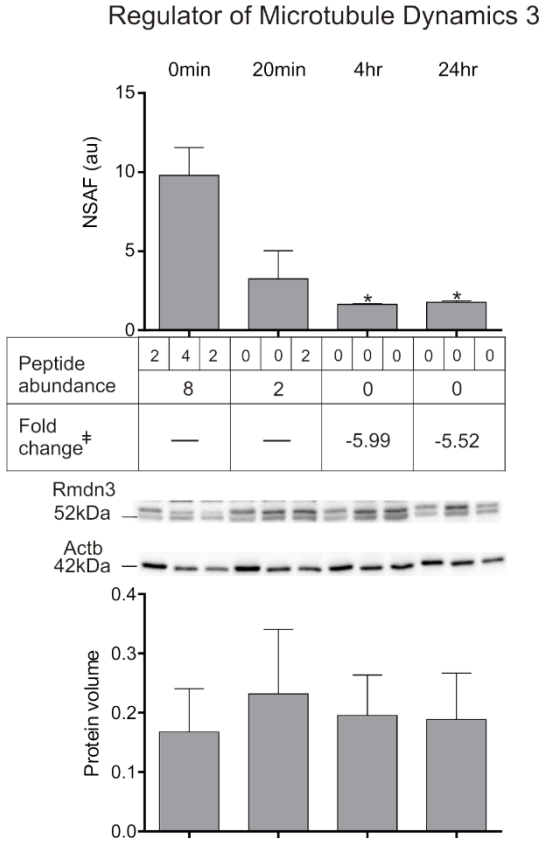
‡ Fold change compared to 0min; $p < 0.05$, Student's t-test

+ Fold change when compared between 50min and 8hr; $p < 0.05$, Student's t-test

A



B



C

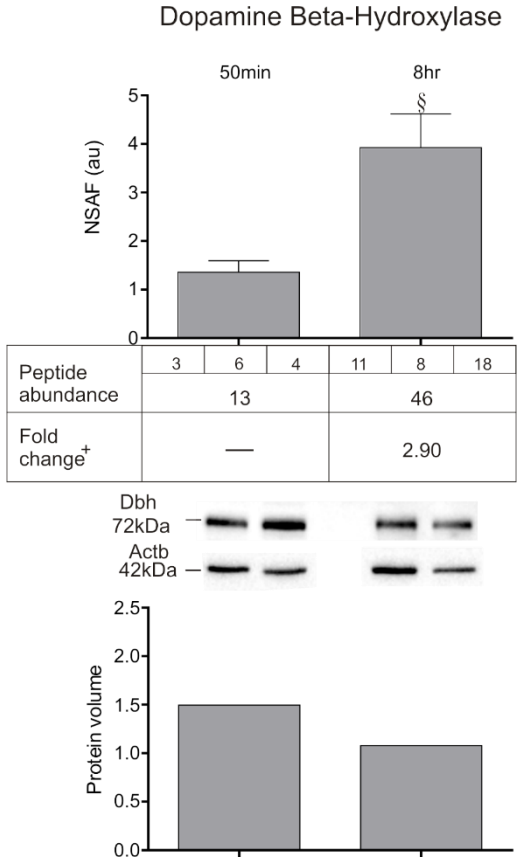


Figure 11. Comparison of MS data and Western blot data. NSAF values, protein abundances and Western blot analysis of individual proteins. A), B) Nsf and Rmdn3 comparisons at time points 0min, 20min, 4hr and 24hr respectively. Each time point in biological triplicate; first 3 bands =0min etc. C) Dbh comparison 50min and 8hr. Western blots done in biological duplicate.
* Differentially expressed compared to 0min; $p < 0.05$, Student's t-test (with the exception of C)
[‡]Fold change compared to 0min; $p < 0.05$, Student's t-test
[‡]Fold change when compared between 50min and 8hr; $p < 0.05$, Student's t-test

Figure 10A shows in the upper panel the NSAF data for Th at each time point with the peptide abundance and fold change acquired using LC-MS/MS analysis. The lower panel shows the Western blot for Th and the housekeeping protein GAPDH as well as the quantification. One-way ANOVA revealed that Th was upregulated at 24hr compared to both 0min and 20min, exhibiting a 2.69 fold increase compared to control. Western blot data was congruent with these results with one-way ANOVA (normalised to GAPDH) showing a significant upregulation of Th at 24hr compared to control showing a 2.3 fold increase (Fig 11A). In order to determine whether differences in expression of Th could be detected between 4hr and 24hr a similar analysis was performed on the 50 min and 8 hr data series (Fig 11C). An unpaired t-test was performed for Th MS acquired data, revealing a 3.43 fold increase at 8hr compared to 50min. Although only two samples were available for Western blot analysis these suggest similarity with the MS expression data. These data together suggest that TH could be upregulated as early as 8 hr after the stimulus and remains upregulated at 24 hr post stimulus.

A similar analysis was performed for insulin degrading enzyme (Ide) (Figure 10B). Ide was upregulated early (20min) as seen in the NSAF with a 2.14 fold increase. The Western blot data showed no significant change at 20min compared with control, however Ide was downregulated at 24hr compared to 20min and control by Western blot (Fig. 11B) a pattern similar to that seen in the MS data. Due to the irregularity of the blot, lane 1 of Figure 11A (Th) and 11B (Ide) were normalised to the mean of lanes 2 and 3 GAPDH.

The 8hr and 50 min data was again used for comparison with the MS analysis. There was no significant difference between 50min and 8hr, so the 3.32 fold increase at 50min compared to 0min was used for analysis. These results were reflected in the available Western blot data (Fig. 11D) however the sample size is too small for quantitative comparison. Nevertheless together the data tentatively suggest that IDE may be decreased a late periods after the stimulus however whether an increase early after the stimulus requires further analysis.

Similar to Figure 10, Figure 11A shows NSAF data for Nsf at each time point in the upper panel along with the peptide abundance and fold change. Nsf was shown to be downregulated at both 20min and 24hr when compared to control, 1.84 and 2.57 fold respectively. The Western blot of Nsf and GAPDH and the quantification shown in the lower panel, though displaying a similar expression pattern, did not show any significant change between any of the time points (Fig. 11A). This analysis was repeated with Rmdn3, another downregulated protein. The MS data show a sharp decrease at both 4hr and 24hr; time points with a peptide

abundance of 0, causing the fold changes to appear great (-5.99 and -5.52 respectively). The Western blot analysis showed no similarities to the MS data, nor were any significant differences observed between time points (Fig. 11B). As described for Ide and Th, a t-test was performed on NSAF values of times 50min and 8hr for the protein Dbh (Fig. 11C). The upper panel shows that Dbh was upregulated at 8hr by 2.90 fold when compared to 50min. However, the Western blot did not correspond to the MS analysis, nor did it show any significant difference between the two time points.

3.10 Localisation using Immunohistochemistry

In order to explore the localisation of some of the proteins within the adrenal medulla identified using both MS and Western blot analysis immunohistochemical analysis was also conducted. As previously stated, tyrosine hydroxylase (Th) is the rate limiting enzyme of catecholamine synthesis, a process that occurs predominantly within the medulla of the adrenal gland (Wurtman and Axelrod, 1966). In order to localise this protein immunohistochemistry was performed on sections of rat adrenal gland. Figure 12A shows that the adrenal cortex is devoid of Th staining, which is confined to the medulla (as described previously (Pickel et al., 1975)). Higher power images of the adrenal medulla reveal tight clusters of chromaffin cells which contained Th within the cytoplasm. Synaptic boutons containing acetylcholine transport vesicles (VaChT) can also be seen localised close to the plasma membranes of the chromaffin cells (Fig. 12B) confirming cholinergic innervation of the adrenal medulla again as described previously (Hamelink et al., 2002).

3.11 Localisation following activation of the adrenal medulla

Th and c-Fos immunoreactivity were assessed in sections of adrenal tissue obtained from rats that received 2DG or saline treatment 2hr prior to perfusion. Visualisation of the early gene product c-Fos is maximal between 90min and 2hr following initial stimulus (Dragunow and Faull, 1989; Stachowiak et al., 1990). Figure 3A shows that the saline treated animal had no c-Fos immunoreactivity whereas the 2DG treated animal (Fig. 3B) shows high levels of c-Fos immunoreactivity, confirming that 2DG as used here activates the adrenal medulla as described previously (Ritter et al., 1995) (Parker et al., 2013).

Although all antibodies tested for Western blot analysis were used also tested for immunohistochemistry no specific labelling was detected in either untreated or 2DG treated tissue.

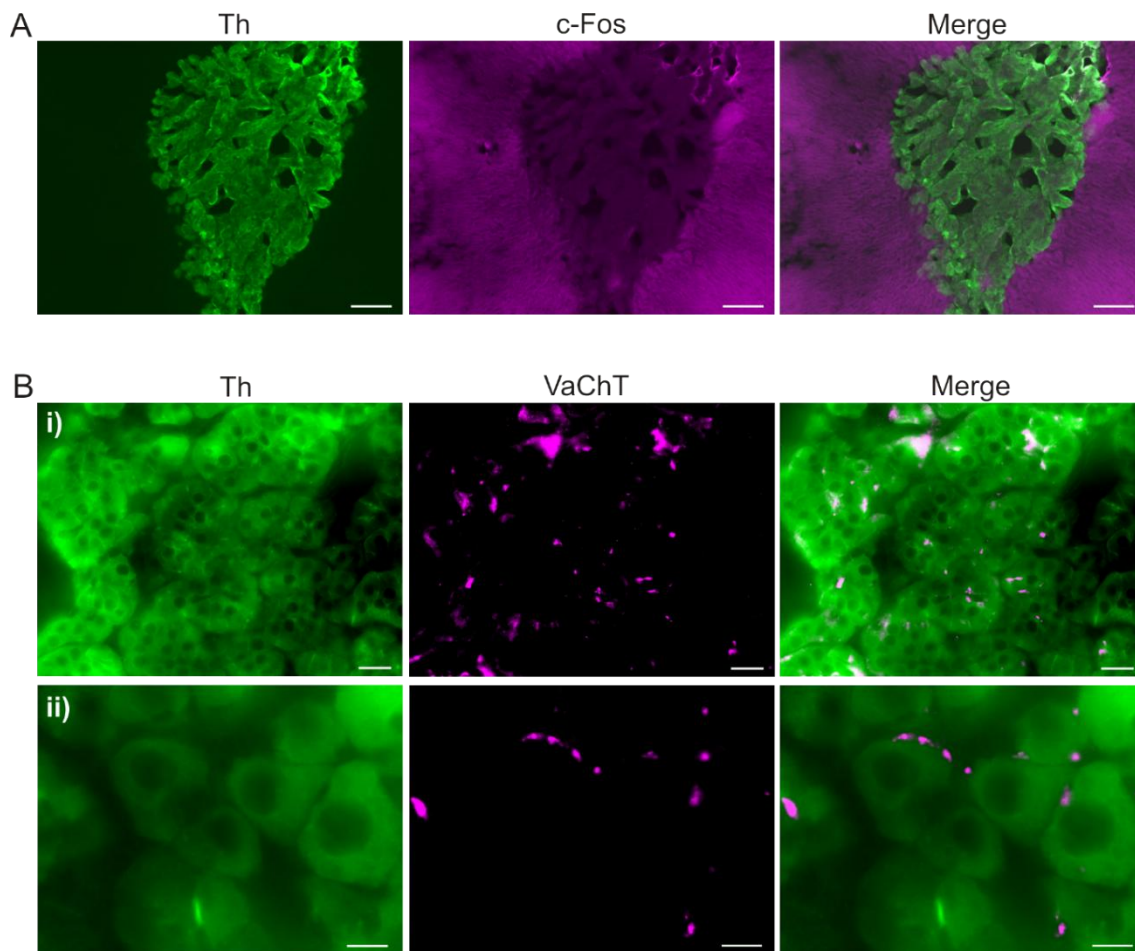


Figure 12. Localisation of tyrosine hydroxylase (Th) and vesicular acetylcholine transporter (VaChT) in a non-2 –deoxyglucose (2DG) treated adrenal. A) Distribution of Th and c-fos immunoreactive cells within Sprague dawely (SD) rat adrenal gland. Merged image shows Th localisation solely within the (chromaffin cells of?) adrenalmedulla (scale bar 200µm). B) Visualisation of cholinergic terminal bouton localisation (VaChT) to membranes of adrenomedullary chromaffin cells (expressing Th). Bi) scale bar=20µm, Bii) scale bar=10µm.

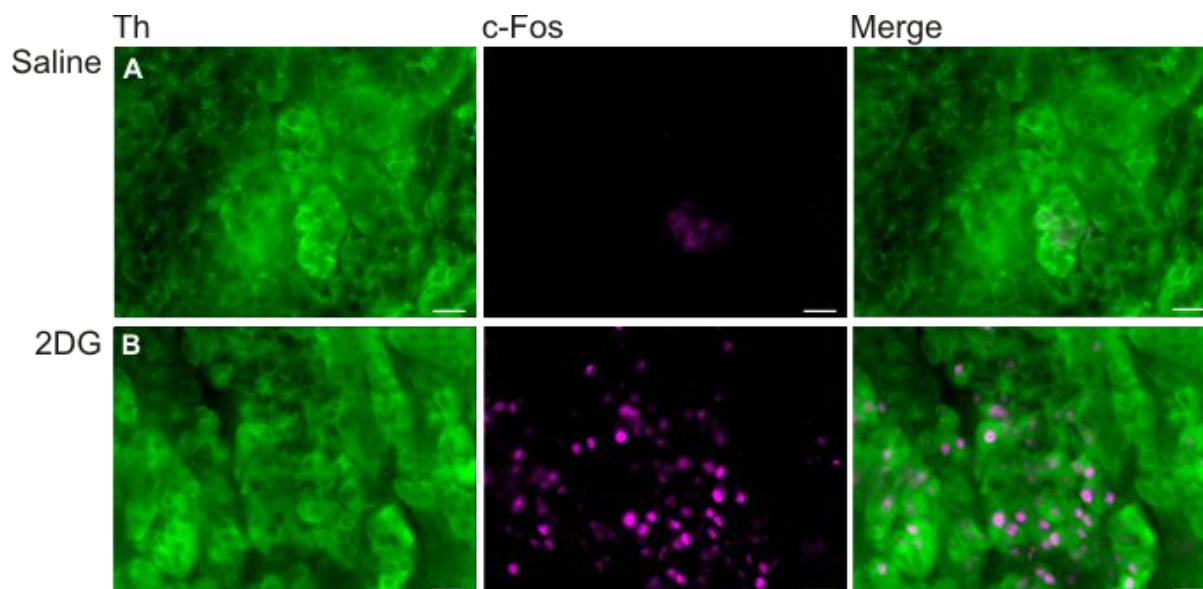


Figure 13. Visualisation of 2DG adrenomedullary activation by c-Fos. Th and c-Fos immunoreactivity in adrenal medulla in SD rats treated with saline (0.4ml i.p)(A) or treated with 2DG (400mg/kg i.p) (B), harvested at 2hr time point (maximal for c-fos visualisation). Merged image shows C-Fos activation is localised to chromaffin nuclei. Scale bar = 20µm

4.0 Discussion

4.1 Major findings and implications

The major findings of this study were to identify the first preliminary protein profile of the adrenal medulla and to identify the protein changes that occur over time in response to systemic 2DG. These changes outline the molecular mechanisms that are responsible for chromaffin cell activation in response to the stress of glucoprivation. Significant protein changes were defined as early as 20 min and for as long as 24 hours following a single episode of glucoprivation with a set of proteins that changed with respect to time. The final observation was that Western blot validation of MS data was not uniformly successful which can be explained by the limitations present in both techniques. Nevertheless overall it can be concluded that the data acquired using MS represents valid changes expected in the adrenal medulla following 2DG.

4.2 Protein profile of the adrenal medulla

A protein profile of the adrenal medulla was achieved using shotgun proteomics which yielded 972 proteins that now comprise the adrenomedullary proteome. Although this represents a large proportion of the proteome there yet remains more to identify. Samples in this study were not enriched to detect low abundance proteins or identify posttranslational modifications, therefore the proteome defined here is incomplete. There are also important membrane bound proteins that were not accounted for as only the supernatant was analysed. A study conducted by Wegrzyn et al. (2007) performed protein profiling on the dense core vesicles of adrenomedullary chromaffin cells. The samples were prepared to include both soluble proteins within these vesicles as well as the proteins in the vesicle membranes. Wegrzyn's group has furthered their attempts at profiling dense core chromaffin granules through use of an affinity column, in order to enhance low abundance proteins (Wegrzyn et al., 2010). As Yasothornsrikul et al. (1998) have shown, it is possible to purify fresh adrenal tissue to isolate the desired organelles to allow for compartmentalised proteomic analysis. Nevertheless a large number of mitochondrial proteins were identified in the present study, however without further purification detection of proteins changed in cellular components such as the inner and outer mitochondrial membranes were likely being missed. It is possible to map the complete adrenomedullary proteome if the analysis is performed on each organelle independently and this information is added to the list described in the present study.

Additional techniques can also be used to supplement the data by adequate purification steps to lessen high abundance proteins and enhance low abundance protein detection (Goshe et al., 2001). This study has contributed to previous efforts to profile the adrenal medulla (Jalili and Dass, 2004). Though there are still many proteins to be identified, this study is the first to catalogue such a significant portion of the proteome of the adrenal medulla and most importantly to track changes to it over time in response to stress.

4.3 Differentially expressed proteins

Two types of analysis were performed on the MS data: one identified proteins changed at each time point with respect to control and the other showed proteins changed at two time point showing a time dependent change. Analysis revealed 289 proteins were differentially expressed at 20min, 4hr, 24hr compared to control. Changes in different functional pathways were identified at each time point segregating into 8 functionally relevant categories; signalling, cellular remodelling, transport, metabolic processes, stress response, protein synthesis and protein degradation. These categories were then further subdivided into more specific functions or pathways in order to understand how cellular processes changed over time. These results revealed the protein systems that were changing to facilitate the chromaffin cells responses to 2DG as well as the how the counter regulatory response to low effective glucose concentrations (hypoglycaemia) were mediated by the adrenal medulla. Though much is known about some of these processes, very little is known about how they change with respect to time. The results of this study elucidate the functional molecular responses to 2DG and the duration and intensity of these responses.

4.4 Methodological considerations

4.4.1 The effects of 2DG

The effects of 2DG on the adrenal medulla were found to elicit two major types of response; the systemic response to glucoprivation will result in catecholamine release and the lack of usable glucose will create cellular stress. These effects can be seen in the changes to the both the stress related proteins and those involved in the glucoprivic response at and across multiple time points. 2DG activates the sympathetic nervous system (SNS) and as a result the activity of the adrenal medulla is increased (Rappaport et al., 1982). This activation can be seen from the immunohistochemical work in the present study showing c-Fos immunoreactive chromaffin cells following 2DG but not saline administration. This stimulates catecholamine release from the chromaffin cells (Scheurink and Ritter, 1993)

causing their cellular structure to alter accordingly. As detailed below, many cytoskeletal remodelling proteins were upregulated as were those facilitating intracellular vesicle transport likely supporting exocytosis of adrenaline. Proteins involved in the stress response pathways to 2DG also showed distinct changes, not only in differentially expressed proteins but also those showing time dependent changes such as transaldolase (Taldo1); the key protein in the non-oxidative branch of the pentose phosphate pathway (Novello and McLean, 1968). Other stress response pathways are also changed at multiple time points including the glutathione/thioredoxin and peroxiredoxin pathways. Similar results were obtained in a study pertaining to neurological oxidative stress in 2DG treated rats, showing upregulation of oxidative stress response proteins (Guo and Mattson, 2000). Of course the sympathoadrenal activation will also likely cause an increase in cellular stress as the stimulus is strong and sustained as evidenced by the degree of c-Fos labelling seen.

2DG is a structural analogue of glucose, with a hydrogen substitution in place of the 2-hydroxyl group in glucose (Woodward and Hudson, 1954), which blocks glycolysis thus preventing the utilisation of glucose. 2DG enters the cell rapidly and competitively inhibits glucose phosphorylation (Wick et al., 1957). Moreover, 2DG is not known to have any cytotoxic effects until doses reach above 2g/kg (Landau and Lubs, 1958). Cells undergoing 2DG-induced glucoprivation behave similarly to those exposed to natural glucose deprivation (Owada et al., 2013). This enables us to accurately simulate naturally occurring glucose deprivation and observe the proteomic response. For instance, glucose deprivation (induced by both starvation and 2DG) results in intracellular production of H_2O_2 and reactive oxygen species (Owada et al., 2013). In turn, H_2O_2 stimulates the pentose phosphate pathway and glutathione/ thioredoxin/ peroxiredoxin systems for detoxification (Averill-Bates and Przybytkowski, 1994; Ahmad et al., 2005). The stress response pathways changed in the current study carried out *in vivo* corresponds largely with those identified in cell culture based studies (Ahmad et al., 2005; Coleman et al., 2008; Owada et al., 2013).

There is also the question as to whether proteins found changed in response to 2DG are also changed in response to other stressors. Based on the literature, it would seem that the stress response on a molecular level is an evolutionarily conserved process even with regard to different cell types, tissues and species (Kultz, 2003). There exists a minimal stress response proteome of 44 proteins conserved between all organisms (Kultz, 2005; Wang et al., 2009). Fourteen of the 44 directly match proteins from the list of Cohort 1 differentially expressed

proteins. This begs the question of why so few from this conserved proteome are unchanged in the adrenal medulla. A possible answer is proffered by Kültz (2005) in that cells exposed to chronic stress already express several stress proteins at high levels. Kültz also suggests that some of the 44 are elements of basic metabolic pathways such as glycolysis and the tricarboxylic acid (TCA) cycle, and thus are present even in the absence of stress. These conserved stress proteins suggests that though many proteins in the adrenal medulla may have changed in response to 2DG, there will be a subset of proteins that will change in response to any stressor (Wang et al., 2009).

4.4.2 Impact of animal age on protein expression

When analysing the initial data set the first heat map revealed a clustering discrepancy showing consistency between 50min and 8hr but differences with the other time points. These two time points were added late in the experimental design and the only available rats were younger by several weeks and weighed approximately half that of the rats in Cohort 1. We tentatively suggest that this is the most probable cause for the unusual protein clustering pattern. While it could be argued that those protein expression patterns could indeed be due to the 2DG, it makes little sense that protein expression at 24hr would be more closely related to the control than 50min. However there are more feasible explanations for this anomaly. Previous studies have shown that the age of rats affects their response to stress (Gomez et al., 2002; Gomez et al., 2004). Rats begin puberty at 6 weeks of age which lasts up to 10 weeks of age (Gomez et al., 2004). As the rats in Cohort 2 were between 7-8 weeks of age, the physiological changes male rats endure during puberty are likely to have influenced the observed difference between cohorts. Testosterone exerts an inhibitory effect on the hypothalamic pituitary adrenal axis (HPA axis) which regulates activity of the adrenal gland (Viau, 2002). An alternate or additional explanation could be that glucose uptake is affected by age (Borst and Snellen, 2001). In this study they showed that a range of muscle types absorbed glucose between 40-70% less in older rats (~14 weeks) when compared to younger rats (~7 weeks). Another study tracking glucose uptake against age further demonstrated that at 8 weeks the glucose uptake was at its greatest while at 16 weeks it had decreased dramatically (Goodman et al., 1983). Such data suggests that the effective glucose time course following 2DG would be different which alter the protein response in the younger rats compared to the older animals used in the present study. Therefore the data obtained from Cohort 2 was not analysed together with Cohort 1 despite interesting and functionally relevant proteins also seen to be changed at these time points. However, independent analysis of the

changes between 50 min and 8 hr yielded independent time course data for key proteins involved in the catecholamine synthesis pathway including Th and dopamine beta hydroxylase (Dbh).

4.4.3 Protein profiling

Though there are many methods available for protein profiling and quantitation, shotgun proteomics was deemed the most appropriate method for this experiment. Shotgun proteomics is a popular mass spectrometry (MS) based method for discovering and quantifying the maximal number of proteins in a sample (Patterson and Aebersold, 2003). Although several types of MS systems exist, one commonly used for shotgun proteomics is liquid chromatography tandem MS (LC-MS/MS) (Hu et al., 2007). LC-MS/MS is a method of achieving protein profiling quickly, inexpensively and *en masse*, hence its use in this experiment.

The adrenal samples were analysed label free despite the availability of several labelling techniques that can be applied to MS for greater sensitivity. Isobaric tags for relative and absolute quantitation (iTRAQ) is technique that could have been used as it is used with shotgun proteomics to study quantitative changes in the proteome between several different samples in a single experiment (Aggarwal et al., 2006). Labelling enables multiple sample processing in the one run, allowing differently treated samples to be visualised at the same time. This may have been useful in this experiment particularly with respect to the different time points, however there is a limit to the number of samples that can be analysed in a single MS run as well as the types of samples to which labelling can be applied (Neilson et al., 2011). Whether greater sensitivity would have resulted is unclear as the preparation process to label samples can cause proteins to be lost (Wang et al., 2012). There is also the expense of isotope labels and software required to be considered, rendering its use unfeasible for this project.

Despite the benefits of MS there are also several short comings that may have hampered identification of the proteome of the adrenal medulla. There is a lack of knowledge on the exact mechanisms of ESI (Knochenmuss, 2006), which hinders further advancements in optimizing sample analysis. Ionization may cause difficulties in identification of isoforms and posttranslational modifications of proteins can be lost unless enriched for (Bruce et al., 2013). In order to identify posttranslational modifications certain enrichment procedures need to be considered such as the inactivation of enzymes responsible for interfering with the PTM

of interest (Olsen and Mann, 2013). Though a large number of proteins were identified and quantified how many have been missed is currently unknown. As previously mentioned, measurement of low abundance proteins in a complex mixture has always proved challenging due to instrument sensitivity and small sample volume (Wienkoop and Weckwerth, 2006) so these may have been missed in the present study. Two options can be used to minimise this; sample enrichment or a procedure called nano-liquid chromatography (nano-LC). The latter was utilised in this study. Nano-LC improves ionization efficiency and subsequently sensitivity (Gaspari and Cuda, 2011; Liu et al., 2014). Reproducibility has been a limitation of Shotgun proteomics. MS/MS has limited quantification capabilities on large sample sets because of random, often irreproducible ion selection in phase I (Baldwin, 2004). However, this was accounted in the present study for by selection of only non-redundant, biologically reproducible proteins. Enriching samples to isolate membrane proteins or posttranslational modifications would be the next step in profiling the adrenomedullary proteome (Hu et al., 2007). However, label free shotgun proteomics has still provided a large list of reproducible, functionally relevant proteins despite sensitivity limitations and contributes at least a proportion of the proteome of the adrenal medulla.

4.4.4 Western blot and IHC validation

In order to explore the validation of MS data, several proteins were selected based on their function, expression at multiple time points and high fold change (for at least one time point) for Western blot analysis.

Tyrosine hydroxylase (Th) was selected for its role in catecholamine synthesis and consequent presence in all chromaffin cells of the adrenal medulla. It was found to be expressed more than two fold higher compared to both control and 20 min by MS analysis 24 hr after 2DG. Western blot analysis revealed a very similar time dependent profile and fold change. Both these changes were also confirmed using the 50 min and 8 hr data set suggesting that Th protein is upregulated as early as 8 hr post stimulus. These data suggest that MS data is well validated by Western blot analysis. Th is a well studied protein of the adrenal medulla (Dunkley et al., 2004). Previous studies also confirm that at 24 hr post 2DG Th protein is more highly expressed and to a similar extent (Bobrovska et al) suggesting that longer term transcriptional regulation takes over from short term phosphorylation evidence at 30 min post 2DG which increases the activity of the Th (Dunkley et al., 2004). Not surprisingly the peptide abundance of Th was high in each sample. However this was not the case for all highly abundant proteins. NSF was down regulated following 2DG with a fold change greater

than 2 and a high peptide count but the Western blot analysis did not match the MS data. On the other hand, although an early increase in *Ide* which showed lower peptide abundance identified in MS data was not matched by Western blot analysis the reduction at time points thereafter was matched. In contrast the down regulation in *Rmdn3* by MS with a very low peptide count was not reflected at all by Western blot analysis. It has been shown in 2D-gels that low abundance proteins are not well visualised (Gygi et al., 2000), which could explain these results. Additionally, antibody specificity may have also played a role. This is particularly a problem when a protein is present in different isoforms, such as splice variants and these may not all be detected by the antibodies used or alternatively antibodies identify multiple proteins. *Dbh*, is a relatively high abundance protein but Western blot results were incongruent with findings in MS data. Nevertheless *Dbh* is well known to be modified by stress (Kvetnansky et al., 2009) which supports the MS findings. Although often used to quantify proteins the team that developed the Western blot technique state that it is not intended as a quantitative technique (Towbin et al., 1979). Though tools have since been created to quantify proteins transferred to the nitrocellulose membrane (Aldridge et al., 2008; Wu et al., 2012; Gürtler et al., 2013), there is still no finite way to ensure total protein quantity.

There is an argument that Western blotting is obsolete for MS validation, particularly when compared to selected reaction monitoring (SRM) (Aebersold et al., 2013). SRM is a more targeted version of MS and is billed as a shotgun proteomics validation technique. Unlike Western blot analysis, SRM is capable of not only confirming the presence of a selected protein but is able to precisely quantify hundreds of peptides per run (Kuhn et al., 2004). However, both techniques have to rely on previously established factors for accuracy. Western blot analysis is reliant on antibody specificity, whereas SRM is dependant on known and tested peptides of a certain length that are compatible with MS (Picotti and Aebersold, 2012). So while Western blot analysis is the “gold standard” for verification the presence of a protein, in terms of quantification, SRM seems the more accurate technique (Aebersold et al., 2013). From data generated by the present study at least it seems that MS data cannot always be validated using Western blotting. These findings contribute to the current debate on whether or not Western blot is capable of accurately validating MS data (Aebersold et al., 2013).

Despite several attempts to visualise the location of proteins used in the western blot analysis within the adrenal medulla, our study was only able to confirm the previously studied expression of Th, c-Fos (Parker et al., 2013) and VaChT. As this was formalin fixed tissue, antigen retrieval was necessary, however the lack of specific staining of the majority of the antibodies suggests that samples need to be incubated in ethanol for a longer period. Another possible reason for the lack of staining could be that some of the adrenal glands used were saline-treated and therefore some proteins may not have been sufficiently highly expressed to be detected.

4.5 Cellular processes and changes in response to 2DG

The MS data revealed changes to many cellular processes over time in response to 2DG. The differentially expressed proteins found in this study for the most part fit into well defined processes and pathways that are involved in the response of the adrenal medulla to a hypoglycemic stimulus as described by the literature (see below) (Aunis and Langley, 1999; Dunkley et al., 2004; Kvetnansky et al., 2009). Protein changes can also be related to oxidative stress response, as this is one of the major localised side effects of 2DG. Proteins identified to be altered by 2DG participate in processes of the adrenal medulla that have described by previous studies. This aids in confirming that the proteins identified by MS likely play a role in these processes.

4.5.1 Metabolic processes

Metabolic processes is the most broadly defined category of protein function. This refers to the tricarboxylic acid cycle, mitochondrial oxidative phosphorylation, lipid oxidation, glucose, pyruvate and inositol metabolisms.

The tricarboxylic acid (TCA) cycle is responsible for driving energy production within cells and is heavily reliant on pyruvate, the end product of glycolysis which begins with glucose. Pyruvate is decarboxylated to acetyl-CoA for entry to the TCA cycle (Coleman et al., 2008). Another source of acetyl-CoA is by fatty acid beta oxidation. The acetyl-CoA is consumed with water, reducing NAD⁺ to produce NADH. The NADH is then utilised in mitochondrial oxidative phosphorylation, finally resulting in the formation of ATP (Fennie et al., 2004). In addition to the glycolysis pathway, an alternate route is available for pyruvate synthesis; the hydroxyproline pathway (Adams and Frank, 1980; Wu et al., 2011). Hydroxyproline is

degraded to glyoxylate and pyruvate by the enzyme 4-hydroxy-2-oxoglutarate aldolase (Riedel et al., 2011).

Normal TCA cycle and oxidative phosphorylation are hampered under stress such as produced by 2DG. For example when exposed to high levels of H₂O₂ key enzymes in the cycle including, succinate dehydrogenase, alpha-ketoglutarate dehydrogenase and most of all aconitase are inhibited (Tretter and Adam-Vizi, 2000). However, Tretter and Adam-Vizi (2000) also state that while multiple enzymes are affected, only alpha-ketoglutarate dehydrogenase limits the amount of NADH production in the TCA cycle. Isocitrate dehydrogenase is yet another enzyme in this pathway that can be affected (Stueland et al., 1988). Because glucose is such a key molecule, its inhibition greatly affects the TCA cycle. Though there are alternate pathways for glucose metabolism, 2DG will inhibit them because it is phosphorylated by hexokinase to 2-deoxyglucose 6-phosphate (2DG6P) which hampers entry in these pathways (Cramer and Woodward, 1952). Therefore pyruvate synthesis by regular or anaerobic glycolysis would be inhibited (Nirenberg and Hogg, 1958).

Despite the inhibitory effects of 2DG on glucose reliant metabolic pathways, there remains an alternate source available for pyruvate synthesis; hydroxyproline (Riedel et al., 2011). In the present study 4-hydroxy-2-oxoglutarate aldolase (Hoga1), the enzyme that catalyses this reaction was upregulated (>3 fold) at 4hr. Another enzyme that produces pyruvate as a by product is mitochondrial malic enzyme 2 (Me2). Found to be upregulated (>3 fold) across 20min and 4hrs, Me2 is a malate degrading enzyme and may act as an alternate supply of pyruvate to increase TCA cycle activity when glucose levels are limited (Guay et al., 2007; Ren et al., 2014).

In the present study many key proteins in the TCA cycle were downregulated over multiple time points including succinate dehydrogenase, aconitase, malate dehydrogenase and even isocitrate dehydrogenase, a protein that was differentially expressed over time. These effects could be due to indirect 2DG inhibition of pyruvate synthesis. However, as previously stated, the TCA cycle can continue to produce NADH despite the changes to these proteins (Tretter and Adam-Vizi, 2000). However, the flow-on effects of these changes can be seen in other mitochondrial proteins. An interesting progression in the oxidative phosphorylation pathway is the changes in protein ATP synthase, H⁺ transporting, mitochondrial Fo complex, subunit D (Atp5h). This protein is a subunit in the mitochondrial H⁺ transporter complex V, involved

in ATP synthesis. At 20min the protein was downregulated however, at 4hr it was upregulated. Conversely a co-subunit, Atp5g1, was downregulated at 4hr. Oxidative stress can reduce the activity of this complex (Mastrocola et al., 2005), however, it has yet to be elucidated why one subunit is upregulated and the other down regulated at the same time. Differentially expressed proteins involved in mitochondrial complex I are downregulated across all time points to varying degrees as complex I has been shown to be inhibited by nitric oxide (Brown and Borutaite, 2004), a compound produced during hypoglycemia (Fioramonti et al., 2010). It appears that 2DG has impeded the TCA cycle by blocking glucose utilisation and over time the cell is finding alternate sources of pyruvate and other metabolites to maintain functionality.

4.5.2 Signalling

Signalling is an all important process in any type of cell, mediating responses to stimuli.

A wide variety of cellular signalling pathways can be induced in response to external stimuli, inducing activation of signalling molecules such as protein tyrosine kinases (PTKs), serine/threonine kinases, phospholipases and Ca^{2+} (Kamata and Hirata, 1999).

A crucial signalling pathway to the adrenal medulla is the glucocorticoid pathway (Hodel, 2001). Secreted by the adrenal cortex, glucocorticoids are a class of steroid hormones that exert various effects on medullary chromaffin cells. One such effect is the modulation of gene expression via activation of glucocorticoid receptors that act as transcription factors and either up or downregulate mRNA synthesis, specifically that of phenylethanolamine N-methyltransferase (PNMT) (Ross et al., 1990) which catalyses the last step in catecholamine synthesis which is the conversion of noradrenaline to adrenaline. This enzyme can also be influenced by adrenocorticotrophic hormone (ACTH) produced by activation of the HPA axis (Wurtman, 2002). Another signalling cascade that is important to adrenomedullary response to glucoprivation is the activation of the Rho/Rab GTPase signalling pathway. These GTPases play a fundamental role in the regulation of membrane and intracellular traffic, exocytosis and endocytosis (Van Aelst and D'Souza-Schorey, 1997; Gasman et al., 1999; Hutagalung and Novick, 2011). Rab proteins act as molecular “switches” to regulate vesicle formation, transport, tethering, and fusion between organelles (Hutagalung and Novick, 2011). Inflammatory mediated signalling has also been associated with 2DG-induced endoplasmic reticulum stress (Yu and Kim, 2010).

2DG administration elicits increased plasma glucocorticoid and progesterone steroid levels (Elman and Breier, 1997; Damanhuri et al., 2012). This may explain the upregulation of progesterone receptors at time points 4 and 24hr after 2DG. A protein involved in the preliminary phase of catecholamine synthesis is downregulated at 4hr. Sepiapterin reductase (Spr) is the enzyme that catalyzes the final step of the synthesis of tetrahydrobiopterin (Bh4), which is the reduced pteridine cofactor for pteridine-requiring enzymes such as tyrosine hydroxylase (Th) (Nagatsu and Ichinose, 1999; Ikemoto et al., 2002) the rate limiting enzyme in catecholamine synthesis (Levine et al., 1990). Th is upregulated at 24hr as shown both in the present study and previously (Bobrovskaya et al. (2010). Another indispensable steroid related protein that was changed with respect to time was steroidogenic acute regulatory protein (Star), which converts cholesterol to prenenolone (the precursor to glucocorticoids). This protein is known to be the rate limiting factor in normal adrenal steroidogenesis (Lin et al., 1995). The presence of this protein suggests that there may have been contamination of the adrenal cortex when the medulla was dissected, though this is unlikely.

The activity of the Rho/Rab GTPase superfamily is downregulated at 20min and upregulated at 4hr. Rho GTPase proteins Nme1, Nme2 are involved in endocytosis (Boissan et al., 2014) and are down regulated at 20min. This may be related to redirected energy requirements to support exocytosis of adrenaline thereby forgoing any endocytotic processes. Rab5c and Rab3b proteins which are upregulated at 4hr play a similar role (Chiariello et al., 1999). It has been suggested that phosphorylated isoforms could specifically modulate their function and these isoforms show a conserved consensus site for serine/threonine phosphorylation (Chiariello et al., 1999). Ppp1cc, a protein also upregulated at 4hr is the catalytic component of a serine/threonine protein phosphatase responsible for dephosphorylation or inactivation of proteins (Chen et al., 2009). Precisely what functions these cells are driving in response to 2DG is unclear however the GTPase family of proteins are part of a larger signalling cascade whose end function is involved in cytoskeletal remodelling and could therefore be classed alternatively in the cellular remodelling process as well (see below). Several inflammatory damage inhibitory proteins are upregulated at multiple time points such as annexin 5 and platelet-activating factor acetylhydrolase 1B2b. While at first there seems to be a minimal signalling response to 2DG administration, the glucocorticoid signalling system and inflammatory mediation systems become activated. The sustained response leads to the need for further Th production to replenish the stores.

4.5.3 Cytoskeletal changes

Cellular remodelling was categorised into 3 primary functions; cytoskeletal remodelling, intracellular movement and cell-cell adhesion. Cytoskeletal remodelling refers to the changes in the actin and myosin structures comprising the cytoskeleton in response to cell activity or stress. Though the microtubules are technically considered part of the cytoskeleton, these structures facilitate intracellular movement (Berberian et al., 2009). Intracellular movement is classified as movement of vesicles or organelles around the inside of the cell. Microfilaments and microtubules are formed by the polymerisation of actin filaments and tubulin respectively, causing them to fuse (Stradal and Scita, 2006).

Cytoskeletal processes are of particular importance regarding catecholamine vesicle release from chromaffin cells of the adrenal medulla. The structural mechanisms for vesicle release have been well documented (Vitale et al., 1995; Trifaró et al., 2008). F-actin, a cytoskeletal protein, acts as an actin barrier at the cortical surface to both cage secretory vesicles and prevent direct vesicle access to the plasma membrane (Burgoyne and Cheek, 1987). It is within the dynamic F-actin framework that readily-releasable vesicles are caged near the plasma membrane (Oheim and Stühmer, 2000). This network is disassembled by Ca^{2+} sensitive actin severing protein, scinderin (Vitale et al., 1991) allowing for vesicle release. In order to replace vesicles released from these cages, dense core vesicles need to be transported to the cortical surface. It has been shown that vesicle transport to the cortical surface for replenishment of these ready-release vesicles is assisted by actin and tubulin microfilaments/tubules. In a study by Maucort et al. (2014) it was found that readily-releasable vesicles were replaced by vesicles from further inside the cell. This movement is accomplished by actin and tubulin microfilaments/tubules as application of respective polymerization inhibitors to the cells showed no change in vesicle activity even when stimulated. This is widely accepted as the means for vesicle trafficking in chromaffin cells (Schliwa, 1999; Trifaró et al., 2008; Berberian et al., 2009) and myosin II has been implicated in facilitating this (Ñeco et al., 2004). However, attempts to identify other potential proteins involved in this system have not been previously explored.

In the present study major changes to proteins related to cytoskeletal remodelling were identified. Several cellular remodelling proteins were upregulated across time points, some significantly changed with respect to multiple time points. One such is F-actin-capping protein (Capza2) which was upregulated. This prevents further actin filament binding at the

cortical surface. This protein is also part of the dynactin complex (Schroer, 2004). This complex, along with other interactions, binds vesicles for microtubule transport over long distances. Actr3, a protein initially chosen for Western blot validation, is key member of the Arp2/3 complex. Billed as cytoskeletal remodelling proteins, Actr3 and its constituents, including Actr2 and Arpc5l, form the Arp2/3 complex which promotes actin nucleation and polymerisation (Rohatgi et al. 1999). As a result these remodelling proteins aid in the formation of microtubules that could be responsible for vesicle trafficking to the plasma membrane. Additionally, a portion of the Arp2/3 complex is associated with secretory granules, supposedly accompanying granules to docking sites at the plasma membrane upon cell activation (Trifaró et al., 2008). In addition to these trafficking proteins, tubulin proteins were also upregulated (Tubb4b, Tubb5). Based on the effect of the tubulin polymerisation inhibitor in Maucort's study (2014), it is possible that these proteins could be involved in vesicle movement. Myoferlin, a downregulated protein at 4hr, promotes rapid resealing of membranes disrupted by mechanical stress such as during endo/exocytosis (Leung et al., 2013). This raises the question as to why it would be downregulated after a protracted period exocytosis, which requires further investigation. These results for the first time define a list of proteins that are likely involved in cytoskeletal remodelling with respect to adrenaline secretion from chromaffin cells following 2DG activation as defined by c-Fos immunoreactivity.

4.5.4 Transport

Transport is defined here as the means of moving a substance, molecule or ion between locations. These processes can be facilitated by vesicle mediated transport, solute carriers/transmembrane transporters.

Vesicle mediated transport encompasses intracellular movement between organelles and the plasma membrane. A well documented vesicular transport pathway is that which exists between endoplasmic reticulum and the Golgi complex (Alberts et al., 2002). Vesicles leave the rough endoplasmic reticulum and are transported to the Golgi complex where they fuse with the Golgi membrane, emptying their contents into the lumen. Here, proteins are modified and sorted prior to further transport. Proteins leaving the Golgi complex first navigate a complex network of membranes and associated vesicles known as the trans-Golgi network (TGN). Proteins are sorted and placed into one of at least three different types of vesicles, depending upon their molecular marker (secretory, endosomal or lysosomal) before

being shipped to their intended destinations (Griffiths and Simons, 1986). The secretory vesicles that emerge from the TGN destined for the plasma membrane are actually large polymorphic structures unable to readily move toward their destination. This is an instance where microtubule dynamics would transport the larger molecules (Toomre et al., 1999). This whole process is assisted by components of the SNARE complex. SNARE proteins have two main functions; those which are anchored in the membrane of a transport vesicle (v-SNAREs) and those anchored in the target membrane (t-SNAREs) (Rothman and Warren, 1994). The primary role of SNARE proteins is to mediate vesicle fusion between the transport vesicles and the cell membrane or an intracellular target compartment (such as a lysosome) (Chen and Scheller, 2001). Different intracellular transport steps are thought to be facilitated by different SNARE family proteins (Fasshauer, 2003).

Transport within the chromaffin cells is extremely important, especially in terms of vesicle mediated transport. Intracellular transport via the SNARE complex are known to be disrupted by hypoglycemia and the resultant oxidative stress. The lack of useable glucose impedes ATP production, an important compound for vesicle trafficking towards the plasma membrane and docking of vesicles for release (Parsons et al., 1995). Reactive oxygen species produced by oxidative stress inhibit the formation of SNARE protein complexes and subsequently inhibit the final steps in vesicle fusion. Oxidative stress may also reduce the degree of SNARE protein availability and possibly functionality (Keating, 2008).

In the present study many proteins comprising various aspects of the SNARE complex were changed across time points, primarily at 4hr after 2DG. An important protein that is upregulated at both 4 and 24hr is vesicle amine transporter 1 (Vat1) which allows the transport of acetylcholine with the assistance of the vesicular acetylcholine transporter VaChT (Eiden et al., 2004). The presence of the latter was confirmed using immunohistochemistry and it is clear that this protein plays a role in adrenomedullary activation as, as describe above, cholinergic fibres innervate the chromaffin cells and are activated by 2DG (Morrison and Cao, 2000). Yet another neuronal related protein, N-ethylmaleimide-sensitive factor (Nsf) is a key protein in synaptic vesicle docking (Tolar and Pallanck, 1998). Also an important protein in Golgi vesicle transport, Nsf (Wilson et al., 1989) is one of the key SNAP proteins that comprise the main SNARE complex. Specific cysteine residues in SNAP-25 are required for SNARE disassembly and exocytosis, but not for membrane targeting. As cysteine residues are commonly affected by redox state, crucial alterations in SNAP-25

structure may underlie the lack of SNARE complex assembly and reduced exocytosis seen in motor nerve endings during conditions of oxidative stress (Keating, 2008). Another interesting SNARE protein associated with the endoplasmic reticulum that was upregulated at 4hr and initially chosen for Western blot analysis is vesicle-associated membrane protein-associated protein B (Vapb). However, this SNARE protein is also responsible for endoplasmic reticulum-mitochondria membrane fusion (Csordás et al., 2006). The corresponding mitochondrial protein is regulator of microtubule dynamics protein 3 (Rmdn3). Together they facilitate calcium exchange between these organelles (Stoica et al., 2014).

It is unclear why some transport proteins are downregulated while others are upregulated. Each plays a specific function in vesicular transport, however the impact of 2DG/hypoglycemia on each individual SNARE processes could not be clearly elucidated and requires further work perhaps by including analysis of vesicle membrane associated proteins.

4.5.5 Stress response

An organism's response to stress will dictate the damage done by the stressor. Stress typically results in deformation of, or damage to proteins and other molecules. Therefore, pathways that mitigate oxidative stress damage will be activated (Kültz, 2005). Some of these evolutionarily conserved pathways are the pentose phosphate pathway, glutathione redox pathway, thioredoxin and the peroxiredoxin pathways. All of these pathways are interlinked (Ahmad et al., 2005).

Beginning with the pentose phosphate pathway, it consists of an oxidative and a non-oxidative phase. When the cell is functioning under normal conditions the oxidative phase is active, providing glucose oxidation in parallel to glycolysis as well as NADPH production (Kruger and von Schaewen, 2003). The non-oxidative phase produces appropriate levels of ribose 5-phosphate and erythrose 4-phosphate, precursors of purines and aromatic amino acids, respectively (Juhnke et al., 1996). The oxidative pentose phosphate pathway provides the glutathione reductase with NADPH in order to reduce glutathione (Averill-Bates and Przybytkowski, 1994), thus beginning the glutathione redox pathway. The NADPH can be used to reduce oxidized glutathione; glutathione disulfide (GSSH) to its reduced form; glutathione (GSH), a process catalysed by a NADPH-dependent glutathione reductase (Juhnke et al., 1996). Under oxidative stress conditions glutathione disulfide is found in larger quantities compared to its reduced form which is generated by antioxidant enzymes

(glutathione peroxidases and peroxiredoxins) during the reduction of peroxides such as hydrogen peroxide (H_2O_2) (Adams et al., 1983; Meister, 1988). Thioredoxin is reduced by the NADPH-dependent thioredoxin reductase (Juhnke et al., 1996) as well as thioredoxin peroxidase (Coleman et al., 2008). Thioredoxin can also react with glutathione disulfide under oxidative stress conditions (Casagrande et al., 2002). Finally, in addition to being a substrate for energy metabolism via the tricarboxylic acid cycle and mitochondrial oxidative phosphorylation, pyruvate acts as a scavenger for hydrogen peroxide (Nath et al., 1995). All these pathways are governed at least in part by NADPH (Averill-Bates and Przybytkowski, 1994).

In the present study following 2DG administration, pathways utilizing phosphorylated glucose (G6P) were blocked. The production of NADPH via the pentose phosphate pathway is reliant on glucose oxidation. As 2DG interferes with glycolysis and the pentose phosphate pathway, NADPH will not be produced in adequate quantities (Downs et al., 1998). Averill-Bates and Przybytkowski (1994) showed that damage done by H_2O_2 was mitigated by the pentose phosphate pathway only in the presence of glucose. Cells they deprived of glucose suffered cytotoxicity due to a malfunctioning pentose phosphate pathway. A study by Downs et al. (1998) used 2DG to demonstrate a similar effect on the pentose phosphate pathway. Therefore glucose is an essential molecule in cellular protection against cytotoxic stress (Ahmad et al., 2005).

Due to the fact that glucose deprivation creates a sharp decline in the availability of NADPH, glutathione peroxidases lack the required H^+ to decompose H_2O_2 (Ahmad et al., 2005). It is possible that the downregulation of glutathione peroxidases seen at 20min in the present study is the result of NADPH unavailability. However, the glutathione S-transferases were upregulated at 4hr. These enzymes also act on peroxide degradation and catalyse the reaction between GSH and xenobiotics (Strange et al., 2001). This could be a potential mechanism by which 2DG is cleared from the cell. Additionally, glutathione S-transferases require a steady supply of GSH (Pemble et al., 1994). An increase in these enzymes could therefore suggest that GSSH is in lower quantities and therefore that cellular stress is reduced (Meister, 1988). At 24hr a number of stress related proteins were downregulated, including peroxiredoxin, thioredoxin reductase and transketolase, a key protein in the pentose phosphate pathway (Juhnke et al., 1996). This most likely indicates that the stress response is diminished and the cell is returning to a more stable condition.

Why would stress proteins be downregulated compared to the control? It is possible that because rats at 24hr were given more time in the laboratory to adjust to their new environment and so the control rats, only having 16hr to acclimate were exhibiting higher levels of stress. Alternatively it is possible that in response to stress there is an overshoot rather than a return to stable baseline. It must be remembered that some stress proteins are always present in cells that undergo a constant steady state of stress under normal cellular conditions (Kültz, 2005).

Though it is already known that 2DG elicits oxidative stress response, the time in which the various mechanisms within the process respond is heavily reliant on the availability of glucose. Until more glucose becomes available as 2DG is metabolised, typical stress response proteins will be affected.

4.5.6 Protein synthesis

Protein synthesis refers to the processes of transcription and translation of new proteins. Before transcription can be achieved, the nucleosomes that block access to the DNA must be moved. This is done by the use of histone chaperones; non-nucleosomal histones H2A–H2B and H3–H4 (Dennehey and Tyler, 2014). These histones are also responsible for the nucleosome reassembly. After the required DNA section has been unravelled, transcription can commence. The process of transcription initiation and elongation lasts approximately 30min (Larson et al., 2011). Once the gene is transcribed into pre-mRNA with the use of RNA polymerase, it then undergoes splicing to remove exons. This is accomplished by a large, multi-protein complex called the spliceosome (Will and Lührmann, 2011).

The mRNA is now ready for translation into an amino acid chain. There are three phases of translation; initiation, elongation and termination. In the initiation phase the ribosome assembles around the mRNA. The two ribosomal subunits surrounding the mRNA are each comprised of many proteins, the smaller of which acts as a translation initiator (Schlunzen et al., 2000), while the larger acts as a ribozyme, catalysing peptide bond formation (Nissen et al., 2000). This ribosome facilitates decoding by inducing the binding of complementary tRNA anticodon sequences to mRNA codons. This is the elongation phase. The tRNA carry specific amino acids that are chained together as the ribosome moves along the mRNA. A stop codon is finally reached, signalling termination of translation (Kisselev et al., 2003). Afterwards the amino acid chain is folded into a functional protein.

A large number of transcription factors including c-Fos are upregulated in response to oxidative stress (Abate et al., 1990). Transcription factors initiate transcription of specific genes, many of which have been identified with respect to oxidative stress (Allen and Tresini, 2000). Certain translation factors can also be affected by stress. For example, phosphorylation of eukaryotic translation initiation factor 2a (Eif2a) can inhibit mRNA translation (Jousse et al., 2003).

There is a pattern of change across time regarding some such proteins identified in the present study. At 20min there is an upregulation of histone-nucleosome related proteins. Part of the FACT complex which facilitates chromatin transcription, suppressor of Ty 16 homolog (Supt16h) interacts specifically with histones H2A–H2B to assist in nucleosome disassembly and thereby transcription elongation (Kari et al., 2011). FACT is composed of 2 subunits one of which is Supt16h (Orphanides et al., 1999). This protein was upregulated at 20min and 24hr suggesting that transcription initiation is being facilitated.

A pattern of translation protein expression was also modified by 2DG. Translation related proteins were downregulated at 20min while at 4hr there was a sharp increase in translation initiation and elongation factors which was also seen at 24hr. The decrease at 20 min is most likely associated with the reduction in availability of energy of the cell due to the reduction in glycolysis due to 2DG. Changes to the translator ribosome were also observed. The large ribosomal subunit is composed of many proteins changed. At 20min some at least are downregulated with an increase in expression with time, however the change to all differentially expressed ribosomal proteins was neither uniformly up nor down. A possible reason for these seemingly sporadic changes is that the ribosome subunit assembly is a complex, multi-step process in which not all the components assemble simultaneously due to the variation in kinetics for different ribosomal proteins (Andersen et al., 2005).

Overall the findings of the present study define the protein synthetic changes which are likely controlled by energy reduction early after 2DG but reflect proteins required at later time points in response to adrenaline secretion and replenishment.

4.5.7 Proteolysis

Proteolysis is the process by which proteins are broken down into smaller polypeptides or amino acid constituents. Several types exist including posttranslational proteolysis, usually

converting an inactive peptide to its active form (Walsh, 2002). Another type of proteolysis is protein degradation wherein proteins are digested down to their amino acids by the lysosome or proteasome. Ubiquitination is an important step in proteasomal protein degradation. Proteins degraded by the proteasome are tagged by covalent attachment of ubiquitin chains, allowing recognition by the proteasome (Hershko, 1998; Voges et al., 1999). Proteolysis is also involved in cellular regulation by activating or deactivating enzymes, transcription factors, and receptors, usually in response to environmental change (Hochstrasser, 1995). Gottesman and Maurizi (1992) coined the term "timing proteins", referring to proteins required for limited periods or under specific metabolic or developmental conditions but are otherwise unnecessary at other times or under other conditions. Once these proteins have executed their respective functions they are degraded. It has been suggested that selective degradation of proteins can also replenish the amino acid pool for production of more functionally relevant proteins (Berghoff et al., 2013).

Under stressful conditions such as hypoglycemia proteins are prone to oxidative damage (Patocková et al., 2002). In order to clear these damaged proteins, proteolytic proteins are upregulated, usually those involved in the proteasomal and lysosomal pathways (Davies, 2005). Another factor influencing protein regulation is the availability of ATP during hypoglycemia. The ubiquitin-proteasome system is dependent on ATP for ubiquitination of proteins (Ouyang and Hu, 2001). Therefore, the reduced glycolysis and TCA cycle activity as in the presence of 2DG could impede ubiquitination of proteins targeted for degradation.

Early in the response to 2DG, several proteolytic proteins are upregulated. A protein involved in "timing protein" recycling, proline, is upregulated at 20min. This protein is responsible for protein degradation to the amino acid form of proline, possibly for collagen resynthesis (Yaron et al., 1993; Surazynski et al., 2008). The expression of a regulatory protein is increased at this time; high-temperature requirement protease A (HtrA). This protein is responsible for multiple cellular functions, including protein quality control, thereby disposing of proteins damaged by stress (Singh et al., 2014). One of the most interesting proteases upregulated at 20min is insulin degrading enzyme (Ide). As the name implies, Ide is a metalloprotease that breaks down insulin and is therefore key in regulating blood glucose levels (Farris et al., 2003). However, this enzyme is inhibited by glutathione disulfide (GSSH), the oxidised form of glutathione that is produced during cellular stress (Cordes et al., 2011). This could be why it is only observed at the early time point when glutathione

peroxidases are inactive due to the lack of glucose. The downregulation of ubiquitination proteins at 4hr is unlikely due to the hindrance in ATP production but may be associated with the protease inhibitory proteins which are upregulated at this time point.

4.5.8 Summary of processes changed

Many of the proteins found are multifunctional and could easily contribute to more than one functional process in the 2DG response. However, the time and the way in which the protein of interest changed influenced the category into which it was placed based on the literature and what is known about stress response and hypoglycemia in the adrenal medulla. Changes to the cytoskeleton of the adrenal medulla are consistent with the process of vesicle exocytosis and trafficking (Maucort et al., 2014), as are those related to catecholamine synthesis (Bobrovskaya et al., 2010). Based on the tyrosine hydroxylase expression in Bobrovskaya et al. (2010) the 24hr time point was chosen. However, the data show that various proteins in each of the 8 processes are still changing. This begs the question of when the response to 2DG ends, if at all. Does the cell ever reset to control conditions or is there a permanent change to the adrenal medulla proteome?

Many of the changed pathways outlined by the differentially expressed proteins from MS analysis interact in some way and are heavily reliant on glucose metabolism to function effectively. Various by-products of metabolic pathways fuel cellular processes that are important for stress response. However, the lack of glucose adds to the cellular stress, forcing it to find alternate methods of energy metabolism. Glycolysis is necessary for pyruvate production, which is in turn required for acetyl-CoA production (Coleman et al., 2008). If there is no acetyl-CoA available to enter the TCA cycle will not produce NADH as a by-product of substrate reduction. The cessation of NADH production will then negatively impact the ATP synthesis of mitochondrial oxidative phosphorylation (Fennie et al., 2004). Many intracellular processes require ATP to operate. One of these processes is SNARE vesicular transport towards the plasma membrane and docking of vesicles for release (Parsons et al., 1995). ATP is also needed for microtubule formation (Dabora and Sheetz, 1988) which could be why we only see the tubulins upregulated at 4hr instead of at 20min along with the actin polymerisation proteins. Ubiquitin-proteasome system is another system dependent on ATP for ubiquitination of proteins (Ouyang and Hu, 2001). Therefore, the reduced glycolysis and TCA cycle activity due to the presence of 2DG could impede ubiquitination of proteins targeted for degradation.

Another pathway directly affected by lack of usable glucose is the pentose phosphate pathway (Kruger and von Schaewen, 2003), impacting oxidative stress pathways. Thioredoxin is normally reduced by the NADPH-dependent thioredoxin reductase (Juhnke et al., 1996) as well as thioredoxin peroxidase (Coleman et al., 2008). Thioredoxin can also react with glutathione disulfide under oxidative stress conditions (Casagrande et al., 2002). However, the limited NADPH that is normally produced by the phosphate pathway would prevent this despite the conditions of oxidative stress. All these pathways are governed at least in part by NADPH (Averill-Bates and Przybytkowski, 1994). Without glucose normal cellular function and even cellular functioning in response to stress is seriously impeded by the lack of glucose. For a cellular stressor like shear stress, hypoxia or even mild cytotoxicity, the response time would most likely be faster than a cell without glucose to fuel its major damage mitigating pathways.

4.6 Future directions

As with most scientific studies, this one has raised more questions than it has answered. The entire adrenomedullary proteome is yet to be mapped, however with the appropriate purification and enrichment procedures this can be accomplished. As previously mentioned, a method of profiling the entire adrenal proteome would be by single organelle profiling. This could advance not only the knowledge of the adrenomedullary proteome but highlight the localisation of the proteins and possibly their movements between organelles at different times during hypoglycemic response.

With the information gleaned from this study, investigating the molecular changes in the adrenal medulla to insulin-induced acute hypoglycemic episodes could lead to greater understanding of the molecular mechanisms changing in type I diabetics. The failure of pancreatic β -cells in type I diabetics necessitates subcutaneous insulin administration to prevent toxic accumulation of glucose (Cryer and Gerich, 1985; Cryer, 1997). Therefore, in type I diabetics and extreme cases of type II diabetics many of normal counter regulatory responses to hypoglycemia are lost or attenuated. Due to this exogenous delivery of insulin the normal physiological feedback mechanisms are not always triggered, muting an otherwise functional hypoglycemic counter regulatory response (McCrimmon and Sherwin, 2010). As the pancreatic α -cells are also non-functional, glucagon as fails to be released, leaving adrenaline the primary CRR in type I diabetics. However, this too is attenuated and

frequently results in recurrent hypoglycemia. Therefore, the next experiment that could follow would be similar to this study in terms of adrenomedullary MS analysis, however instead of 2DG-induced glucoprivation, inducing hyperinsulinemia in animals that are either partially pancreatectomised or treated with streptozotocin would better mimic the type I diabetic condition.

Another major concern surrounding hypoglycemia in diabetics is hypoglycemic unawareness. This is the absence of the common neurogenic symptoms that would otherwise alert the person to this condition. Hypoglycemia-associated autonomic failure (HAAF) (Cryer, 2004) is the amalgamation of the reduced sympathoadrenal response, dulling neurogenic symptoms and a reduced adrenomedullary response in the absence of glucagon, inhibiting adequate glucose regulation (Sanders and Ritter, 2000). Using the adrenal medulla protein profile obtained in this study, exploration of the effects of impaired glucose regulation on the adrenal glands during recurrent hypoglycemic episodes could be the next step in illuminating possible molecular mechanisms responsible. Alternatively, a similar experiment could be conducted on regions of the brain that have involved in glucose regulation (Verberne and Sartor, 2010; Verberne et al., 2014).

4.7 Conclusion

This study has defined pathways and mechanisms that are changing in the adrenal medulla in response to 2DG-induced glucoprivation. The exact proteins that are involved in previously described processes have been shown to be differentially expressed during an acute hypoglycemic event. The two major responses of the adrenal medulla were the sympathetically innervated release of adrenaline from the chromaffin cells and the second is the localised, cellular response to oxidative stress produced by 2DG. Changes to the structural proteins directly involved in vesicle movement and release over time were identified. This study was able to track the time course of protein changes involved in glucose dependent functions such as ATP production and oxidative stress. A large portion of the adrenal medulla proteome has been mapped.

5.0 References

- Abate, C., Patel, L., Rauscher Iii, F.J., and Curran, T. (1990). Redox regulation of Fos and Jun DNA-binding activity in vitro. *Science* 249, 1157-1161.
- Adams, E., and Frank, L. (1980). Metabolism of proline and the hydroxyprolines. *Annual review of biochemistry* 49, 1005-1061.
- Adams, J., Lauterburg, B., and Mitchell, J. (1983). Plasma glutathione and glutathione disulfide in the rat: regulation and response to oxidative stress. *Journal of Pharmacology and Experimental Therapeutics* 227, 749-754.
- Aebersold, R., Burlingame, A.L., and Bradshaw, R.A. (2013). Western Blots versus Selected Reaction Monitoring Assays: Time to Turn the Tables? *Molecular & Cellular Proteomics* 12, 2381-2382.
- Aggarwal, K., Choe, L.H., and Lee, K.H. (2006). Shotgun proteomics using the iTRAQ isobaric tags. *Briefings in Functional Genomics & Proteomics* 5, 112-120.
- Ahmad, I.M., Aykin-Burns, N., Sim, J.E., Walsh, S.A., Higashikubo, R., Buettner, G.R., Venkataraman, S., Mackey, M.A., Flanagan, S.W., and Oberley, L.W. (2005). Mitochondrial and H₂O₂ Mediate Glucose Deprivation-induced Stress in Human Cancer Cells. *Journal of Biological Chemistry* 280, 4254-4263.
- Alberts, B., Johnson, A., Lewis, J., Walter, P., Raff, M., and Roberts, K. (2002). *Molecular Biology of the Cell 4th Edition: International Student Edition*. Routledge.
- Aldridge, G.M., Podrebarac, D.M., Greenough, W.T., and Weiler, I.J. (2008). The use of total protein stains as loading controls: An alternative to high-abundance single-protein controls in semi-quantitative immunoblotting. *Journal of Neuroscience Methods* 172, 250-254.
- Allen, R.G., and Tresini, M. (2000). Oxidative stress and gene regulation. *Free Radical Biology and Medicine* 28, 463-499.
- Altschul, S.F., Gish, W., Miller, W., Myers, E.W., and Lipman, D.J. (1990). Basic local alignment search tool. *Journal of Molecular Biology* 215, 403-410.
- Andersen, J.S., Lam, Y.W., Leung, A.K., Ong, S.-E., Lyon, C.E., Lamond, A.I., and Mann, M. (2005). Nucleolar proteome dynamics. *Nature* 433, 77-83.
- Aunis, D., and Langley, K. (1999). Physiological aspects of exocytosis in chromaffin cells of the adrenal medulla. *Acta physiologica scandinavica* 167, 89-97.
- Averill-Bates, D.A., and Przybytkowski, E. (1994). The role of glucose in cellular defences against cytotoxicity of hydrogen peroxide in Chinese hamster ovary cells. *Arch Biochem Biophys* 312, 52-58.
- Baldwin, M.A. (2004). Protein Identification by Mass Spectrometry: Issues to be Considered. *Molecular & Cellular Proteomics* 3, 1-9.
- Balfoussia, E., Skenderi, K., Tsironi, M., Anagnostopoulos, A.K., Parthimos, N., Vougas, K., Papassotiriou, I., Tsangaris, G.T., and Chrousos, G.P. (2014). A proteomic study of plasma protein changes under extreme physical stress. *Journal of Proteomics* 98, 1-14.
- Berberian, K., Torres, A.J., Fang, Q., Kisler, K., and Lindau, M. (2009). F-actin and myosin II accelerate catecholamine release from chromaffin granules. *The Journal of Neuroscience* 29, 863-870.
- Berghoff, B.A., Konzer, A., Mank, N.N., Looso, M., Rische, T., Förstner, K.U., Krüger, M., and Klug, G. (2013). Integrative “omics”-approach discovers dynamic and regulatory features of bacterial stress responses. *PLoS genetics* 9, e1003576.
- Bobrovskaya, L., Cheah, T.B., Bunn, S.J., and Dunkley, P.R. (1998). Tyrosine hydroxylase in bovine adrenal chromaffin cells: angiotensin II-stimulated activity and phosphorylation of Ser19, Ser31, and Ser40. *J Neurochem* 70, 2565-2573.
- Bobrovskaya, L., Damanhuri, H.A., Ong, L.K., Schneider, J.J., Dickson, P.W., Dunkley, P.R., and Goodchild, A.K. (2010). Signal transduction pathways and tyrosine hydroxylase

- regulation in the adrenal medulla following glucoprivation: An in vivo analysis. *Neurochemistry International* 57, 162-167.
- Boissan, M., Montagnac, G., Shen, Q., Griparic, L., Guitton, J., Romao, M., Sauvonnet, N., Lagache, T., Lascu, I., Raposo, G., Desbordes, C., Schlattner, U., Lacombe, M.-L., Polo, S., Van Der Blik, A.M., Roux, A., and Chavrier, P. (2014). Nucleoside diphosphate kinases fuel dynamin superfamily proteins with GTP for membrane remodeling. *Science* 344, 1510-1515.
- Borst, S.E., and Snellen, H.G. (2001). Metformin, but not exercise training, increases insulin responsiveness in skeletal muscle of Sprague-Dawley rats. *Life Sci* 69, 1497-1507.
- Breker, M., Gymrek, M., and Schuldiner, M. (2013). A novel single-cell screening platform reveals proteome plasticity during yeast stress responses. *The Journal of Cell Biology* 200, 839-850.
- Brown, G.C., and Borutaite, V. (2004). Inhibition of mitochondrial respiratory complex I by nitric oxide, peroxynitrite and S-nitrosothiols. *Biochimica et Biophysica Acta (BBA) - Bioenergetics* 1658, 44-49.
- Bruce, C., Stone, K., Gulcicek, E., and Williams, K. (2013). Proteomics and the analysis of proteomic data: 2013 overview of current protein-profiling technologies. *Curr. Protoc. Bioinformatics* Ch. 13, Unit 13 21.
- Burgoyne, R.D., and Cheek, T.R. (1987). Role of fodrin in secretion. *Nature* 326, 448-448.
- Casagrande, S., Bonetto, V., Fratelli, M., Gianazza, E., Eberini, I., Massignan, T., Salmona, M., Chang, G., Holmgren, A., and Ghezzi, P. (2002). Glutathionylation of human thioredoxin: A possible crosstalk between the glutathione and thioredoxin systems. *Proceedings of the National Academy of Sciences* 99, 9745-9749.
- Chen, S., Kesler, C.T., Paschal, B.M., and Balk, S.P. (2009). Androgen Receptor Phosphorylation and Activity Are Regulated by an Association with Protein Phosphatase 1. *Journal of Biological Chemistry* 284, 25576-25584.
- Chen, Y.A., and Scheller, R.H. (2001). SNARE-mediated membrane fusion. *Nature Reviews Molecular Cell Biology* 2, 98-106.
- Chiariello, M., Bruni, C.B., and Bucci, C. (1999). The small GTPases Rab5a, Rab5b and Rab5c are differentially phosphorylated in vitro. *FEBS Letters* 453, 20-24.
- Coleman, M.C., Asbury, C.R., Daniels, D., Du, J., Aykin-Burns, N., Smith, B.J., Li, L., Spitz, D.R., and Cullen, J.J. (2008). 2-Deoxy-d-glucose causes cytotoxicity, oxidative stress, and radiosensitization in pancreatic cancer. *Free Radical Biology and Medicine* 44, 322-331.
- Cordes, C.M., Bennett, R.G., Siford, G.L., and Hamel, F.G. (2011). Redox regulation of insulin degradation by insulin-degrading enzyme. *PLoS One* 6, e18138.
- Cramer, F.B., and Woodward, G.E. (1952). 2-Desoxy-D-glucose as an antagonist of glucose in yeast fermentation. *Journal of the Franklin Institute* 253, 354-360.
- Cryer, P.E. (1997). *Hypoglycemia : pathophysiology, diagnosis, and treatment*. New York: Oxford University Press.
- Cryer, P.E. (2004). Diverse Causes of Hypoglycemia-Associated Autonomic Failure in Diabetes. *New England Journal of Medicine* 350, 2272-2279.
- Cryer, P.E. (2005). Mechanisms of Hypoglycemia-Associated Autonomic Failure and Its Component Syndromes in Diabetes. *Diabetes* 54, 3592-3601.
- Cryer, P.E. (2013). Mechanisms of Hypoglycemia-Associated Autonomic Failure in Diabetes. *New England Journal of Medicine* 369, 362-372.
- Cryer, P.E., and Gerich, J.E. (1985). Glucose Counterregulation, Hypoglycemia, and Intensive Insulin Therapy in Diabetes Mellitus. *New England Journal of Medicine* 313, 232-241.

- Csordás, G., Renken, C., Várnai, P., Walter, L., Weaver, D., Buttle, K.F., Balla, T., Mannella, C.A., and Hajnóczky, G. (2006). Structural and functional features and significance of the physical linkage between ER and mitochondria. *The Journal of cell biology* 174, 915-921.
- Dabora, S.L., and Sheetz, M.F. (1988). The microtubule-dependent formation of a tubulovesicular network with characteristics of the ER from cultured cell extracts. *Cell* 54, 27-35.
- Damanhuri, H.A., Burke, P.G.R., Ong, L.K., Bobrovskaya, L., Dickson, P.W., Dunkley, P.R., and Goodchild, A.K. (2012). Tyrosine Hydroxylase Phosphorylation in Catecholaminergic Brain Regions: A Marker of Activation following Acute Hypotension and Glucoprivation. *PLoS ONE* 7, e50535.
- Davies, M.J. (2005). The oxidative environment and protein damage. *Biochimica et Biophysica Acta (BBA) - Proteins and Proteomics* 1703, 93-109.
- Dennehey, B.K., and Tyler, J. (2014). "Histone Chaperones in the Assembly and Disassembly of Chromatin," in *Fundamentals of Chromatin*. Springer), 29-67.
- Derosa, M.A., and Cryer, P.E. (2004). Hypoglycemia and the sympathoadrenal system: neurogenic symptoms are largely the result of sympathetic neural, rather than adrenomedullary, activation. *Am J Physiol Endocrinol Metab* 287, E32-41.
- Downs, S.M., Humpherson, P.G., and Leese, H.J. (1998). Meiotic induction in cumulus cell-enclosed mouse oocytes: involvement of the pentose phosphate pathway. *Biology of reproduction* 58, 1084-1094.
- Dragunow, M., and Faull, R. (1989). The use of c-fos as a metabolic marker in neuronal pathway tracing. *Journal of Neuroscience Methods* 29, 261-265.
- Dun, N.J., Tang, H., Dun, S.L., Huang, R., Dun, E.C., and Wakade, A.R. (1996). Pituitary adenylate cyclase activating polypeptide-immunoreactive sensory neurons innervate rat adrenal medulla. *Brain Research* 716, 11-21.
- Dunkley, P.R., Bobrovskaya, L., Graham, M.E., Von Nagy-Felsobuki, E.I., and Dickson, P.W. (2004). Tyrosine hydroxylase phosphorylation: regulation and consequences. *Journal of Neurochemistry* 91, 1025-1043.
- Egea, J., Rosa, A.O., Cuadrado, A., García, A.G., and López, M.G. (2007). Nicotinic receptor activation by epibatidine induces heme oxygenase-1 and protects chromaffin cells against oxidative stress. *Journal of neurochemistry* 102, 1842-1852.
- Eiden, L., Schäfer, M.H., Weihe, E., and Schütz, B. (2004). The vesicular amine transporter family (SLC18): amine/proton antiporters required for vesicular accumulation and regulated exocytotic secretion of monoamines and acetylcholine. *Pflügers Archiv* 447, 636-640.
- Eisenhofer, G., Huynh, T.-T., Elkahoul, A., Morris, J.C., Bratslavsky, G., Linehan, W.M., Zhuang, Z., Balgley, B.M., Lee, C.S., Mannelli, M., Lenders, J.W.M., Bornstein, S.R., and Pacak, K. (2008). Differential expression of the regulated catecholamine secretory pathway in different hereditary forms of pheochromocytoma. *American Journal of Physiology - Endocrinology and Metabolism* 295, E1223-E1233.
- Elman, I., and Breier, A. (1997). Effects of acute metabolic stress on plasma progesterone and testosterone in male subjects: relationship to pituitary-adrenocortical axis activation. *Life Sci* 61, 1705-1712.
- Farris, W., Mansourian, S., Chang, Y., Lindsley, L., Eckman, E.A., Frosch, M.P., Eckman, C.B., Tanzi, R.E., Selkoe, D.J., and Guénette, S. (2003). Insulin-degrading enzyme regulates the levels of insulin, amyloid β -protein, and the β -amyloid precursor protein intracellular domain in vivo. *Proceedings of the National Academy of Sciences* 100, 4162-4167.

- Fasshauer, D. (2003). Structural insights into the SNARE mechanism. *Biochimica et Biophysica Acta (BBA) - Molecular Cell Research* 1641, 87-97.
- Fernie, A.R., Carrari, F., and Sweetlove, L.J. (2004). Respiratory metabolism: glycolysis, the TCA cycle and mitochondrial electron transport. *Current Opinion in Plant Biology* 7, 254-261.
- Fioramonti, X., Marsollier, N., Song, Z., Fakira, K.A., Patel, R.M., Brown, S., Duparc, T., Pica-Mendez, A., Sanders, N.M., Knauf, C., Valet, P., Mccrimmon, R.J., Beuve, A., Magnan, C., and Routh, V.H. (2010). Ventromedial Hypothalamic Nitric Oxide Production Is Necessary for Hypoglycemia Detection and Counterregulation. *Diabetes* 59, 519-528.
- Francis, H.M., Mirzaei, M., Pardey, M.C., Haynes, P.A., and Cornish, J.L. (2013). Proteomic analysis of the dorsal and ventral hippocampus of rats maintained on a high fat and refined sugar diet. *Proteomics* 13, 3076-3091.
- Gammulla, C.G., Pascovici, D., Atwell, B.J., and Haynes, P.A. (2011). Differential proteomic response of rice (*Oryza sativa*) leaves exposed to high- and low-temperature stress. *PROTEOMICS* 11, 2839-2850.
- Gasman, S., Chasserot-Golaz, S., Popoff, M.R., Aunis, D., and Bader, M.F. (1999). Involvement of Rho GTPases in calcium-regulated exocytosis from adrenal chromaffin cells. *Journal of Cell Science* 112, 4763-4771.
- Gaspari, M., and Cuda, G. (2011). Nano LC-MS/MS: a robust setup for proteomic analysis. *Methods Mol Biol* 790, 115-126.
- Gomez, F., Houshyar, H., and Dallman, M.F. (2002). Marked Regulatory Shifts in Gonadal, Adrenal, and Metabolic System Responses to Repeated Restraint Stress Occur within a 3-Week Period in Pubertal Male Rats. *Endocrinology* 143, 2852-2862.
- Gomez, F., Manalo, S., and Dallman, M.F. (2004). Androgen-Sensitive Changes in Regulation of Restraint-Induced Adrenocorticotropin Secretion between Early and Late Puberty in Male Rats. *Endocrinology* 145, 59-70.
- Goodman, M., Dluz, S., Mcelaney, M., Belur, E., and Ruderman, N. (1983). Glucose uptake and insulin sensitivity in rat muscle: changes during 3-96 weeks of age. *The American journal of physiology* 244, E93.
- Goshe, M.B., Veenstra, T.D., Panisko, E.A., Conrads, T.P., Angell, N.H., and Smith, R.D. (2001). Phosphoprotein Isotope-Coded Affinity Tags: Application to the Enrichment and Identification of Low-Abundance Phosphoproteins. *Analytical Chemistry* 74, 607-616.
- Gottesman, S., and Maurizi, M.R. (1992). Regulation by proteolysis: energy-dependent proteases and their targets. *Microbiological Reviews* 56, 592-621.
- Griffiths, G., and Simons, K. (1986). The trans Golgi network: sorting at the exit site of the Golgi complex. *Science* 234, 438-443.
- Guay, C., Madiraju, S.R., Aumais, A., Joly, E., and Prentki, M. (2007). A role for ATP-citrate lyase, malic enzyme, and pyruvate/citrate cycling in glucose-induced insulin secretion. *J Biol Chem* 282, 35657-35665.
- Guo, Z.H., and Mattson, M.P. (2000). In Vivo 2-Deoxyglucose Administration Preserves Glucose and Glutamate Transport and Mitochondrial Function in Cortical Synaptic Terminals after Exposure to Amyloid β -Peptide and Iron: Evidence for a Stress Response. *Experimental Neurology* 166, 173-179.
- Gürtler, A., Kunz, N., Gomolka, M., Hornhardt, S., Friedl, A.A., McDonald, K., Kohn, J.E., and Posch, A. (2013). Stain-Free technology as a normalization tool in Western blot analysis. *Analytical Biochemistry* 433, 105-111.

- Gygi, S.P., Corthals, G.L., Zhang, Y., Rochon, Y., and Aebersold, R. (2000). Evaluation of two-dimensional gel electrophoresis-based proteome analysis technology. *Proc. Natl. Acad. Sci. U.S.A* 97, 9390-9395.
- Hamelink, C., Tjurmina, O., Damadzic, R., Young, W.S., Weihe, E., Lee, H.-W., and Eiden, L.E. (2002). Pituitary adenylate cyclase-activating polypeptide is a sympathoadrenal neurotransmitter involved in catecholamine regulation and glucohomeostasis. *Proceedings of the National Academy of Sciences* 99, 461-466.
- Haycock, J. (1993). Multiple signaling pathways in bovine chromaffin cells regulate tyrosine hydroxylase phosphorylation at Ser19, Ser31, and Ser40. *Neurochemical Research* 18, 15-26.
- Hershko, A. (1998). "The Ubiquitin System," in *Ubiquitin and the Biology of the Cell*, eds. J.-M. Peters, J.R. Harris & D. Finley. Springer US), 1-17.
- Hill, J., Chan, S.-A., Kuri, B., and Smith, C. (2011). Pituitary Adenylate Cyclase-activating Peptide (PACAP) Recruits Low Voltage-activated T-type Calcium Influx under Acute Sympathetic Stimulation in Mouse Adrenal Chromaffin Cells. *Journal of Biological Chemistry* 286, 42459-42469.
- Hochstrasser, M. (1995). Ubiquitin, proteasomes, and the regulation of intracellular protein degradation. *Current Opinion in Cell Biology* 7, 215-223.
- Hodel, A. (2001). Effects of Glucocorticoids on Adrenal Chromaffin Cells. *Journal of Neuroendocrinology* 13, 216-220.
- Hu, L., Ye, M., Jiang, X., Feng, S., and Zou, H. (2007). Advances in hyphenated analytical techniques for shotgun proteome and peptidome analysis—A review. *Analytica Chimica Acta* 598, 193-204.
- Hutagalung, A.H., and Novick, P.J. (2011). *Role of Rab GTPases in Membrane Traffic and Cell Physiology*.
- Ikemoto, K., Suzuki, T., Ichinose, H., Ohye, T., Nishimura, A., Nishi, K., Nagatsu, I., and Nagatsu, T. (2002). Localization of sepiapterin reductase in the human brain. *Brain Research* 954, 237-246.
- Jalili, P.R., and Dass, C. (2004). Proteome analysis in the bovine adrenal medulla using liquid chromatography with tandem mass spectrometry. *Rapid Communications in Mass Spectrometry* 18, 1877-1884.
- Jousse, C., Oyadomari, S., Novoa, I., Lu, P., Zhang, Y., Harding, H.P., and Ron, D. (2003). Inhibition of a constitutive translation initiation factor 2 α phosphatase, CREP, promotes survival of stressed cells. *The Journal of cell biology* 163, 767-775.
- Juhnke, H., Krems, B., Kötter, P., and Entian, K.D. (1996). Mutants that show increased sensitivity to hydrogen peroxide reveal an important role for the pentose phosphate pathway in protection of yeast against oxidative stress. *Molecular and General Genetics MGG* 252, 456-464.
- Kamata, H., and Hirata, H. (1999). Redox Regulation of Cellular Signalling. *Cellular Signalling* 11, 1-14.
- Kari, V., Shchebet, A., Neumann, H., and Johnsen, S.A. (2011). The H2B ubiquitin ligase RNF40 cooperates with SUPT16H to induce dynamic changes in chromatin structure during DNA double-strand break repair. *Cell Cycle* 10, 3495-3504.
- Keating, D.J. (2008). Mitochondrial dysfunction, oxidative stress, regulation of exocytosis and their relevance to neurodegenerative diseases. *Journal of neurochemistry* 104, 298-305.
- Kisselev, L., Ehrenberg, M., and Frolova, L. (2003). Termination of translation: interplay of mRNA, rRNAs and release factors? *The EMBO Journal* 22, 175-182.
- Knochenmuss, R. (2006). Ion formation mechanisms in UV-MALDI. *Analyst* 131, 966-986.

- Kruger, N.J., and Von Schaewen, A. (2003). The oxidative pentose phosphate pathway: structure and organisation. *Current Opinion in Plant Biology* 6, 236-246.
- Kuhn, E., Wu, J., Karl, J., Liao, H., Zolg, W., and Guild, B. (2004). Quantification of C-reactive protein in the serum of patients with rheumatoid arthritis using multiple reaction monitoring mass spectrometry and ¹³C-labeled peptide standards. *PROTEOMICS* 4, 1175-1186.
- Kultz, D. (2003). Evolution of the cellular stress proteome: from monophyletic origin to ubiquitous function. *J Exp Biol* 206, 3119-3124.
- Kültz, D. (2005). Molecular and evolutionary basis of the cellular stress response. *Annu. Rev. Physiol.* 67, 225-257.
- Kvetnansky, R., Sabban, E.L., and Palkovits, M. (2009). Catecholaminergic systems in stress: structural and molecular genetic approaches. *Physiological reviews* 89, 535-606.
- Landau, B.R., and Lubs, H.A. (1958). Animal Responses to 2-Deoxy-D-Glucose Administration. *Experimental Biology and Medicine* 99, 124-127.
- Larson, D.R., Zenklusen, D., Wu, B., Chao, J.A., and Singer, R.H. (2011). Real-Time Observation of Transcription Initiation and Elongation on an Endogenous Yeast Gene. *Science* 332, 475-478.
- Leung, S.K.C., Yu, C., Lin, M.I., Tognon, C., and Bernatchez, P. (2013). Abstract A186: Novel target to control lung tumor growth: Disruption of cell membrane remodeling by modulating myoferlin expression. *Molecular Cancer Therapeutics* 12, A186-A186.
- Levine, R.A., Kapatos, G., Kaufman, S., and Milstien, S. (1990). Immunological evidence for the requirement of sepiapterin reductase for tetrahydrobiopterin biosynthesis in brain. *Journal of neurochemistry* 54, 1218-1224.
- Lin, D., Sugawara, T., Strauss, J., Clark, B., Stocco, D., Saenger, P., Rogol, A., and Miller, W. (1995). Role of steroidogenic acute regulatory protein in adrenal and gonadal steroidogenesis. *Science* 267, 1828-1831.
- Liu, Q., Cobb, J.S., Johnson, J.L., Wang, Q., and Agar, J.N. (2014). Performance Comparisons of Nano-LC Systems, Electrospray Sources and LC-MS-MS Platforms. *Journal of Chromatographic Science* 52, 120-127.
- Martins, A.C.P., Souza, K.L.A., Shio, M.T., Mathias, P.C.F., Lelkes, P.I., and Garcia, R.M.G. (2004). Adrenal medullary function and expression of catecholamine-synthesizing enzymes in mice with hypothalamic obesity. *Life Sciences* 74, 3211-3222.
- Marty, N., Dallaporta, M., and Thorens, B. (2007). Brain glucose sensing, counterregulation, and energy homeostasis. *Physiology* 22, 241-251.
- Mastrocola, R., Restivo, F., Vercellinato, I., Danni, O., Brignardello, E., Aragno, M., and Boccuzzi, G. (2005). Oxidative and nitrosative stress in brain mitochondria of diabetic rats. *Journal of Endocrinology* 187, 37-44.
- Maucort, G., Kasula, R., Papadopulos, A., Nieminen, T.A., Rubinsztein-Dunlop, H., and Meunier, F.A. (2014). Mapping Organelle Motion Reveals a Vesicular Conveyor Belt Spatially Replenishing Secretory Vesicles in Stimulated Chromaffin Cells. *PloS one* 9, e87242.
- Mccrimmon, R.J., and Sherwin, R.S. (2010). Hypoglycemia in type 1 diabetes. *Diabetes* 59, 2333-2339.
- Meister, A. (1988). Glutathione metabolism and its selective modification. *J Biol Chem* 263, 17205-17208.
- Millaruelo, A., Sagarral, M., Delicado, E., Torres, M., and Miras-Portugal, M. (1986). Enzymes and pathways of glucose utilization in bovine adrenal medulla. *Molecular and cellular biochemistry* 70, 67-76.

- Mirzaei, M., Pascovici, D., Atwell, B.J., and Haynes, P.A. (2012a). Differential regulation of aquaporins, small GTPases and V-ATPases proteins in rice leaves subjected to drought stress and recovery. *Proteomics* 12, 864-877.
- Mirzaei, M., Soltani, N., Sarhadi, E., Pascovici, D., Keighley, T., Salekdeh, G.H., Haynes, P.A., and Atwell, B.J. (2012b). Shotgun proteomic analysis of long-distance drought signaling in rice roots. *J Proteome Res* 11, 348-358.
- Morrison, S.F., and Cao, W.-H. (2000). Different adrenal sympathetic preganglionic neurons regulate epinephrine and norepinephrine secretion. *American Journal of Physiology - Regulatory, Integrative and Comparative Physiology* 279, R1763-R1775.
- Nagatsu, T., and Ichinose, H. (1999). Regulation of pteridine-requiring enzymes by the cofactor tetrahydrobiopterin. *Molecular neurobiology* 19, 79-96.
- Nath, K.A., Ngo, E.O., Hebbel, R.P., Croatt, A.J., Zhou, B., and Nutter, L.M. (1995). alpha-Ketoacids scavenge H₂O₂ in vitro and in vivo and reduce menadione-induced DNA injury and cytotoxicity. *Am J Physiol* 268, C227-236.
- Ñeco, P., Giner, D., Viniegra, S., Borges, R., Villarroel, A., and Gutiérrez, L.M. (2004). New roles of myosin II during vesicle transport and fusion in chromaffin cells. *Journal of Biological Chemistry* 279, 27450-27457.
- Neher, E. (2006). A comparison between exocytic control mechanisms in adrenal chromaffin cells and a glutamatergic synapse. *Pflügers Archiv* 453, 261-268.
- Neilson, K.A., Ali, N.A., Muralidharan, S., Mirzaei, M., Mariani, M., Assadourian, G., Lee, A., Van Sluyter, S.C., and Haynes, P.A. (2011). Less label, more free: Approaches in label-free quantitative mass spectrometry. *Proteomics* 11, 535-553.
- Neilson, K.A., Keighley, T., Pascovici, D., Cooke, B., and Haynes, P.A. (2013). "Label-free quantitative shotgun proteomics using normalized spectral abundance factors," in *Proteomics for Biomarker Discovery*. Springer), 205-222.
- Nirenberg, M.W., and Hogg, J.F. (1958). Inhibition of Anaerobic Glycolysis in Ehrlich Ascites Tumor Cells by 2-Deoxy-d-Glucose. *Cancer Research* 18, 518-521.
- Nissen, P., Hansen, J., Ban, N., Moore, P.B., and Steitz, T.A. (2000). The Structural Basis of Ribosome Activity in Peptide Bond Synthesis. *Science* 289, 920-930.
- Novello, F., and Mclean, P. (1968). The pentose phosphate pathway of glucose metabolism. Measurement of the non-oxidative reactions of the cycle. *Biochem. J* 107, 775-791.
- Oheim, M., and Stühmer, W. (2000). Tracking chromaffin granules on their way through the actin cortex. *European Biophysics Journal* 29, 67-89.
- Olsen, J.V., and Mann, M. (2013). Status of Large-scale Analysis of Post-translational Modifications by Mass Spectrometry. *Molecular & Cellular Proteomics* 12, 3444-3452.
- Ong, L.K., Guan, L., Damanhuri, H., Goodchild, A.K., Bobrovskaya, L., Dickson, P.W., and Dunkley, P.R. (2014). Neurobiological consequences of acute footshock stress: effects on tyrosine hydroxylase phosphorylation and activation in the rat brain and adrenal medulla. *J Neurochem* 128, 547-560.
- Orphanides, G., Wu, W.H., Lane, W.S., Hampsey, M., and Reinberg, D. (1999). The chromatin-specific transcription elongation factor FACT comprises human SPT16 and SSRP1 proteins. *Nature* 400, 284-288.
- Ouyang, Y.-B., and Hu, B.-R. (2001). Protein ubiquitination in rat brain following hypoglycemic coma. *Neuroscience Letters* 298, 159-162.
- Owada, S., Shimoda, Y., Tsuchihara, K., and Esumi, H. (2013). Critical Role of H₂O₂ Generated by NOX4 during Cellular Response under Glucose Deprivation. *PLoS ONE* 8, e56628.

- Parker, L.M., Kumar, N.N., Lonergan, T., McMullan, S., and Goodchild, A.K. (2013). Distribution and neurochemical characterization of neurons in the rat ventrolateral medulla activated by glucoprivation. *Brain Structure and Function*, 1-18.
- Parker, T., Kesse, W., Mohamed, A., and Afework, M. (1993). The innervation of the mammalian adrenal gland. *Journal of anatomy* 183, 265.
- Parsons, T.D., Coorssen, J.R., Horstmann, H., and Almers, W. (1995). Docked granules, the exocytic burst, and the need for ATP hydrolysis in endocrine cells. *Neuron* 15, 1085-1096.
- Patocková, J., Marhol, P., Tůmová, E., Krsiak, M., Rokyta, R., Stípek, S., Crkovská, J., and Andel, M. (2002). Oxidative stress in the brain tissue of laboratory mice with acute post insulin hypoglycemia. *Physiological research/Academia Scientiarum Bohemoslovaca* 52, 131-135.
- Patterson, S.D., and Aebersold, R.H. (2003). Proteomics: the first decade and beyond. *Nat Genet* 33 Suppl, 311-323.
- Pemble, S., Schroeder, K., Spencer, S., Meyer, D., Hallier, E., Bolt, H., Ketterer, B., and Taylor, J. (1994). Human glutathione S-transferase theta (GSTT1): cDNA cloning and the characterization of a genetic polymorphism. *Biochem. J* 300, 271-276.
- Pickel, V.M., Joh, T.H., Field, P.M., Becker, C.G., and Reis, D.J. (1975). Cellular localization of tyrosine hydroxylase by immunohistochemistry. *J Histochem Cytochem* 23, 1-12.
- Picotti, P., and Aebersold, R. (2012). Selected reaction monitoring-based proteomics: workflows, potential, pitfalls and future directions. *Nat Methods* 9, 555-566.
- Rappaport, E.B., Young, J.B., and Landsberg, L. (1982). Effects of 2-deoxy-D-glucose on the cardiac sympathetic nerves and the adrenal medulla in the rat: further evidence for a dissociation of sympathetic nervous system and adrenal medullary responses. *Endocrinology* 110, 650-656.
- Ren, J.-G., Seth, P., Clish, C.B., Lorkiewicz, P.K., Higashi, R.M., Lane, A.N., Fan, T.W.M., and Sukhatme, V.P. (2014). Knockdown of Malic Enzyme 2 Suppresses Lung Tumor Growth, Induces Differentiation and Impacts PI3K/AKT Signaling. *Sci. Rep.* 4.
- Riedel, T.J., Johnson, L.C., Knight, J., Hantgan, R.R., Holmes, R.P., and Lowther, W.T. (2011). Structural and Biochemical Studies of Human 4-hydroxy-2-oxoglutarate Aldolase: Implications for Hydroxyproline Metabolism in Primary Hyperoxaluria. *PLoS ONE* 6, e26021.
- Ritter, S., Scheurink, A., and Singer, L.K. (1995). 2-Deoxy-D-Glucose but not 2-Mercaptoacetate Increases Fos-Like Immunoreactivity in Adrenal Medulla and Sympathetic Preganglionic Neurons. *Obesity research* 3, 729S-734S.
- Ross, M.E., Evinger, M.J., Hyman, S.E., Carroll, J.M., Mucke, L., Comb, M., Reis, D.J., Joh, T.H., and Goodman, H.M. (1990). Identification of a functional glucocorticoid response element in the phenylethanolamine N-methyltransferase promoter using fusion genes introduced into chromaffin cells in primary culture. *J Neurosci* 10, 520-530.
- Rothman, J.E., and Warren, G. (1994). Implications of the SNARE hypothesis for intracellular membrane topology and dynamics. *Curr Biol* 4, 220-233.
- Sanders, N.M., and Ritter, S. (2000). Repeated 2-deoxy-D-glucose-induced glucoprivation attenuates Fos expression and glucoregulatory responses during subsequent glucoprivation. *Diabetes* 49, 1865-1874.
- Scheurink, A., and Ritter, S. (1993). Sympathoadrenal responses to glucoprivation and lipoprivation in rats. *Physiology & Behavior* 53, 995-1000.
- Schliwa, M. (1999). Protein transport: Molecular motors join forces. *Nature* 397, 204-205.
- Schlutzen, F., Tocilj, A., Zarivach, R., Harms, J., Gluehmann, M., Janell, D., Bashan, A., Bartels, H., Agmon, I., Franceschi, F., and Yonath, A. (2000). Structure of

- Functionally Activated Small Ribosomal Subunit at 3.3 Å Resolution. *Cell* 102, 615-623.
- Schroer, T.A. (2004). Dynactin. *Annual review of cell and developmental biology* 20, 759-779.
- Singh, N., D'souza, A., Cholleti, A., Sastry, G.M., and Bose, K. (2014). Dual regulatory switch confers tighter control on HtrA2 proteolytic activity. *Febs j* 281, 2456-2470.
- Sprague, J.E., and Arbeláez, A.M. (2011). Glucose counterregulatory responses to hypoglycemia. *Pediatric endocrinology reviews: PER* 9, 463.
- Stachowiak, M.K., Sar, M., Tuominen, R.K., Jiang, H.K., An, S., Iadarola, M.J., Poisner, A.M., and Hong, J.S. (1990). Stimulation of adrenal medullary cells in vivo and in vitro induces expression of c-fos proto-oncogene. *Oncogene* 5, 69-73.
- Stoica, R., De Vos, K.J., Paillusson, S., Mueller, S., Sancho, R.M., Lau, K.-F., Vizcay-Barrena, G., Lin, W.-L., Xu, Y.-F., Lewis, J., Dickson, D.W., Petrucelli, L., Mitchell, J.C., Shaw, C.E., and Miller, C.C.J. (2014). ER-mitochondria associations are regulated by the VAPB-PTPIP51 interaction and are disrupted by ALS/FTD-associated TDP-43. *Nat Commun* 5.
- Stradal, T.E.B., and Scita, G. (2006). Protein complexes regulating Arp2/3-mediated actin assembly. *Current Opinion in Cell Biology* 18, 4-10.
- Strange, R.C., Spiteri, M.A., Ramachandran, S., and Fryer, A.A. (2001). Glutathione-S-transferase family of enzymes. *Mutation Research/Fundamental and Molecular Mechanisms of Mutagenesis* 482, 21-26.
- Stueland, C.S., Gorden, K., and Laporte, D.C. (1988). The isocitrate dehydrogenase phosphorylation cycle. Identification of the primary rate-limiting step. *Journal of Biological Chemistry* 263, 19475-19479.
- Surazynski, A., Milyk, W., Palka, J., and Phang, J.M. (2008). Prolidase-dependent regulation of collagen biosynthesis. *Amino Acids* 35, 731-738.
- Tesfaye, N., and Seaquist, E.R. (2010). Neuroendocrine responses to hypoglycemia. *Annals of the New York Academy of Sciences* 1212, 12-28.
- The Uniprot Consortium (2014). Activities at the Universal Protein Resource (UniProt). *Nucleic Acids Research* 42, D191-D198.
- Thomas, G., Haavik, J., and Cohen, P. (1997). Participation of a stress-activated protein kinase cascade in the activation of tyrosine hydroxylase in chromaffin cells. *European Journal of Biochemistry* 247, 1180-1189.
- Tolar, L.A., and Pallanck, L. (1998). NSF function in neurotransmitter release involves rearrangement of the SNARE complex downstream of synaptic vesicle docking. *The Journal of neuroscience* 18, 10250-10256.
- Toomre, D., Keller, P., White, J., Olivo, J.C., and Simons, K. (1999). Dual-color visualization of trans-Golgi network to plasma membrane traffic along microtubules in living cells. *Journal of Cell Science* 112, 21-33.
- Towbin, H., Staehelin, T., and Gordon, J. (1979). Electrophoretic transfer of proteins from polyacrylamide gels to nitrocellulose sheets: procedure and some applications. *Proc Natl Acad Sci U S A* 76, 4350-4354.
- Tretter, L., and Adam-Vizi, V. (2000). Inhibition of Krebs cycle enzymes by hydrogen peroxide: A key role of α -ketoglutarate dehydrogenase in limiting NADH production under oxidative stress. *The Journal of Neuroscience* 20, 8972-8979.
- Trifaró, J.M., Gasman, S., and Gutiérrez, L.M. (2008). Cytoskeletal control of vesicle transport and exocytosis in chromaffin cells. *Acta Physiologica* 192, 165-172.
- Van Aelst, L., and D'souza-Schorey, C. (1997). Rho GTPases and signaling networks. *Genes & Development* 11, 2295-2322.

- Vaudry, D., Falluel-Morel, A., Bourgault, S., Basille, M., Burel, D., Wurtz, O., Fournier, A., Chow, B.K.C., Hashimoto, H., Galas, L., and Vaudry, H. (2009). Pituitary Adenylate Cyclase-Activating Polypeptide and Its Receptors: 20 Years after the Discovery. *Pharmacological Reviews* 61, 283-357.
- Verberne, A.J., Sabetghadam, A., and Korim, W.S. (2014). Neural pathways that control the glucose counterregulatory response. *Frontiers in neuroscience* 8.
- Verberne, A.J., and Sartor, D.M. (2010). Rostroventrolateral medullary neurons modulate glucose homeostasis in the rat. *American Journal of Physiology-Endocrinology and Metabolism* 299, E802-E807.
- Viau, V. (2002). Functional cross-talk between the hypothalamic-pituitary-gonadal and-adrenal axes. *Journal of neuroendocrinology* 14, 506-513.
- Vitale, M., Del Castillo, A.R., Tchakarov, L., and Trifaro, J. (1991). Cortical filamentous actin disassembly and scinderin redistribution during chromaffin cell stimulation precede exocytosis, a phenomenon not exhibited by gelsolin. *The Journal of cell biology* 113, 1057-1067.
- Vitale, M., Seward, E., and Trifaro, J.-M. (1995). Chromaffin cell cortical actin network dynamics control the size of the release-ready vesicle pool and the initial rate of exocytosis. *Neuron* 14, 353-363.
- Voelckel, C., Mirzaei, M., Reichelt, M., Luo, Z., Pascovici, D., Heenan, P.B., Schmidt, S., Janssen, B., Haynes, P.A., and Lockhart, P.J. (2010). Transcript and protein profiling identify candidate gene sets of potential adaptive significance in New Zealand Pachycladon. *BMC evolutionary biology* 10, 151.
- Vogel, C., Silva, G.M., and Marcotte, E.M. (2011). Protein expression regulation under oxidative stress. *Molecular & Cellular Proteomics* 10.
- Voges, D., Zwickl, P., and Baumeister, W. (1999). The 26S proteasome: a molecular machine designed for controlled proteolysis. *Annual review of biochemistry* 68, 1015-1068.
- Walsh, G. (2002). *Proteins: Biochemistry and Biotechnology*. Wiley.
- Wang, H., Alvarez, S., and Hicks, L.M. (2012). Comprehensive comparison of iTRAQ and label-free LC-based quantitative proteomics approaches using two *Chlamydomonas reinhardtii* strains of interest for biofuels engineering. *J Proteome Res* 11, 487-501.
- Wang, P., Bouwman, F.G., and Mariman, E.C.M. (2009). Generally detected proteins in comparative proteomics – A matter of cellular stress response? *PROTEOMICS* 9, 2955-2966.
- Watanabe, T., Shimamoto, N., Takahashi, A., and Fujino, M. (1995). PACAP stimulates catecholamine release from adrenal medulla: a novel noncholinergic secretagogue. *Am J Physiol* 269, E903-909.
- Wegrzyn, J., Lee, J., Neveu, J.M., Lane, W.S., and Hook, V. (2007). Proteomics of neuroendocrine secretory vesicles reveal distinct functional systems for biosynthesis and exocytosis of peptide hormones and neurotransmitters. *Journal of proteome research* 6, 1652-1665.
- Wegrzyn, J.L., Bark, S.J., Funkelstein, L., Mosier, C., Yap, A., Kazemi-Esfarjani, P., La Spada, A.R., Sigurdson, C., O'connor, D.T., and Hook, V. (2010). Proteomics of dense core secretory vesicles reveal distinct protein categories for secretion of neuroeffectors for cell-cell communication. *J Proteome Res* 9, 5002-5024.
- Wick, A.N., Drury, D.R., Nakada, H.I., Wolfe, J.B., Britton, W.T.T.a.O.B., and Grabowski, R. (1957). Localization of the Primary Metabolic Block Produced by 2-Deoxyglucose. *Journal of Biological Chemistry* 224, 963-969.
- Wienkoop, S., and Weckwerth, W. (2006). Relative and absolute quantitative shotgun proteomics: targeting low-abundance proteins in *Arabidopsis thaliana*. *Journal of experimental botany* 57, 1529-1535.

- Will, C.L., and Lührmann, R. (2011). Spliceosome Structure and Function. *Cold Spring Harbor Perspectives in Biology* 3.
- Wilson, D.W., Wilcox, C.A., Flynn, G.C., Chen, E., Kuang, W.-J., Henzel, W.J., Block, M.R., Ullrich, A., and Rothman, J.E. (1989). A fusion protein required for vesicle-mediated transport in both mammalian cells and yeast. *Nature* 339, 355-359.
- Woodward, G.E., and Hudson, M.T. (1954). The Effect of 2-Desoxy-d-glucose on Glycolysis and Respiration of Tumor and Normal Tissues. *Cancer Research* 14, 599-605.
- Wu, G., Bazer, F., Burghardt, R., Johnson, G., Kim, S., Knabe, D., Li, P., Li, X., Mcknight, J., Satterfield, M.C., and Spencer, T. (2011). Proline and hydroxyproline metabolism: implications for animal and human nutrition. *Amino Acids* 40, 1053-1063.
- Wu, X., Wiater, M.F., and Ritter, S. (2010). NPAS2 deletion impairs responses to restricted feeding but not to metabolic challenges. *Physiology & Behavior* 99, 466-471.
- Wu, Y., Wu, M., He, G., Zhang, X., Li, W., Gao, Y., Li, Z., Wang, Z., and Zhang, C. (2012). Glyceraldehyde-3-phosphate dehydrogenase: a universal internal control for Western blots in prokaryotic and eukaryotic cells. *Anal Biochem* 423, 15-22.
- Wurtman, R.J. (2002). Stress and the adrenocortical control of epinephrine synthesis. *Metabolism* 51, 11-14.
- Wurtman, R.J., and Axelrod, J. (1966). Control of Enzymatic Synthesis of Adrenaline in the Adrenal Medulla by Adrenal Cortical Steroids. *Journal of Biological Chemistry* 241, 2301-2305.
- Yaron, A., Naider, F., and Scharpe, S. (1993). Proline-dependent structural and biological properties of peptides and proteins. *Critical reviews in biochemistry and molecular biology* 28, 31-81.
- Yasothornsrikul, S., Toneff, T., Hwang, S.R., and Hook, V.Y. (1998). Arginine and lysine aminopeptidase activities in chromaffin granules of bovine adrenal medulla: relevance to prohormone processing. *J Neurochem* 70, 153-163.
- Yu, S.-M., and Kim, S.-J. (2010). Endoplasmic reticulum stress (ER-stress) by 2-deoxy-D-glucose (2DG) reduces cyclooxygenase-2 (COX-2) expression and N-glycosylation and induces a loss of COX-2 activity via a Src kinase-dependent pathway in rabbit articular chondrocytes. *Exp Mol Med* 42, 777-786.
- Zybailov, B., Mosley, A.L., Sardi, M.E., Coleman, M.K., Florens, L., and Washburn, M.P. (2006). Statistical Analysis of Membrane Proteome Expression Changes in *Saccharomyces cerevisiae*. *Journal of proteome research* 5, 2339-2347.

6.0 Appendix

Table A1. Adrenomedullary Proteome

Identifier	Symbol	Description
gi 407970992	Ali3	alpha-1-inhibitor 3 precursor
gi 209862801	Aars	alanine--tRNA ligase, cytoplasmic
gi 403224993	Abhd11	abhydrolase domain containing 11
gi 56090461	Abhd14b	alpha/beta hydrolase domain-containing protein 14B
gi 157820211	Abhd3	abhydrolase domain containing 3 (Predicted)
gi 6978429	Acaa1a	3-ketoacyl-CoA thiolase A, peroxisomal
gi 18426866	Acaa2	3-ketoacyl-CoA thiolase, mitochondrial
gi 11559962	Acaca	acetyl-CoA carboxylase 1
gi 392341831	Acad8	acyl-CoA dehydrogenase family, member 8
gi 197313734	Acad9	acyl-CoA dehydrogenase family member 9
gi 6978431	Acadl	long-chain specific acyl-CoA dehydrogenase
gi 292494885	Acadm	medium-chain specific acyl-CoA dehydrogenase
gi 11968090	Acads	short-chain specific acyl-CoA dehydrogenase
gi 6978435	Acadvl	very long-chain specific acyl-CoA dehydrogenase
gi 401461805	Acat1	acetyl-CoA acetyltransferase 1
gi 55741502	Acat2	acetyl-CoA acetyltransferase 2
gi 8394162	Aco1	cytoplasmic aconitate hydratase
gi 40538860	Aco2	aconitate hydratase, mitochondrial precursor
gi 48675862	Acot2	acyl-CoA thioesterase 2
gi 10863989	Acp1	low molecular weight phosphotyrosine protein phosphatase isoform A
gi 293355295	Acsf3	PREDICTED: acyl-CoA synthetase family member 3, mitochondrial
gi 25742739	Acs11	long-chain-fatty-acid--CoA ligase 1
gi 16758426	Acs14	long-chain-fatty-acid--CoA ligase 4
gi 13592133	Actb	beta-actin, cytoplasmic 1
gi 157823033	Actbl2	beta-actin-like protein 2
gi 77993370	Actc1	actin, alpha cardiac muscle 1
gi 13591902	Actn1	alpha-actinin-1
gi 77539778	Actn4	alpha-actinin-4
gi 70912366	Actr3	actin-related protein 3
gi 169636413	Adcy3	adenylate cyclase 3
gi 186972146	Adh5	alcohol dehydrogenase class-3
gi 52345435	Adk	adenosine kinase
gi 198442897	Afg3l2	AFG3-like protein 2
gi 27229290	Afm	afamin precursor
gi 72255513	Aga	N(4)-(Beta-N-acetylglucosaminyl)-L-asparaginase
gi 157822109	Agpat2	1-acylglycerol-3-phosphate O-acyltransferase 2 (Predicted)
gi 8392878	Ahcy	adenosylhomocysteinase

gi 157819079	Ahcy1l	putative adenosylhomocysteinase 2
gi 300794574	Ahnak	neuroblast differentiation-associated protein AHNAK
gi 6978477	Ahsg	alpha-2-HS-glycoprotein precursor
gi 25742626	Aifm1	apoptosis-inducing factor 1, mitochondrial
gi 213385255	Aifm2	apoptosis-inducing factor, mitochondrion-associated, 2
gi 75832035	Aimp1	aminoacyl tRNA synthase complex-interacting multifunctional protein 1
gi 61889092	Ak1	adenylate kinase isoenzyme 1
gi 390125192	Ak2	adenylate kinase 2
gi 6978479	Ak3	GTP:AMP phosphotransferase, mitochondrial
gi 13591894	Akr1a1	alcohol dehydrogenase
gi 6978491	Akr1b1	aldose reductase
gi 61556894	Akr1b10	aldo-keto reductase family 1 member B10
gi 148540194	Akr1b14	aldose reductase-related protein 1
gi 27465603	Akr1b8	aldose reductase-like protein
gi 19705537	Akr7a2	aflatoxin B1 aldehyde reductase member 2
gi 158138568	Alb	serum albumin precursor
gi 11968144	Aldh1l1	cytosolic 10-formyltetrahydrofolate dehydrogenase
gi 14192933	Aldh2	aldehyde dehydrogenase, mitochondrial precursor
gi 197927423	Aldh4a1	delta-1-pyrroline-5-carboxylate dehydrogenase, mitochondrial
gi 145651820	Aldh6a1	methylmalonate-semialdehyde dehydrogenase
gi 402766107	Aldh7a1	alpha-aminoadipic semialdehyde dehydrogenase
gi 75905479	Aldh9a1	4-trimethylaminobutyraldehyde dehydrogenase
gi 408772019	Aldoa	fructose-bisphosphate aldolase A
gi 213511844	Alg2	alpha-1,3-mannosyltransferase ALG2
gi 6978497	Ambp	bikunin
gi 157822539	Ank1	ankyrin-1
gi 404501461	Ankfy1	ankyrin repeat and FYVE domain containing 1
gi 18777770	Anp32b	acidic leucine-rich nuclear phosphoprotein 32 family member B
gi 6978501	Anxa1	Annexin A1
gi 9845234	Anxa2	annexin A2
gi 55742832	Anxa4	annexin A4
gi 6978505	Anxa5	annexin A5
gi 130502086	Anxa6	annexin A6
gi 148539909	Anxa7	annexin A7
gi 8392872	Ap1b1	AP-1 complex subunit beta-1
gi 189491695	Ap1g1	AP-1 complex subunit gamma-1
gi 157823677	Ap2a1	AP-2 complex subunit alpha-1
gi 162138932	Ap2a2	AP-2 complex subunit alpha-2
gi 198278523	Ap3d1	AP-3 complex subunit delta-1
gi 6978513	Apeh	acylamino-acid-releasing enzyme
gi 13162337	Apex1	DNA-(apurinic or apyrimidinic site) lyase
gi 188497679	Api5	apoptosis inhibitor 5

gi 6978515	Apoa1	apolipoprotein A-I preproprotein
gi 157823671	Apoa1bp	NAD(P)H-hydrate epimerase
gi 161783809	Apob	apolipoprotein B-100
gi 397529602	Apoe	apolipoprotein E precursor
gi 61556832	Aprt	adenine phosphoribosyltransferase
gi 6978527	Aqp1	aquaporin-1
gi 11968098	Arf1	ADP-ribosylation factor 1
gi 13162343	Arf4	ADP-ribosylation factor 4
gi 13162339	Arf5	ADP-ribosylation factor 5
gi 13162345	Arf6	ADP-ribosylation factor 6
gi 211065497	Arhgap1	Rho GTPase activating protein 1
gi 55742827	Arhgdia	Rho GDP-dissociation inhibitor 1
gi 57527565	Arhgdib	Rho GDP dissociation inhibitor (GDI) beta
gi 157818451	Arl8a	ADP-ribosylation factor-like protein 8A
gi 157817229	Arpc2	actin-related protein 2/3 complex subunit 2
gi 157786926	Arpc3	actin-related protein 2/3 complex subunit 3
gi 319020750	Arpc4	actin-related protein 2/3 complex subunit 4
gi 40254747	Asah1	acid ceramidase precursor
gi 48675845	Atic	bifunctional purine biosynthesis protein
gi 112984140	Atl3	atlastin-3
gi 6978543	Atp1a1	sodium/potassium-transporting ATPase subunit alpha-1 precursor
gi 161016776	Atp2a2	sarcoplasmic/endoplasmic reticulum calcium ATPase 2 isoform a
gi 16758008 :reversed	Atp2b1	plasma membrane calcium-transporting ATPase 1
gi 40538742	Atp5a1	ATP synthase subunit alpha, mitochondrial precursor
gi 54792127	Atp5b	ATP synthase subunit beta, mitochondrial precursor
gi 39930503	Atp5c1	ATP synthase subunit gamma, mitochondrial
gi 20806153	Atp5d	ATP synthase subunit delta, mitochondrial precursor
gi 19705465	Atp5f1	ATP synthase subunit b, mitochondrial precursor
gi 8392939	Atp5g1	ATP synthase F(0) complex subunit C1, mitochondrial
gi 9506411	Atp5h	ATP synthase subunit d, mitochondrial
gi 20302061	Atp5o	ATP synthase subunit O, mitochondrial precursor
gi 157819953	Atp6v1a	V-type proton ATPase catalytic subunit A
gi 38454230	Atp6v1e1	V-type proton ATPase subunit E 1
gi 157822275	Auh	methylglutaconyl-CoA hydratase, mitochondrial
gi 77020272	Bag6	large proline-rich protein BAG6
gi 51948420	Bcap31	B-cell receptor-associated protein 31
gi 11693174	Bcat2	branched-chain-amino-acid aminotransferase, mitochondrial
gi 158517950	Bckdk	branched chain ketoacid dehydrogenase kinase
gi 16758714	Blvra	biliverdin reductase A precursor

gi 157819619	Blvrb	flavin reductase
gi 81295385	Bphl	valacyclovir hydrolase precursor
gi 25282455	Bpnt1	3-(2-),5--bisphosphate nucleotidase 1
gi 37693510	Bst2	bone marrow stromal antigen 2
gi 48675371	C1qbp	complement component 1 Q subcomponent-binding protein, mitochondrial precursor
gi 158138561	C3	complement C3 precursor
gi 50657362	C4a	complement component 4A
gi 16924006	C9	complement component C9
gi 157817869	Ca1	carbonic anhydrase 1
gi 51948388	Cacybp	calcyclin-binding protein
gi 158534057	Cad	carbamoyl-phosphate synthetase 2, aspartate transcarbamylase, and dihydroorotase
gi 6978589	Cald1	non-muscle caldesmon
gi 14010863	Calm1	calmodulin
gi 11693172	Calr	calreticulin precursor
gi 16758920	Cand1	cullin-associated NEDD8-dissociated protein 1
gi 25282419	Canx	calnexin precursor
gi 59709467	Cap1	adenylyl cyclase-associated protein 1
gi 87239978	Caprin1	caprin-1
gi 161086978	Capza1	F-actin-capping protein subunit alpha-1
gi 57163991	Capza2	F-actin-capping protein subunit alpha-2
gi 54400732	Capzb	F-actin-capping protein subunit beta
gi 9506445	Car2	carbonic anhydrase 2
gi 6978607	Cat	catalase
gi 32996723	Cbr4	carbonyl reductase family member 4
gi 56799436	Cbx3	chromobox homolog 3 (HP1 gamma homolog, Drosophila)
gi 54400730	Cct2	T-complex protein 1 subunit beta
gi 40018616	Cct3	T-complex protein 1 subunit gamma
gi 33414505	Cct4	T-complex protein 1 subunit delta
gi 51890219	Cct5	T-complex protein 1 subunit epsilon
gi 76253725	Cct6a	T-complex protein 1 subunit zeta
gi 157819651	Cct7	T-complex protein 1 subunit eta
gi 347800699	Cct8	T-complex protein 1 subunit theta
gi 48675379	Cd36	CD36 molecule (Thrombospondin receptor)
gi 6978635	Cd59	CD59 glycoprotein precursor
gi 6978639	Cd81	CD81 antigen
gi 148229054	Cd9	CD9 antigen
gi 61889112	Cdc42	cell division control protein 42 homolog precursor
gi 76257394	Cdc42bpb	serine/threonine-protein kinase MRCK beta
gi 20302093	Cdipt	CDP-diacylglycerol--inositol 3-phosphatidyltransferase
gi 392351269	Cenpv	centromere protein V
gi 57529187	Ces1c	carboxylesterase 1C
gi 281604082	Cf9	coagulation factor IX
gi 77861917	Cfh	complement factor H

gi 8393101	Cfl1	cofilin-1
gi 62543533	Chchd2	coiled-coil-helix-coiled-coil-helix domain containing 2
gi 157817027	Chchd3	coiled-coil-helix-coiled-coil-helix domain-containing protein 3, mitochondrial
gi 127139019	Chga	chromogranin A (parathyroid secretory protein 1)
gi 397174784	Chgb	secretogranin-1
gi 300798020	Cisd2	CDGSH iron sulfur domain-containing protein 2
gi 401461784	Ckb	creatine kinase B-type
gi 50657380	Clic1	chloride intracellular channel protein 1
gi 50300479	Clint1	clathrin interactor 1
gi 9506497	Cltc	clathrin heavy chain 1
gi 392351341	Cluh	clustered mitochondria protein homolog
gi 56912206	Cmb1	carboxymethylenebutenolidase homolog
gi 71043752	Cmpk1	UMP-CMP kinase
gi 117606182	Cnpy2	protein canopy homolog 2 precursor
gi 392346358	Cobl1	cordon-bleu WH2 repeat protein-like
gi 157822161	Comtd1	catechol O-methyltransferase domain-containing protein 1
gi 197384345	Copa	coatamer subunit alpha
gi 18158449	Copb1	coatamer subunit beta 1
gi 11120716	Copb2	coatamer subunit beta 2
gi 73532768	Copg1	coatamer subunit gamma-1
gi 51948518	Cops4	COP9 signalosome complex subunit 4
gi 157824117	Copz1	coatamer protein complex, subunit zeta 1 (Predicted)
gi 164518906	Cox15	cytochrome c oxidase assembly homolog 15 (yeast)
gi 110189718	COX2	cytochrome c oxidase subunit II (mitochondrion)
gi 8393180	Cox4i1	cytochrome c oxidase subunit 4 isoform 1, mitochondrial precursor
gi 401461788	Cp	ceruloplasmin isoform 2 precursor
gi 406035338	Cpamd8	C3 and PZP-like, alpha-2-macroglobulin domain containing 8
gi 6978699	Cpd	carboxypeptidase D
gi 157818555	Cpsf6	cleavage and polyadenylation specificity factor subunit 6
gi 162287173	Cpt1a	carnitine O-palmitoyltransferase 1, liver isoform
gi 6978705	Cpt2	carnitine O-palmitoyltransferase 2, mitochondrial precursor
gi 157787004	Creg1	cellular repressor of E1A-stimulated genes (Predicted)
gi 11968068	Crip2	cysteine-rich protein 2
gi 9506515	Crk	v-crk avian sarcoma virus CT10 oncogene homolog
gi 8393197	Crp	C-reactive protein precursor

gi 18543177	Cs	citrate synthase, mitochondrial precursor
gi 157820325	Cse1l	exportin-2
gi 55742755	Ctnna1	catenin alpha-1
gi 82830420	Ctsb	cathepsin B preproprotein
gi 42476045	Ctsd	cathepsin D precursor
gi 11560046	Cyb5a	cytochrome b5
gi 13399338	Cyb5b	cytochrome b5 type B precursor
gi 20302049	Cyb5r3	NADH-cytochrome b5 reductase 3
gi 194473626	Cyc1	cytochrome c-1
gi 6978725	Cycs	cytochrome c, somatic
gi 8393224	Cyp11a1	cholesterol side-chain cleavage enzyme, mitochondrial
gi 292494921	Cyp11b1	cytochrome P450, family 11, subfamily b, polypeptide 1
gi 6978737	Cyp1b1	cytochrome P450 1B1
gi 259906405	Cyp21a1	steroid 21-hydroxylase
gi 6978751	Cyp51a1	lanosterol 14-alpha demethylase
gi 157818371	D2hgdh	D-2-hydroxyglutarate dehydrogenase
gi 16758642	Dars	aspartate-tRNA ligase, cytoplasmic
gi 140970928	Dbh	dopamine beta-hydroxylase
gi 158749632	Dbt	dihydrolipoamide branched chain transacylase E2
gi 56090393	Dcakd	dephospho-CoA kinase domain-containing protein
gi 13162302	Dctn1	dynactin subunit 1
gi 413081953	Ddb1	DNA damage-binding protein 1
gi 13162287	Ddt	D-dopachrome decarboxylase
gi 61097941	Ddx1	ATP-dependent RNA helicase DDX1
gi 51592092	Ddx39b	spliceosome RNA helicase Ddx39b
gi 56090441	Ddx5	DEAD (Asp-Glu-Ala-Asp) box helicase 5
gi 292781228	Decr1	2,4-dienoyl-CoA reductase, mitochondrial precursor
gi 62079131	Derl1	Der1-like domain family, member 1
gi 11693158	Dhcr7	7-dehydrocholesterol reductase
gi 71043640	Dhtkd1	probable 2-oxoglutarate dehydrogenase E1 component DHKTD1, mitochondrial
gi 300797788	Dhx15	DEAH (Asp-Glu-Ala-His) box polypeptide 15 (Predicted)
gi 157821633	Dhx9	DEAH (Asp-Glu-Ala-His) box helicase 9
gi 56605642	Diablo	diablo homolog, mitochondrial
gi 403224997	Diaph1	diaphanous-related formin 1
gi 78365255	Dlat	dihydrolipoamide S-acetyltransferase
gi 40786469	Dld	dihydrolipoyl dehydrogenase, mitochondrial precursor
gi 195927000	Dlst	dihydrolipoamide S-succinyltransferase (E2 component of 2-oxo-glutarate complex)
gi 84370368	Dnaja3	dnaJ homolog subfamily A member 3, mitochondrial isoform 2
gi 392350322	Dnajc13	DnaJ (Hsp40) homolog, subfamily C, member

gi 61557163	Dnajc8	DnaJ homolog subfamily C member 8
gi 77917614	Dnm1l	dynamamin-1-like protein
gi 6978771	Dnm2	dynamamin-2
gi 67846036	Dnpep	aspartyl aminopeptidase
gi 157818409	Dpm1	dolichol-phosphate mannosyltransferase
gi 16758578	Dpp3	dipeptidyl peptidase 3
gi 6978773	Dpp4,	dipeptidyl peptidase 4
gi 13591940	Dpyd	dihydropyrimidine dehydrogenase [NADP(+)]
gi 157786744	Dpysl2	dihydropyrimidinase-related protein 2
gi 392355146	Dstnl1	PREDICTED: destrin
gi 148491097	Dync1h1	cytoplasmic dynein 1 heavy chain 1
gi 157823277	Dysf	dysferlin (Predicted), isoform CRA_a
gi 155369702	Echdc3	enoyl-CoA hydratase domain-containing protein 3, mitochondria
gi 162287040	Eci1	enoyl-CoA delta isomerase 1, mitochondrial precursor
gi 55741520	Eci2	enoyl-CoA delta isomerase 2, mitochondrial
gi 61556967	Eef1d	elongation factor 1-delta
gi 51948418	Eef1g	elongation factor 1-gamma
gi 8393296	Eef2	elongation factor 2
gi 62078909	Eepd1	endonuclease/exonuclease/phosphatase family domain-containing protein 1
gi 109491989	Eftud2	elongation factor Tu GTP binding domain containing 2
gi 34536836	Ehd3	EH domain-containing protein 3
gi 25282453	Eif2b1	translation initiation factor eIF-2B subunit alpha
gi 55741628	Eif2b5	translation initiation factor eIF-2B subunit epsilon
gi 261337190	Eif3a	eukaryotic translation initiation factor 3 subunit A
gi 72255511	Eif3b	eukaryotic translation initiation factor 3 subunit B
gi 198386358	Eif3c	eukaryotic translation initiation factor 3 subunit C
gi 270483841	Eif3m	eukaryotic translation initiation factor 3, subunit M
gi 40786436	Eif4a1	eukaryotic initiation factor 4A-I
gi 157821621	Eif4a3	eukaryotic initiation factor 4A-III
gi 56605726	Eif4b	eukaryotic translation initiation factor 4B
gi 55741853	Eif4h	eukaryotic translation initiation factor 4H
gi 76096304	Eif5a	eukaryotic translation initiation factor 5A-1
gi 158635983	Eif5b	eukaryotic translation initiation factor 5B
gi 157818153	Elavl1	ELAV-like protein 1
gi 51948432	Emcn	endomucin
gi 158186651	Eno1	alpha-enolase
gi 40786479	Entpd5	ectonucleoside triphosphate diphosphohydrolase 5
gi 392349592 :reversed	Eppk1	epiplakin 1

gi 66793366	Eprs	bifunctional aminoacyl-tRNA synthetase
gi 13540638	Erap1	endoplasmic reticulum aminopeptidase 1 precursor
gi 399498540	Esd	S-formylglutathione hydrolase
gi 75832132	Esyt1	extended synaptotagmin-1
gi 293348426	Esyt2	extended synaptotagmin-2
gi 57527204	Etfa	electron transfer flavoprotein subunit alpha, mitochondrial
gi 51948412	Etfb	electron transfer flavoprotein subunit beta
gi 52138635	Etfdh	electron transfer flavoprotein-ubiquinone oxidoreductase, mitochondrial precursor
gi 52138521	Ezr	ezrin
gi 161333847	F2	prothrombin
gi 198386332	Fahd2a	fumarylacetoacetate hydrolase domain-containing protein 2
gi 223972702 :reversed	Fam71e2	family with sequence similarity 71, member E2
gi 157822917	Farp1	FERM, RhoGEF and pleckstrin domain-containing protein 1
gi 51948478	Farsb	phenylalanyl-tRNA synthetase, beta subunit
gi 8394158	Fasn	fatty acid synthase
gi 71043704	Fbl	rRNA 2'-O-methyltransferase fibrillarin
gi 13929206	Fdps	farnesyl pyrophosphate synthase
gi 8393355	Fdx1	adrenodoxin, mitochondrial
gi 13162347	Fdxr	NADPH:adrenodoxin oxidoreductase, mitochondrial
gi 58865400	Fermt2	fermitin family homolog 2
gi 17865327	Fetub	fetuin-B
gi 144922622	Fga	fibrinogen alpha chain
gi 158186678	Fgb	fibrinogen beta chain
gi 61098186	Fgg	fibrinogen gamma chain
gi 158186722	Fh	fumarate hydratase, mitochondrial precursor
gi 81295379	Fkbp8	peptidyl-prolyl cis-trans isomerase FKBP8
gi 197386807	Flna	filamin-A
gi 157818975	Flnb	filamin-B
gi 158636004	Flot1	flotillin-1
gi 399154173	Flot2	flotillin-2 isoform 2
gi 6978847	Fmo1	dimethylaniline monooxygenase [N-oxide-forming] 1
gi 186972114	Fn1	fibronectin 1
gi 6978859	Fth1	ferritin heavy chain
gi 84000579	Ftl	ferritin light chain 1
gi 83320094	Fubp1	far upstream element-binding protein 1
gi 58865844	Fus	RNA-binding protein FUS
gi 71043780	Fusip1	FUS interacting protein (Serine-arginine rich) 1
gi 281306781	G3bp1	GTPase activating protein (SH3 domain) binding protein 1
gi 8393381	G6pd	glucose-6-phosphate 1-dehydrogenase
gi 13591947	Gak	cyclin-G-associated kinase
gi 157822919	Ganab	neutral alpha-glucosidase AB

gi 8393418	Gapdh	glyceraldehyde-3-phosphate dehydrogenase
gi 402794806	Gars	glycine-tRNA ligase
gi 62945328	Gbas	glioblastoma amplified sequence
gi 401709952	Gc	group specific component
gi 157820807	Gcdh	glutaryl-CoA dehydrogenase, mitochondrial
gi 25742748	Gclc	glutamate-cysteine ligase catalytic subunit
gi 274327131	Gcn11l	GCN1 general control of amino-acid synthesis 1-like 1
gi 126723054	Gcsh	glycine cleavage system H protein, mitochondrial precursor
gi 148747414	Gda	guanine deaminase
gi 71534276	Gdi1	rab GDP dissociation inhibitor alpha
gi 40254781	Gdi2	rab GDP dissociation inhibitor beta
gi 16758432	Gfm1	elongation factor G, mitochondrial
gi 8393450	Glg1	golgi apparatus protein 1 precursor
gi 46485429	Glo1	lactoylglutathione lyase
gi 62079189	Glod4	glyoxalase domain-containing protein 4
gi 48976085	Gm2a	GM2 ganglioside activator
gi 13624295	Gmfb	glia maturation factor beta
gi 17105340	Gmpr	GMP reductase 1
gi 67078508	Gmps	GMP synthase
gi 61557109	Gna14	guanine nucleotide-binding protein subunit alpha-14
gi 406035317	Gnb21l	guanine nucleotide-binding protein subunit beta-2-like 1
gi 401461792	Got1	aspartate aminotransferase, cytoplasmic
gi 6980972	Got2	aspartate aminotransferase, mitochondrial
gi 57527919	Gpd1	glycerol-3-phosphate dehydrogenase
gi 300798457	Gpd1l	glycerol-3-phosphate dehydrogenase 1-like protein
gi 46485440	Gpi	glucose-6-phosphate isomerase
gi 145275165	Gpx1	glutathione peroxidase 1
gi 41053837	Gpx3	glutathione peroxidase 3 precursor
gi 90903229	Gpx4	phospholipid hydroperoxide glutathione peroxidase, mitochondrial
gi 300798184	Gramd1b	GRAM domain containing 1B
gi 166091519	Grhpr	glyoxylate reductase/hydroxypyruvate reductase
gi 13324704	Grpel1	grpE protein homolog 1, mitochondrial precursor
gi 51854227	Gsn	gelsolin precursor
gi 392342264	Gsta3	PREDICTED: glutathione S-transferase alpha-3
gi 31077128	Gstk1	glutathione S-transferase kappa 1
gi 8393502	Gstm1	glutathione S-transferase Mu 1
gi 13592152	Gstm7	glutathione S-transferase Yb-3
gi 56090550	Gsto1	glutathione S-transferase omega-1
gi 25453420	Gstp1	glutathione S-transferase P
gi 16757988	Gstt1	glutathione S-transferase theta 1
gi 6980992	Gstt2	glutathione S-transferase theta-2
gi 212549647	Gstt3	glutathione S-transferase, theta 3

gi 157822229	Gstz1	maleylacetoacetate isomerase
gi 157822499	H2afv	histone H2A
gi 8393519	H2afy	core histone macro-H2A.1
gi 157821675	H6pd	hexose-6-phosphate dehydrogenase
gi 17105336	Hadh	hydroxyacyl-coenzyme A dehydrogenase, mitochondrial precursor
gi 148747393	Hadha	trifunctional enzyme subunit alpha, mitochondrial precursor
gi 19424338	Hadhb	trifunctional enzyme subunit beta, mitochondrial precursor
gi 315630402	Hagh	hydroxyacylglutathione hydrolase, mitochondrial precursor
gi 14091775	Hao2	hydroxyacid oxidase 2
gi 6981010	Hba1	hemoglobin subunit alpha-1/2
gi 17985949	Hbb	hemoglobin subunit beta-1
gi 40445397	Hbb-b1	hemoglobin, beta adult major chain
gi 148540175	Hdhd2	haloacid dehalogenase-like hydrolase domain- containing protein 2 precursor
gi 162287194	Hdlbp	vigilin
gi 77539444	Hgs	hepatocyte growth factor-regulated tyrosine kinase substrate
gi 83977457	Hibadh	3-hydroxyisobutyrate dehydrogenase, mitochondrial precursor
gi 61556993	Hibch	3-hydroxyisobutyryl-CoA hydrolase
gi 157819527	Hint1	histidine triad nucleotide-binding protein 1
gi 164565401	Hint2	histidine triad nucleotide binding protein 2
gi 34853298	Hint3	PREDICTED: histidine triad nucleotide-binding protein 3
gi 198041635	Hip1r	huntingtin interacting protein 1 related isoform 1
gi 157821427	Hist1h1b	histone H1.5
gi 12025524	Hist1h2ba	histone H2B type 1-A
gi 403420588	Hist1h4m	histone H4
gi 162459050	Hist2h2ab	histone H2A
gi 6981022	Hk1	hexokinase-1
gi 6981026	Hmgb1	high mobility group protein B1
gi 392339776	Hmgb1 [#]	high mobility group protein B1
gi 392351997	Hmgb2	high mobility group box 2
gi 13242293	Hmgcl	hydroxymethylglutaryl-CoA lyase, mitochondrial
gi 157265559	Hnrnpa2b1	heterogeneous nuclear ribonucleoproteins A2/B1
gi 162329579	Hnrnpa3	heterogeneous nuclear ribonucleoprotein A3 isoform b
gi 140971918	Hnrnpab	heterogeneous nuclear ribonucleoprotein A/B
gi 62078769	Hnrnpb2	heterogeneous nuclear ribonucleoprotein H2
gi 16923998	Hnrnpk	heterogeneous nuclear ribonucleoprotein K
gi 197927211	Hnrnpl	heterogeneous nuclear ribonucleoprotein L isoform a

gi 158186698	Hnrnmp	heterogeneous nuclear ribonucleoprotein M isoform a
gi 148747541	Hnrnpu	heterogeneous nuclear ribonucleoprotein U
gi 18266700	Hnrph1	heterogeneous nuclear ribonucleoprotein H
gi 114145636	Hnrpq	heterogeneous nuclear ribonucleoprotein Q
gi 209869999	Hook3	protein Hook homolog 3
gi 40018592	Hp1bp3	heterochromatin protein 1-binding protein 3
gi 392356055	Hprt1	PREDICTED: hypoxanthine-guanine phosphoribosyltransferase
gi 16758014	Hpx	hemopexin precursor
gi 14269572	Hrsp12	ribonuclease UK114
gi 8393573	Hsd11b2	corticosteroid 11-beta-dehydrogenase isozyme 2
gi 13994225	Hsd17b10	3-hydroxyacyl-CoA dehydrogenase type-2
gi 162287198	Hsd17b4	peroxisomal multifunctional enzyme type 2
gi 47087119	Hsd17b8	estradiol 17-beta-dehydrogenase 8
gi 110835753	Hsd3b	3 beta-hydroxysteroid dehydrogenase/Delta 5-->4-isomerase type 2
gi 59797058	Hsd3b1	3 beta-hydroxysteroid dehydrogenase/Delta 5-->4-isomerase type 1
gi 71043858	Hsd12	hydroxysteroid dehydrogenase-like protein 2
gi 28467005	Hsp90aa1	heat shock protein HSP 90-alpha
gi 148747365	Hsp90ab1	heat shock protein HSP 90-beta
gi 210032365	Hsp90b1	endoplasmic precursor
gi 157818467 :reversed	Hspa12a	heat shock 70kDa protein 12A (Predicted), isoform CRA_a
gi 260064045	Hspa1a	heat shock 70 kDa protein 1A/1B
gi 24025637	Hspa4	heat shock 70 kDa protein 4
gi 25742763	Hspa5	78 kDa glucose-regulated protein precursor
gi 13242237	Hspa8	heat shock cognate 71 kDa protein
gi 410110929	Hspa9	stress-70 protein, mitochondrial
gi 94400790	Hspb1	heat shock protein beta-1
gi 206597443	Hspd1	60 kDa heat shock protein, mitochondrial
gi 6981052	Hspe1	10 kDa heat shock protein, mitochondrial
gi 58865372	Hsph1	heat shock protein 105 kDa
gi 157819535	Htra2	HtrA serine peptidase 2
gi 189339236	Htt	huntingtin
gi 77404380	Hyou1	hypoxia up-regulated protein 1 precursor
gi 392332936	Iars2	PREDICTED: isoleucine--tRNA ligase, mitochondrial
gi 157818919	Iba57	uncharacterized protein LOC363611
gi 6981076	Ide	insulin-degrading enzyme
gi 13928690	Idh1	isocitrate dehydrogenase
gi 62079055	Idh2	isocitrate dehydrogenase
gi 16758446	Idh3a	isocitrate dehydrogenase
gi 309951088	Ifi47	immunity-related GTPase family, M
gi 18266706	Ikbkap	elongator complex protein 1
gi 157823815	Ilvbl	ilvB (Bacterial acetolactate synthase)-like (Predicted)
gi 77917546	Immt	mitochondrial inner membrane protein

gi 14091736	Impa1	inositol monophosphatase 1
gi 157820505	Impdh1	inosine 5'-phosphate dehydrogenase 1
gi 392345809	Ints3	integrator complex subunit 3
gi 157820315	Ipo7	importin-7
gi 157821073	Ipo9	importin-9
gi 210032529	Iqgap1	IQ motif containing GTPase activating protein 1 (Predicted), isoform CRA_b
gi 392345265	Iqgap2	IQ motif containing GTPase activating protein 2
gi 62079215	Isoc1	isochorismatase domain-containing protein 1
gi 13591884	Itga1	Integrin alpha-1
gi 158303324	Itgb1	integrin beta-1 precursor
gi 313151177	Itih1	inter-alpha trypsin inhibitor, heavy chain 1 (Predicted)
gi 8393899	Itih3	inter-alpha-trypsin inhibitor heavy chain H3 precursor
gi 126722991	Itih4	inter alpha-trypsin inhibitor, heavy chain 4
gi 157821079	Itpa	inosine triphosphate pyrophosphatase
gi 6981112	Ivd	isovaleryl-CoA dehydrogenase, mitochondrial precursor
gi 55741637	Kars	lysine-tRNA ligase
gi 19424312	Khsrp	far upstream element-binding protein 2
gi 47155563	Kif13b	kinesin 13B
gi 83776543	Kif5b	kinesin-1 heavy chain
gi 8393610	Kpnb1	importin subunit beta-1
gi 392353440	Ktn1	PREDICTED: LOW QUALITY PROTEIN: kinectin
gi 157821989	Lage3	L antigen family, member 3
gi 40254785	Lamp2	lysosome-associated membrane glycoprotein 2 precursor
gi 58865398	Lap3	cytosol aminopeptidase
gi 8393706	Ldha	L-lactate dehydrogenase A chain
gi 54400736	Letm1	LETM1 and EF-hand domain-containing protein 1, mitochondrial precursor
gi 9845261	Lgals1	galectin-1
gi 6981154	Lgals5	galectin-5
gi 77917572	Lipa	lysosomal acid lipase/cholesteryl ester hydrolase precursor
gi 50355947	Lmna	prelamin-A/C isoform C2
gi 16758782	Lmnbl	lamin-B1
gi 164448680	LOC100134871	hemoglobin subunit beta-2
gi 392340011	LOC100360057	PREDICTED: 60S ribosomal protein L22-like
gi 392340776	LOC100360180	PREDICTED: 6-phosphogluconate dehydrogenase
gi 293353258	LOC100360491	PREDICTED: 60S ribosomal protein L13-like
gi 398303848	LOC100360501	ribonuclease inhibitor isoform a
gi 392332289	LOC100360601	carbonyl reductase 2-like
gi 392349506	LOC100360868	PREDICTED: histone H3.3-like
gi 392354356	LOC100362339	PREDICTED: 40S ribosomal protein S19-like
gi 392334162	LOC100362479	PREDICTED: 60S ribosomal protein L15-like

gi 392343218	LOC100362640	PREDICTED: 40S ribosomal protein S4, X isoform-like
gi 392348563	LOC100362830	PREDICTED: 40S ribosomal protein S7-like
gi 392346819	LOC100363271	PREDICTED: 40S ribosomal protein S2-like
gi 392341003	LOC100363439	PREDICTED: 40S ribosomal protein S10-like
gi 392343176	LOC100363782	PREDICTED: ras-related protein Rab-1B-like
gi 392355306	LOC100364062	PREDICTED: pyruvate kinase isozymes M1/M2-like
gi 392343927	LOC100364427	40S ribosomal protein S12
gi 392345917	LOC100909441	PREDICTED: tubulin alpha-1C chain-like isoform 2
gi 392343762	LOC100909466	PREDICTED: 40S ribosomal protein S9-like
gi 392346424	LOC100909983	PREDICTED: acidic leucine-rich nuclear phosphoprotein 32 family member A-like
gi 392354394	LOC100910554	histone H2A
gi 300797934	LOC100911178	Protein LOC100911178
gi 392344353	LOC100911186	PREDICTED: enoyl-CoA hydratase, mitochondrial-like
gi 392355494	LOC100911286	PREDICTED: proSAAS-like
gi 392350599	LOC100911515	PREDICTED: triosephosphate isomerase-like
gi 392344748	LOC100911575	PREDICTED: 60S acidic ribosomal protein P2-like
gi 403420634	LOC100911576	heterogeneous nuclear ribonucleoproteins C1/C2-like
gi 392349606	LOC100911597	PREDICTED: myosin-9-like
gi 392340703	LOC100911847	PREDICTED: 40S ribosomal protein S14-like
gi 392346176	LOC100911966	PREDICTED: 60S ribosomal protein L7a-like
gi 392344389	LOC100911991	PREDICTED: elongation factor 1-alpha 1-like
gi 392348146	LOC100912024	PREDICTED: uncharacterized protein LOC100912024
gi 392353337	LOC100912032	PREDICTED: ubiquitin-40S ribosomal protein S27a-like
gi 392351429	LOC100912146	PREDICTED: AP-1 complex subunit beta-1-like
gi 392332261	LOC100912203	PREDICTED: carbonyl reductase
gi 198278428	LOC100912534	Protein LOC100912534
gi 392342833	LOC100912917	PREDICTED: phosphoribosylformylglycinamide synthase-like, partial
gi 392352643	LOC101552443	ubiquitin-40S ribosomal protein S27a-like
gi 392356141	LOC101992510	40S ribosomal protein S25-like
gi 392355778	LOC103234934	40S ribosomal protein S26-like
gi 32563565	LOC299282	serine protease inhibitor
gi 114145740	LOC306079	LRRGT00066
gi 66730521	LOC501110	glutathione S-transferase A6
gi 392354344	LOC679994	PREDICTED: uncharacterized protein LOC679994
gi 392354401	LOC680498	similar to CG31613-PA
gi 392354145	LOC681410	PREDICTED: heterogeneous nuclear

gi 109494630	LOC681544	ribonucleoprotein A0-like
gi 114158668	LOC682105	similar to histidine-rich glycoprotein
gi 392347927	LOC683961	receptor expression-enhancing protein 2
gi 392343883	LOC684270	PREDICTED: 40S ribosomal protein S13-like
		PREDICTED: isochorismatase domain-containing protein 2A, mitochondrial-like isoform 2
gi 392354330	LOC684681	PREDICTED: uncharacterized protein LOC684681
gi 392337504	LOC687295	PREDICTED: mitochondrial import inner membrane translocase subunit TIM50-like isoform 2
gi 19173766	Lonp1	ion protease homolog, mitochondrial precursor
gi 56605990	Lrprrc	leucine-rich PPR motif-containing protein, mitochondrial precursor
gi 71795621	Lta4h	leukotriene A-4 hydrolase
gi 6981362	Lypla1	acyl-protein thioesterase 1
gi 13786178	Lypla2	acyl-protein thioesterase 2
gi 157787089	Lyplal1	lysophospholipase-like 1 (Predicted)
gi 21326475	Macrodl,	acetyl-ADP-ribose deacetylase MACROD1
gi 189339241	Man2a1	alpha-mannosidase 2
gi 21245094	Man2c1	alpha-mannosidase 2C1
gi 270288740	Maoa	monoamine oxidase A
gi 66730360	Map4	microtubule-associated protein 4
gi 62461582	Mapk14	mitogen activated protein kinase 14
gi 78097100	Mapre1	microtubule-associated protein RP/EB family member 1
gi 402744019	Marcks	myristoylated alanine-rich C-kinase substrate
gi 189083764	Mars	methionine-tRNA ligase, cytoplasmic
gi 61889073	Matr3	matrin-3
gi 57528264	Mccc1	methylcrotonoyl-CoA carboxylase subunit alpha, mitochondrial
gi 58865926	Mccc2	methylcrotonoyl-CoA carboxylase beta chain, mitochondrial
gi 15100179	Mdh1	malate dehydrogenase, cytoplasmic
gi 42476181	Mdh2	malate dehydrogenase, mitochondrial precursor
gi 157823059	Mdp1	magnesium-dependent phosphatase 1
gi 158341689	Me1	NADP-dependent malic enzyme
gi 8393848	Mecr	trans-2-enoyl-CoA reductase, mitochondrial precursor
gi 157818123	Mgarp	mitochondria-localized glutamic acid-rich protein
gi 18777747	Mgea5	meningioma expressed antigen 5 (hyaluronidase)
gi 19923092	Mgll	monoglyceride lipase
gi 19705453	Mgst1	microsomal glutathione S-transferase 1
gi 300797728	Mgst3	microsomal glutathione S-transferase 3
gi 117647218	Mpc2	mitochondrial pyruvate carrier 2
gi 20304123	Mpst	3-mercaptopyruvate sulfurtransferase

gi 148277635	Mpv17l	MPV17 mitochondrial membrane protein-like
gi 157822935	Mrc1	mannose receptor, C type 1
gi 58219514	Mri1	methylthioribose-1-phosphate isomerase
gi 16758936	Mrp5	multidrug resistance-associated protein 5
gi 81295383	Mrpl47	mitochondrial ribosomal protein L47
gi 13540689	Msn	moesin
gi 114145534	Mtap	methylthioadenosine phosphorylase precursor
gi 197313797	Mtch1	mitochondrial carrier homolog 1
gi 158819029	Mtch2	mitochondrial carrier homolog 2
gi 11968082	Mthfd1	C-1-tetrahydrofolate synthase, cytoplasmic
gi 157820897	Mthfd2	methylenetetrahydrofolate dehydrogenase 2
gi 125630382	Mtus1	microtubule-associated tumor suppressor 1 homolog
gi 56605654	Mtx2	metaxin-2
gi 12831225	Mug1	murinoglobulin-1 precursor
gi 392342260	Mut	methylmalonyl CoA mutase
gi 41055865	Mvp	major vault protein
gi 13928926	Mybbp1a	myb-binding protein 1A
gi 203097140	Myl12a	myosin regulatory light chain RLC-A
gi 157823377	Myl6	myosin light polypeptide 6
gi 287328046	Myo18a	myosin 18a
gi 124107592	Myo1c	unconventional myosin-Ic
gi 56799396	Myo1d	unconventional myosin-Id
gi 300798598	Myof	myoferlin
gi 157786942	Naca	nascent polypeptide-associated complex subunit alpha isoform 1
gi 112984180	Nadkd1	NAD kinase domain-containing protein 1, mitochondrial
gi 164663874	Nans	N-acetylneuraminic acid synthase
gi 161760644	Ncl	nucleolin
gi 399498533	Ndrp2	N-Myc Downstream Regulator 2
gi 114145517	Ndufa8	NADH dehydrogenase
gi 198278533	Ndufa9	NADH dehydrogenase
gi 157822175	Ndufb10	NADH dehydrogenase
gi 53850628	Ndufs1	NADH-ubiquinone oxidoreductase 75 kDa subunit, mitochondrial precursor
gi 56606108	Ndufs7	NADH dehydrogenase (ubiquinone) Fe-S protein 7
gi 158186672	Nedd4	E3 ubiquitin-protein ligase NEDD4
gi 392346880	Nfs1	NFS1 nitrogen fixation 1 homolog (S. cerevisiae)
gi 282154799	Nfu1	histone cell cycle regulation defective interacting protein 5 (Predicted)
gi 209969744	Nipsnap1	4-nitrophenylphosphatase domain and non-neuronal SNAP25-like protein homolog 1
gi 128485844	Nit1	nitrilase homolog 1 isoform b
gi 77628000	Nit2	omega-amidase NIT2
gi 19924089	Nme1	nucleoside diphosphate kinase A
gi 55926145	Nme2	nucleoside diphosphate kinase B

gi 16758266	Nme3	nucleoside diphosphate kinase 3 precursor
gi 61557127	Nnt	NAD(P) transhydrogenase, mitochondrial
gi 157816949	Nomo1	nodal modulator 1 precursor
gi 59891440	Nono	non-POU domain-containing octamer-binding protein
gi 311771778	Npc1	Niemann-Pick disease, type C1
gi 158749540	Npepps	puromycin-sensitive aminopeptidase precursor
gi 7242160	Npm1	nucleophosmin
gi 109463944	Npm3	nucleophosmin/nucleoplasmin 3
gi 13489067	Nsf	N-ethylmaleimide-sensitive factor
gi 403225015	Nt5c	5', 3'-nucleotidase, cytosolic
gi 403420618	Numa1	nuclear mitotic apparatus protein 1
gi 157820537	Nup205	nucleoporin 205kDa (Predicted)
gi 270483728	Nup214	nucleoporin 214
gi 58865420	Nup93	nuclear pore complex protein Nup93
gi 62945278	Ogdh	2-oxoglutarate dehydrogenase, mitochondrial precursor
gi 148747459	Opa1	dynammin-like 120 kDa protein, mitochondrial precursor
gi 189303591	Osgep	probable tRNA threonylcarbamoyladenosine biosynthesis protein Osgep
gi 61889110	Ostf1	osteoclast-stimulating factor 1
gi 157821731	Otub1	ubiquitin thioesterase OTUB1
gi 189181716	Oxct1	succinyl-CoA:3-ketoacid coenzyme A transferase 1, mitochondrial precursor
gi 6981324	P4hb	protein disulfide-isomerase precursor
gi 51948384	Pa2g4	proliferation-associated protein 2G4
gi 19705459	Pabpc1	polyadenylate-binding protein 1
gi 11693154	Pafah1b2	platelet-activating factor acetylhydrolase IB subunit beta
gi 16924002	Park7	protein DJ-1 isoform 2
gi 300793858	Parp14	poly (ADP-ribose) polymerase family, member 14
gi 31543464	Pc	pyruvate carboxylase, mitochondrial precursor
gi 392340090	Pcbp1	PREDICTED: poly(rC)-binding protein 1, partial KH-I, K homology RNA-binding domain, type I
gi 158303308	Pcca	propionyl-CoA carboxylase alpha chain, mitochondrial
gi 148747119	Pccb	propionyl coenzyme A carboxylase, beta polypeptide
gi 56961640	Pcmt1	protein-L-isoaspartate(D-aspartate) O-methyltransferase
gi 157818653	Pdcd6	programmed cell death 6 (Predicted)
gi 210032180	Pdcd6ip	programmed cell death 6-interacting protein
gi 396578149	Pde2a	phosphodiesterase 2A, cGMP-stimulated
gi 124430510	Pdha1	pyruvate dehydrogenase E1 component subunit alpha, somatic form, mitochondrial precursor
gi 56090293	Pdhb	pyruvate dehydrogenase E1 component subunit

		beta, mitochondrial precursor
gi 8393322	Pdia3	protein disulfide-isomerase A3 precursor
gi 16758712	Pdia4	protein disulfide-isomerase A4 precursor
gi 52345385	Pdia6	protein disulfide-isomerase A6 precursor
gi 13929082	Pdxk	pyridoxal kinase
gi 61557370	Pea15	astrocytic phosphoprotein PEA-15
gi 8393910	Pebp1	phosphatidylethanolamine-binding protein 1
gi 157786806	Pfas	phosphoribosylformylglycinamide synthase
gi 6981352	Pfk1	6-phosphofructokinase, liver type
gi 57977273	Pfkip	6-phosphofructokinase type C
gi 42476144	Pfn1	profilin-1
gi 16757984	Pgam1	phosphoglycerate mutase 1
gi 8393948	Pgam2	phosphoglycerate mutase 2
gi 40254752	Pgk1	phosphoglycerate kinase 1
gi 157823471	Pgls	6-phosphogluconolactonase
gi 77627971	Pgm1	phosphoglucomutase-1
gi 11120720	Pgrmc1	membrane-associated progesterone receptor component 1
gi 56605824	Pgrmc2	membrane-associated progesterone receptor component 2
gi 13937353	Phb	prohibitin
gi 61556754	Phb2	prohibitin-2
gi 164663846	Phpt1	phosphohistidine phosphatase 1
gi 25742825	Pi4ka	phosphatidylinositol 4-kinase alpha
gi 16758324	Picalm	phosphatidylinositol-binding clathrin assembly protein
gi 157817696	Pin1	peptidyl-prolyl cis-trans isomerase NIMA-interacting 1
gi 157819139	Pitrm1	pitrilysin metallopeptidase 1 (Predicted)
gi 158341684	Plaa	phospholipase A-2-activating protein
gi 62078583	Plbd1	phospholipase B-like 1
gi 256221749	Plec	plectin isoform 1d
gi 16758216	Plg	plasminogen
gi 157821883	Plxnb2	plexin-B2 precursor
gi 54234052	Pmpca	mitochondrial-processing peptidase subunit alpha
gi 11693166	Pmpcb	Mitochondrial-processing peptidase subunit beta
gi 158081717	Pnmt	phenylethanolamine N-methyltransferase
gi 157822819	Pnp	purine nucleoside phosphorylase
gi 293351610	POLR2A	polymerase (RNA) II (DNA directed) polypeptide A
gi 13928780	Por	NADPH-cytochrome P450 reductase
gi 213972586	Ppa1	inorganic pyrophosphatase
gi 8394009	Ppia	peptidyl-prolyl cis-trans isomerase A
gi 11968126	Ppib	peptidyl-prolyl cis-trans isomerase B precursor
gi 28461153	Ppm1f	protein phosphatase 1F
gi 11968062	Ppp1cc	serine/threonine-protein phosphatase PP1-gamma catalytic subunit isoform 1

gi 57634526	Ppp1r7	protein phosphatase 1 regulatory subunit 7
gi 55926139	Ppp2r1a	serine/threonine-protein phosphatase 2A 65 kDa regulatory subunit A alpha isoform
gi 16758910	Ppp2r2a	serine/threonine-protein phosphatase 2A 55 kDa regulatory subunit B alpha isoform
gi 157819489	Ppp2r4	serine/threonine-protein phosphatase 2A activator
gi 16923958	Prdx1	peroxiredoxin-1
gi 8394432	Prdx2	peroxiredoxin-2
gi 11968132	Prdx3	thioredoxin-dependent peroxide reductase, mitochondrial precursor
gi 16758404	Prdx5	peroxiredoxin-5, mitochondrial precursor
gi 16758348	Prdx6	peroxiredoxin-6
gi 117647220	Prkacb	cAMP-dependent protein kinase catalytic subunit beta
gi 6981396	Prkar1a	cAMP-dependent protein kinase type I-alpha regulatory subunit
gi 157818781	Prkcsh	glucosidase 2 subunit beta precursor
gi 300797649	Prpf8	pre-mRNA-processing-splicing factor 8
gi 8394060	Psma1	proteasome subunit alpha type-1
gi 8394063	Psma2	proteasome subunit alpha type-2
gi 76573881	Psma3l	proteasome subunit alpha type-3
gi 8394069	Psma4	proteasome subunit alpha type-4
gi 8394072	Psma5	proteasome subunit alpha type-5
gi 8394076	Psma6	proteasome subunit alpha type-6
gi 56550075	Psma7	proteasome subunit alpha type-7
gi 16758370	Psmb1	proteasome subunit beta type-1 precursor
gi 71043724	Psmb10	proteasome subunit beta type-10
gi 8394079	Psmb2	proteasome subunit beta type-2
gi 8394082	Psmb3	proteasome subunit beta type-3
gi 13928866	Psmb4	Proteasome subunit beta type-4
gi 54019419	Psmb6	proteasome subunit beta type-6
gi 258614012	Psmb8	proteasome subunit beta type-8
gi 258614009	Psmb9	proteasome subunit beta type-9
gi 25742677	Psmc4	26S protease regulatory subunit 6B
gi 14010879	Psmd1	26S proteasome non-ATPase regulatory subunit 1
gi 157821581	Psmd13	26S proteasome non-ATPase regulatory subunit 13
gi 72255509	Psmd2	26S proteasome non-ATPase regulatory subunit 2
gi 61098214	Psme1	proteasome activator subunit 1
gi 392334544	Psme2	proteasome activator subunit 2
gi 402765974	Ptbp1	polypyrimidine tract binding protein 1
gi 197927097	Ptcd3	pentatricopeptide repeat-containing protein 3, mitochondrial
gi 157822395	Ptges2	prostaglandin E synthase 2
gi 195976800	Ptges3	prostaglandin E synthase 3
gi 20302022	Ptgr1	prostaglandin reductase 1

gi 157819829	Ptplad1	protein tyrosine phosphatase-like A domain containing 1
gi 157787111	Ptpmt1	phosphatidylglycerophosphatase and protein-tyrosine phosphatase 1
gi 309384274	Ptpn23	tyrosine-protein phosphatase non-receptor type 23
gi 392354626	Pura	PREDICTED: transcriptional activator protein Pur-alpha isoform 1
gi 62945366	Purb	transcriptional activator protein Pur-beta
gi 158187544	Pygb	glycogen phosphorylase, brain form
gi 51948490	Pyroxd2	pyridine nucleotide-disulfide oxidoreductase domain-containing protein 2
gi 307746876	Pzp	alpha-1-macroglobulin precursor
gi 56090285	Qars	glutaminyl-tRNA synthetase
gi 11693160	Qdpr	dihydropteridine reductase
gi 61889071	Rab10	ras-related protein Rab-10
gi 14249144	Rab11b	ras-related protein Rab-11B
gi 16758368	Rab14	ras-related protein Rab-14
gi 45433570	Rab1a	ras-related protein Rab-1A
gi 51948448	Rab21	ras-related protein Rab-21
gi 13929006	Rab2a	ras-related protein Rab-2A
gi 61556789	Rab35	ras-related protein Rab-35
gi 13592037	Rab3b	ras-related protein Rab-3B
gi 281604211	Rab3gap2	rab3 GTPase-activating protein non-catalytic subunit
gi 121583768	Rab5b	ras-related protein Rab-5B
gi 347800697	Rab5c	ras-related protein Rab-5C
gi 213972608	Rab6a	ras-related protein Rab-6A
gi 13027392	Rab7a	ras-related protein Rab-7a
gi 162287395	Rab8a	ras-related protein Rab-8A
gi 54607147	Rac1	ras-related C3 botulinum toxin substrate 1 precursor
gi 16758182	Ran	GTP-binding nuclear protein Ran
gi 349501086	Rangap1	Ran GTPase activating protein 1
gi 52138628	Rap1b	ras-related protein Rap-1b precursor
gi 157817007	Rbbp4	histone-binding protein RBBP4
gi 158187535	Rbp4	retinol binding protein 4, plasma
gi 40363270	Rdh2	retinol dehydrogenase 2
gi 56799432	Rdx	radixin
gi 270288782	Reep5	receptor expression-enhancing protein 5
gi 21489985	Retsat	all-trans-retinol 13,14-reductase
gi 51948422	RGD1303003	ES1 protein homolog, mitochondrial precursor
gi 62079139	RGD1309534	ester hydrolase C11orf54 homolog
gi 157819755	RGD1309586	uncharacterized protein LOC364073
gi 62079015	RGD1309676	redox-regulatory protein FAM213A
gi 281427190	RGD1309922	uncharacterized protein LOC306007
gi 157818445	RGD1564804	protein RGD1564804
gi 109484558	RGD1565368	PREDICTED: glyceraldehyde-3-phosphate dehydrogenase-like

gi 13928740	Rgn	regucalcin
gi 16923986	Rhoa	transforming protein RhoA precursor
gi 157819711	Rhot1	mitochondrial Rho GTPase 1
gi 81295355	Rmdn2	regulator of microtubule dynamics 2
gi 62078823	Rmdn3	regulator of microtubule dynamics protein 3
gi 13592053	Rpl10	60S ribosomal protein L10
gi 71043900	Rpl11	60S ribosomal protein L11
gi 157822227	Rpl12	60S ribosomal protein L12
gi 77404207	Rpl13a	60S ribosomal protein L13a
gi 13592057	Rpl18	60S ribosomal protein L18
gi 47059006	Rpl18a	60S ribosomal protein L18a
gi 14389297	Rpl19	60S ribosomal protein L19
gi 392343039	Rpl21	ribosomal protein L21
gi 56090279	Rpl23	60S ribosomal protein L23
gi 11968096	Rpl24	60S ribosomal protein L24
gi 157786616	Rpl26	60S ribosomal protein L26
gi 293353295	Rpl28	ribosomal protein L28
gi 12083659	Rpl30	60S ribosomal protein L30
gi 392340583	Rpl32	60S ribosomal protein L32
gi 47059004	Rpl35	60S ribosomal protein L35
gi 11968086	Rpl4	60S ribosomal protein L4
gi 13592051	Rpl5	60S ribosomal protein L5
gi 162287391	Rpl6	60S ribosomal protein L6
gi 198278505	Rpl7	60S ribosomal protein L7
gi 145207974	Rpl9	60S ribosomal protein L9
gi 11693176	Rplp0	60S acidic ribosomal protein P0
gi 56090277	Rplp1	60S acidic ribosomal protein P1
gi 6981486	Rpn1	dolichyl-diphosphooligosaccharide-protein glycosyltransferase subunit 1 precursor
gi 13928974	Rpn2	dolichyl-diphosphooligosaccharide-protein glycosyltransferase subunit 2 precursor
gi 13592071	Rps11	40S ribosomal protein S11
gi 8394212	Rps15	40S ribosomal protein S15
gi 392345425	Rps15a2	40S ribosomal protein S15a-like
gi 310703682	Rps16	40S ribosomal protein S16
gi 297515469	Rps17	40S ribosomal protein S17
gi 56090271	Rps20	40S ribosomal protein S20
gi 17530965	Rps23	40S ribosomal protein S23
gi 57164151	Rps3	40S ribosomal protein S3
gi 157786754	Rps5	40S ribosomal protein S5
gi 392348112	Rps6	40S ribosomal protein S6
gi 13928986	Rps8	40S ribosomal protein S8
gi 8393693	Rpsa	40S ribosomal protein SA
gi 157824216	Rras	Ras-related protein R-Ras
gi 157821061	Rsu1	ras suppressor protein 1
gi 158261988	Rtn3	reticulon-3 isoform A1
gi 13929188	Rtn4	reticulon-4
gi 16758640	Sacm11	phosphatidylinositide phosphatase SAC1

gi 56090263	Sar1a	GTP-binding protein SAR1a
gi 57528164	Sar1b	GTP-binding protein SAR1b
gi 25742657	Sardh	sarcosine dehydrogenase, mitochondrial
gi 158749626	Scamp1	secretory carrier-associated membrane protein 1
gi 13928730	Scarb1	scavenger receptor class B member 1
gi 16758914	Scarb2	lysosome membrane protein 2 precursor
gi 12083601	Scg2	secretogranin-2 precursor
gi 50356003	Scp2	non-specific lipid-transfer protein
gi 19173736	Scpep1	retinoid-inducible serine carboxypeptidase
gi 18426858	Sdha	succinate dehydrogenase complex, subunit A, flavoprotein (Fp)
gi 209915614	Sdhb	succinate dehydrogenase
gi 71043604	Sec22b	vesicle-trafficking protein SEC22b precursor
gi 157786714	Sec23a	protein transport protein Sec23A
gi 14717392	Sec31a	SEC31 homolog A (<i>S. cerevisiae</i>)
gi 40538882	Sec61a1	protein transport protein Sec61 subunit alpha isoform 1
gi 157820673	Sec61b	protein transport protein Sec61 subunit beta
gi 157821523	Sept11	septin-11
gi 16924010	Sept2	septin-2
gi 51036655	Serpina1	alpha-1-antiproteinase
gi 347800746	Serpina3k	serine protease inhibitor A3K precursor
gi 40018548	Serpib6	serpin B6
gi 56090431	Serpib9	serpin B9
gi 8393057	Serpinh1	serpin H1 precursor
gi 157821905	Sf3a1	splicing factor 3a, subunit 1
gi 189339231	Sf3b1	splicing factor 3b, subunit 1
gi 297207121	Sf3b3	splicing factor 3B subunit 3
gi 70778983	Sfpq	splicing factor, proline- and glutamine-rich
gi 58865994	Sfxn1	sideroflexin-1
gi 290563454	Sh3bgr1	SH3 domain-binding glutamic acid-rich-like protein
gi 56090475	Skp1	S-phase kinase-associated protein 1
gi 293355421	Slc18b1	solute carrier family 18, subfamily B, member 1
gi 347921120	Slc23a2	solute carrier family 23 member 2
gi 8394297	Slc25a1	tricarboxylate transport protein, mitochondrial precursor
gi 19173788	Slc25a10	mitochondrial dicarboxylate carrier
gi 11693170	Slc25a11	mitochondrial 2-oxoglutarate/malate carrier protein
gi 52138624	Slc25a20	mitochondrial carnitine/acylcarnitine carrier protein
gi 19424330	Slc25a21	mitochondrial 2-oxodicarboxylate carrier
gi 189011598	Slc25a24	calcium-binding mitochondrial carrier protein SCaMC-1
gi 399124780	Slc25a3	phosphate carrier protein, mitochondrial isoform 2 precursor
gi 61557225	Slc25a30	kidney mitochondrial carrier protein 1
gi 32189355	Slc25a4	ADP/ATP translocase 1

gi 32189350	Slc25a5	ADP/ATP translocase 2
gi 157823505	Slc27a3	solute carrier family 27 (fatty acid transporter), member 3
gi 402743472	Slc3a2	4F2 cell-surface antigen heavy chain isoform 1
gi 82734227	Slc41a3	solute carrier family 41 member 3
gi 76443687	Slc4a1	band 3 anion transport protein
gi 396080336	Slco1b2	solute carrier organic anion transporter family member 1B2
gi 77404395	Snd1	staphylococcal nuclease domain-containing protein 1
gi 281371480	Snrnp200	U5 small nuclear ribonucleoprotein 200 kDa helicase
gi 157818069	Snrpd1	small nuclear ribonucleoprotein Sm D1
gi 157820925	Snrpd2	small nuclear ribonucleoprotein D2 polypeptide
gi 13592087	Soat1	sterol O-acyltransferase 1
gi 8394328	Sod1	superoxide dismutase 1
gi 8394331	Sod2	superoxide dismutase 2
gi 16758606	Sorbs2	sorbin and SH3 domain-containing protein 2
gi 397529553	Spg20	spastic paraplegia 20
gi 158711683	Spr	sepiapterin reductase
gi 83642822	Spryd4	SPRY domain-containing protein 4
gi 158533972	Spta1	erythroid spectrin alpha
gi 31543764	Sptan1	spectrin alpha chain, non-erythrocytic 1
gi 47058982	Sptb	spectrin beta chain, erythrocyte
gi 61557085	Sptbn1	spectrin beta chain, brain 1
gi 282158053	Srp72	signal recognition particle 72
gi 61676217	Srprb	signal recognition particle receptor subunit beta
gi 157818019	Srsf1	splicing factor, arginine/serine-rich 1B
gi 114145746	Srsf3	splicing factor, arginine/serine-rich 3
gi 8394364	Ssr4	translocon-associated protein subunit delta precursor
gi 13928754	Star	steroidogenic acute regulatory protein
gi 77695926	Stat1	signal transducer and activator of transcription
gi 20302113	Stip1	stress-induced-phosphoprotein 1
gi 58865500	Stom	stomatin
gi 72255527	Stoml2	stomatin-like protein 2, mitochondrial
gi 77695930	Stx12	syntaxin-12
gi 158749584	Suc1a2	succinyl-CoA ligase
gi 139948224	Suc1g1	succinyl-CoA ligase
gi 189491689	Suc1g2	succinate-CoA ligase, GDP-forming, beta subunit
gi 19424298	Sumo2	small ubiquitin-related modifier 2 precursor
gi 76443685	Surf4	surfeit 4
gi 61557028	Tagln2	transgelin-2
gi 42476292	Taldo1	transaldolase
gi 58865526	Tardbp	TAR DNA binding protein
gi 55741823	Tars	threonine-tRNA ligase, cytoplasmic
gi 62078811	Tars2	threonine-tRNA ligase, mitochondrial

gi 13592105	Tceb2	transcription elongation factor B polypeptide 2
gi 6981642	Tcp1	T-complex protein 1 subunit alpha
gi 19924091	Tecr	very-long-chain enoyl-CoA reductase
gi 86129590	Tes	testin
gi 61556986	Tf	serotransferrin precursor
gi 6981652	Th	tyrosine 3-monooxygenase
gi 392339355	Timm23	translocase of inner mitochondrial membrane 23 homolog (yeast)
gi 8394449	Timm44	mitochondrial import inner membrane translocase subunit TIM44
gi 157823439	Tjp1	tight junction protein 1
gi 12018252	Tkt	transketolase
gi 189181726	Tln1	talin-1
gi 293361202	Tln2	PREDICTED: talin-2
gi 392352824	Tmco1	transmembrane and coiled-coil domains 1
gi 16758214	Tmed10	transmembrane emp24 domain-containing protein 10 precursor
gi 57528337	Tmed9	transmembrane emp24 domain-containing protein 9
gi 11067391	Tmem33	transmembrane protein 33 isoform 1
gi 67078422	Tmx1	thioredoxin-related transmembrane protein 1 precursor
gi 300796899	Tns1	tensin 1
gi 47058998	Tomm22	mitochondrial import receptor subunit TOM22 homolog
gi 291045133	Top2b	DNA topoisomerase 2
gi 166157530	Tp53i3	tumor protein p53 inducible protein 3
gi 78000203	Tpm1	tropomyosin alpha-1 chain isoform i
gi 29336093	Tpm3	tropomyosin alpha-3 chain
gi 6981672	Tpm4	tropomyosin alpha-4 chain
gi 13786206	Tpp1	tripeptidyl-peptidase 1 precursor
gi 13592121	Tpp2	tripeptidyl-peptidase 2
gi 158508582	Tpr	translocated promoter region
gi 16758734	Tpt1	translationally-controlled tumor protein
gi 84781723	Trap1	heat shock protein 75 kDa, mitochondrial precursor
gi 209870077	Trim28	transcription intermediary factor 1-beta
gi 11120712	Tsn	translin
gi 6978575	Tspo	translocator protein
gi 57528682	Tst	thiosulfate sulfurtransferase
gi 209571551	Ttll12	tubulin-tyrosine ligase-like protein 12
gi 333033763	Ttr	transthyretin precursor
gi 112984124	Tuba1b	tubulin alpha-1B chain
gi 40018568	Tubb4b	tubulin beta-4B chain
gi 27465535	Tubb5	tubulin beta-5 chain
gi 157820845	Tufm	elongation factor Tu, mitochondrial precursor
gi 16758644	Txn	thioredoxin
gi 404501500	Txndc5	thioredoxin Domain Containing 5 (Endoplasmic Reticulum)

gi 18266686	Txn1l	thioredoxin-like protein 1
gi 78191795	Txnrd1	thioredoxin reductase 1, cytoplasmic
gi 12018236	Txnrd2	thioredoxin reductase 2, mitochondrial
gi 62078893	Uba1	ubiquitin-like modifier-activating enzyme 1
gi 197384571	Uba2	SUMO-activating enzyme subunit 2
gi 157821599	Uba6	ubiquitin-like modifier-activating enzyme 6
gi 82617581	Ube2d2	ubiquitin-conjugating enzyme E2 D2
gi 16758810	Ube2n	ubiquitin-conjugating enzyme E2 N
gi 188536073	Ube2v1	ubiquitin-conjugating enzyme E2 variant 1
gi 157818175	Ubqln2	ubiquilin-2
gi 84781733	Ubr4	E3 ubiquitin-protein ligase UBR4
gi 61098212	Uchl1	ubiquitin carboxyl-terminal hydrolase isozyme L1
gi 158749588	Uchl3	ubiquitin carboxyl-terminal hydrolase isozyme L3
gi 51172600	Ufc1	ubiquitin-fold modifier-conjugating enzyme 1
gi 13786146	Ugdh	UDP-glucose 6-dehydrogenase
gi 19424302	Uggt1	UDP-glucose:glycoprotein glucosyltransferase 1 precursor
gi 83320084	Unc45a	protein unc-45 homolog A
gi 56090401	UPF0598	UPF0598 protein C8orf82 homolog
gi 392353859	Upf1	up-Frameshift Suppressor 1 Homolog
gi 51948476	Uqcrc1	cytochrome b-c1 complex subunit 1, mitochondrial precursor
gi 55741544	Uqcrc2	cytochrome b-c1 complex subunit 2, mitochondrial precursor
gi 57114330	Uqcrfs1	cytochrome b-c1 complex subunit Rieske, mitochondrial
gi 158749613	Urod	uroporphyrinogen decarboxylase
gi 9507177	Uso1	general vesicular transport factor p115
gi 157819971	Usp5	ubiquitin carboxyl-terminal hydrolase 5
gi 67078438	Usp7	ubiquitin carboxyl-terminal hydrolase 7
gi 209571464	Usp9x	probable ubiquitin carboxyl-terminal hydrolase FAF-X isoform 1
gi 6981696	Utrn	utrophin
gi 118142811	Vapa	vesicle-associated membrane protein-associated protein A
gi 11177880	Vapb	vesicle-associated membrane protein-associated protein B
gi 158186770	Vars	valine-tRNA ligase
gi 76096306	Vat1	synaptic vesicle membrane protein VAT-1 homolog
gi 157822133	Vcl	vinculin
gi 17865351	Vcp	transitional endoplasmic reticulum ATPase
gi 13786200	Vdac1	voltage-dependent anion-selective channel protein 1
gi 13786202	Vdac2	voltage-dependent anion-selective channel protein 2
gi 13786204	Vdac3	voltage-dependent anion-selective channel

gi 14389299	Vim	protein 3
gi 219275534	Vps13a	vimentin
gi 205360969	Vps35	vacuolar protein sorting 13 homolog A
gi 162287178	Vtn	maternal embryonic message 3
gi 392346920	Vwa5a	vitronectin
gi 392353662	Vwa8	von Willebrand factor A domain containing 5A
gi 62078997	Wdr1	von Willebrand factor A domain containing 8
gi 293356234	Wdr11	WD repeat-containing protein 1
gi 13929176	Wfs1	PREDICTED: WD repeat-containing protein 11
gi 8394544	Xdh	wolfram syndrome 1
gi 18777778	Xpnpep1	xanthine dehydrogenase/oxidase
gi 29789299	Xpo1	xaa-Pro aminopeptidase 1
gi 405113040	Xpo7	exportin-1
gi 92373398	Ybx1	exportin-7
gi 9507243	Ywhab	Y box binding protein 1
gi 13928824	Ywhae	14-3-3 protein beta/alpha
gi 9507245	Ywhag	14-3-3 protein epsilon
gi 6981710	Ywhah	14-3-3 protein gamma
gi 6981712	Ywhaq	14-3-3 protein eta
gi 62990183	Ywhaz	14-3-3 protein theta
gi 27545350 :reversed	Yy1	14-3-3 protein zeta/delta
gi 157817316	Zadh2	YY1 transcription factor
		zinc-binding alcohol dehydrogenase domain-containing protein 2

Table A2. Individual proteins differentially expressed at one or more time points*

Gene identifier	Symbol	Name
gi 209862801	Aars	alanyl-tRNA synthetase
gi 16758936	Abcc5	ATP-binding cassette, sub-family C, member 5
gi 158081775	Abcf1	ATP-binding cassette sub-family F member 1
gi 56090461	Abhd14b	alpha/beta hydrolase domain-containing protein 14B
gi 157820211	Abhd3	Abhydrolase domain containing 3
gi 6978429	Acaa1a	3-ketoacyl-CoA thiolase A, peroxisomal
gi 392341831	Acad8	acyl-CoA dehydrogenase family, member 8
gi 392349899 [†]	Acad8	acyl-CoA dehydrogenase family, member 8
gi 11968090	Acads	short-chain specific acyl-CoA dehydrogenase, mitochondrial precursor
gi 8394162	Aco1	aconitase 1, soluble
gi 40538860	Aco2	aconitate hydratase, mitochondrial precursor
gi 48675862	Acot2	acyl-CoA thioesterase 2
gi 16758426	Acs14	acyl-CoA synthetase long-chain family member 4
gi 57164143	Actr2	actin-related protein 2
gi 70912366	Actr3	actin-related protein 3
gi 52851387	Acy1	aminoacylase-1A
gi 186972146	Adh5	alcohol dehydrogenase class-3
gi 72255513	Aga	aspartylglucosaminidase
gi 157819079	Ahcy11	putative adenosylhomocysteinase 2
gi 6978477	Ahsg	alpha-2-HS-glycoprotein precursor
gi 75832035	Aimp1	aminoacyl tRNA synthase complex-interacting multifunctional protein 1
gi 6978479	Ak3	Adenylate kinase
gi 13591894	Akr1a1	aldo-keto reductase family 1, member A1 (aldehyde reductase)
gi 61556894	Akr1b10	aldo-keto reductase family 1 member B10
gi 148540194	Akr1b7	aldose reductase-related protein 1
gi 27465603	Akr1b8	aldose reductase-related protein 2
gi 158138568	Alb	albumin
gi 197927423	Aldh4a1	aldehyde dehydrogenase 4 family, member A1
gi 6978497	Ambp	alpha-1-microglobulin/bikunin precursor
gi 157822539	Ank1	ankyrin-1
gi 6978505	Anxa5	annexin A5
gi 148539909	Anxa7	annexin A7
gi 205360945	Ap1s1	adaptor protein complex AP-1, sigma 1
gi 162138932	Ap2a2	adaptor protein-2 complex subunit alpha-2
gi 6978515	Apoa1	apolipoprotein A-I preproprotein
gi 161783809	Apob	Apolipoprotein B-100
gi 11968098	Arf1	ADP-ribosylation factor 1
gi 57527565	Arhgdib	Rho GDP dissociation inhibitor (GDI) beta
gi 157818451	Arl8a	ADP-ribosylation factor-like protein 8A
gi 290650356	Arpc51	actin-related protein 2/3 complex subunit 5-like protein

gi 114145540 reverse d	Arse	arylsulfatase E
gi 40254747	Asah1	N-acylsphingosine amidohydrolase 1
gi 48675845	Atic	5-aminoimidazole-4-carboxamide ribonucleotide formyltransferase/IMP cyclohydrolase
gi 16758008 reversed	Atp2b1	calcium-transporting ATPase 1, plasma membrane
gi 40538742	Atp5a1	ATP synthase subunit alpha, mitochondrial precursor
gi 39930503	Atp5c1	ATP synthase subunit gamma, mitochondrial
gi 8392939	Atp5g1	ATP synthase F(0) complex subunit C1, mitochondrial
gi 9506411	Atp5h	ATP synthase subunit d, mitochondrial
gi 51948420	Bcap31	B-cell receptor-associated protein 31
gi 25282455	Bpnt1	3-(2-),5--bisphosphate nucleotidase 1
gi 37693510	Bst2	bone marrow stromal antigen 2
gi 62079139	C11orf54	chromosome 11 open reading frame 54
gi 48675371	C1qbp	complement component 1 Q subcomponent- binding protein, mitochondrial precursor
gi 50657362	C4b	Complement component 4
gi 16924006	C9	Complement component C9
gi 8393038	Capn2	calpain-2 catalytic subunit precursor
gi 87239978	Caprin1	caprin-1
gi 57163991	Capza2	F-actin-capping protein subunit alpha-2
gi 6978607	Cat	catalase
gi 50657362	Cb4	complement component 4, gene 2
gi 32996723	Cbr4	carbonyl reductase family member 4
gi 293351800	Cbx1	chromobox protein homolog 1 isoform X3
gi 33414505	Cct4	chaperonin containing TCP1, subunit 4 (delta)
gi 157819651	Cct7	chaperonin containing TCP1, subunit 7 (eta)
gi 392351269	Cenpv	centromere protein V-like isoform X1
gi 57529187	Ces1c	carboxylesterase 1C
gi 281604082	Cf9	coagulation factor IX
gi 77861917	Cfh	complement inhibitory factor H
gi 50300479	Clint1	clathrin interactor 1
gi 61557351	Cops8	COP9 signalosome complex subunit 8
gi 401461788	Cp	ceruloplasmin isoform 2 precursor
gi 162287173	Cpt1a	carnitine O-palmitoyltransferase 1, liver isoform
gi 157787004	Creg1	Cellular repressor of E1A-stimulated genes 1
gi 28461157	Cryl1	Lambda-crystallin homolog
gi 8393206	Csrp1	cysteine and glycine-rich protein 1
gi 194473626	Cyc1	cytochrome c-1
gi 259906405	Cyp21a1	steroid 21-hydroxylase
gi 139949139	Cyp27a1	sterol 26-hydroxylase, mitochondrial
gi 56090393	Dcakd	dephospho-CoA kinase domain-containing protein
gi 157823027	Ddx3x	DEAD/H (Asp-Glu-Ala-Asp/His) box

gi 292781228	Decr1	polypeptide 2,4-dienoyl-CoA reductase, mitochondrial precursor
gi 56090381	Dhrs1	dehydrogenase/reductase SDR family member 1
gi 71043640	Dhtkd1	dehydrogenase E1 and transketolase domain containing 1
gi 78365255	Dlat	dihydrolipoyllysine-residue acetyltransferase
gi 61557163	Dnajc8	DnaJ homolog subfamily C member 8
gi 67846036	Dnpep	aspartyl aminopeptidase
gi 157818409	Dpm1	dolichol-phosphate mannosyltransferase
gi 6978773	Dpp4	dipeptidyl peptidase 4
gi 148747184	Ece1	endothelin converting enzyme 1
gi 157818179	Eef1b2	elongation factor 1-beta
gi 61556967	Eef1d	elongation factor 1-delta
gi 51948418	Eef1g	elongation factor 1-gamma
gi 8393296	Eef2	elongation factor 2
gi 62078909	Eepd1	endonuclease/exonuclease/phosphatase family
gi 194474054	Efr3a	protein EFR3 homolog A
gi 25282453	Eif2b1	translation initiation factor eIF-2B subunit alpha
gi 55741628	Eif2b5	translation initiation factor eIF-2B subunit epsilon
gi 72255511	Eif3B	Eukaryotic translation initiation factor 3 subunit B
gi 55741853	Eif4h	eukaryotic translation initiation factor 4H
gi 76096304	Eif5a	eukaryotic translation initiation factor 5A-1
gi 82654198	Eif6	eukaryotic translation initiation factor 6
gi 51948432	Emcn	endomucin
gi 392349592 :reverse d	Eppk1	epiplakin 1
gi 66793366	Eprs	glutamyl-prolyl-tRNA synthetase
gi 42491372	Ermp1	endoplasmic reticulum metallopeptidase 1
gi 75832132	Esyt1	extended synaptotagmin-1
gi 293348426	Esyt2	extended synaptotagmin-2
gi 56090371	Fam210a	protein FAM210A
gi 157822917	Farp1	FERM, RhoGEF and pleckstrin domain-containing protein 1
gi 8393355	Fdx1	ferredoxin-1
gi 13162347	Fdxr	ferredoxin reductase
gi 17865327	Fetub	fetuin-B
gi 158186678	Fgb	fibrinogen beta chain
gi 157786896	Fis1	mitochondrial fission 1 protein
gi 197313696	Fkbp2	FK506 Binding Protein 2, 13kDa
gi 399154173	Flot2	flotillin-2 isoform 2
gi 83320094	Fubp1	Far upstream element-binding protein 1
gi 58865844	Fus	translocated In Liposarcoma Protein
gi 8393381	G6pd	glucose-6-phosphate 1-dehydrogenase
gi 157822919	Ganab	neutral alpha-glucosidase AB

gi 402794806	Gars	glycyl-tRNA synthetase
gi 401709952	Gc	group specific component, isoform CRA_b
gi 25742748	Gclc	glutamate--cysteine ligase catalytic subunit
gi 71534276	Gdi1	rab GDP dissociation inhibitor alpha
gi 40254781	Gdi2	rab GDP dissociation inhibitor beta
gi 254281180	Get4	golgi to ER traffic protein 4 homolog (S. cerevisiae)
gi 16758432	Gfm1	elongation factor G, mitochondrial
gi 46485429	Glo1	glyoxalase I
gi 406035317	Gnb2l1	guanine nucleotide-binding protein subunit beta-2-like 1
gi 401461792	Got1	aspartate aminotransferase, cytoplasmic
gi 145275165	Gpx1	glutathione peroxidase 1
gi 90903229	Gpx4	glutathione peroxidase 4
gi 392342264	Gsta3	glutathione S-transferase alpha-3
gi 25453420	Gstp1	glutathione S-transferase P
gi 16757988	Gstt1	glutathione S-transferase theta-1
gi 6980992	Gstt2	glutathione S-transferase theta-2
gi 212549647	Gstt3	glutathione S-transferase, theta 3
gi 78214356	Gtf2i	general transcription factor II-I
gi 6981004	H1f0	histone H1.0
gi 157817664	H2afx	H2A histone family, member X
gi 8393519	H2afy	H2A histone family, member Y
gi 17105336	Hadh	hydroxyacyl-coenzyme A dehydrogenase
gi 148747393	Hadha	hydroxyacyl-CoA dehydrogenase/3-ketoacyl-CoA thiolase/enoyl-CoA hydratase (trifunctional protein), alpha subunit
gi 315630402	Hagh	hydroxyacylglutathione hydrolase
gi 213385315	Hcfc1	host cell factor 1
gi 61556993	Hibch	3-hydroxyisobutyryl-CoA hydrolase
gi 34853298	Hint3	histidine triad nucleotide-binding protein 3
gi 157821427	Hist1h1b	histone H1.5
gi 12025524	Hist1h2ba	histone H2B type 1-A
gi 392351997	Hmgb2	high mobility group protein B2
gi 8393547	Hnrnpa1	heterogeneous nuclear ribonucleoprotein A1
gi 62078769	Hnrnpb2	heterogeneous nuclear ribonucleoprotein H2
gi 157818423	Hnrnpb3	heterogeneous nuclear ribonucleoprotein H3
gi 158186698	Hnrnpm	heterogeneous nuclear ribonucleoprotein M isoform a
gi 157822207	Hoga1	4-hydroxy-2-oxoglutarate aldolase
gi 209869999	Hook3	protein Hook homolog 3
gi 392356055	Hprt1	hypoxanthine-guanine phosphoribosyltransferase
gi 8393573	Hsd11b2	hydroxysteroid (11-beta) dehydrogenase 2
gi 13994225	Hsd17b10	hydroxysteroid (17-beta) dehydrogenase 10
gi 162287198	Hsd17b4	hydroxysteroid (17-beta) dehydrogenase 4
gi 47087119	Hsd17b8	hydroxysteroid (17-beta) dehydrogenase 8
gi 59797058	Hsd3b1	hydroxy-delta-5-steroid dehydrogenase, 3 beta- and steroid delta-isomerase 1

gi 260064045	Hspa1a	heat shock 70 kDa protein 1A/1B
gi 11177910	Hspa2	heat shock-related 70 kDa protein 2
gi 25742763	Hspa5	heat shock 70kDa protein 5 (glucose-regulated protein, 78kDa)
gi 13242237	Hspa8	heat shock 70kDa protein 8
gi 410110929	Hspa9	heat shock 70kDa protein 9 (mortalin)
gi 206597443	Hspd1	heat shock 60kDa protein 1 (chaperonin)
gi 157819535	Htra2	HtrA serine peptidase 2
gi 189339236	Htt	huntingtin
gi 77404380	Hyou1	hypoxia up-regulated protein 1 precursor
gi 392332936	Iars2	PREDICTED: isoleucine--tRNA ligase
gi 392352912 [†]	Iars2	PREDICTED: isoleucine--tRNA ligase
gi 6981076	Ide	insulin-degrading enzyme
gi 77917546	Immt	mitochondrial inner membrane protein
gi 14091736	Impa1	inositol monophosphatase 1
gi 157823031	Ipo4	importin-4
gi 157821073	Ipo9	importin-9
gi 62079215	Isoc1	isochorismatase domain-containing protein 1
gi 189163481	Isyn1	inositol-3-phosphate synthase 1
gi 13591884	Itga1	integrin alpha-1
gi 55741637	Kars	lysyl-tRNA synthetase
gi 47155563	Kif13b	kinesin 13B
gi 83776543	Kif5b	kinesin-1 heavy chain
gi 8393610	Kpnb1	importin subunit beta-1
gi 6981144	Lamp1	lysosome-associated membrane glycoprotein 1
gi 40254785	Lamp2	lysosome-associated membrane glycoprotein 2 precursor
gi 57526927	Lars	leucyl-tRNA synthetase
gi 8393706	Ldha	L-lactate dehydrogenase A chain
gi 54400736	Letm1	LETM1 and EF-hand domain-containing protein 1
gi 9845261	Lgals1	galectin-1
gi 6981154	Lgals5	galectin-5
gi 169234844	Lman2	vesicular integral-membrane protein VIP36 precursor
gi 392332289	LOC100360601	carbonyl reductase [NADPH] 1-like
gi 392348563	LOC100362830	PREDICTED: 40S ribosomal protein S7-like
gi 392346819	LOC100363271	PREDICTED: 40S ribosomal protein S2-like
gi 392341003	LOC100363439	PREDICTED: 40S ribosomal protein S10-like
gi 293350511	LOC100364062	PREDICTED: pyruvate kinase isozymes M1/M2-like isoform 1
gi 392355306 [†]	LOC100364062	PREDICTED: pyruvate kinase isozymes M1/M2-like
gi 392343927	LOC100364427	40S ribosomal protein S12
gi 62078633	LOC100909415	sperm motility kinase W-like
gi 392343762	LOC100909466	PREDICTED: 40S ribosomal protein S9-like
gi 392346880	LOC100911034	NFS1 nitrogen fixation 1 homolog
gi 392346649	LOC100911313	regulator of microtubule dynamics protein 3-like

gi 392350599	LOC100911515	PREDICTED: triosephosphate isomerase-like
gi 392346176	LOC100911966	PREDICTED: 60S ribosomal protein L7a-like
gi 392348146	LOC100912024	PREDICTED: uncharacterized protein LOC100912024
gi 392353337	LOC100912032	PREDICTED: ubiquitin-40S ribosomal protein S27a-like
gi 198278428	LOC100912534	RCG36803, isoform CRA_a
gi 392352643	LOC101552443	ubiquitin-40S ribosomal protein S27a-like
gi 62821815	LOC297756	ribosomal protein S8-like
gi 392354344	LOC679994	PREDICTED: uncharacterized protein LOC679994
gi 109494630	LOC681544	similar to histidine-rich glycoprotein
gi 392349174	LOC685179	similar to SWI/SNF-related matrix-associated actin-dependent regulator of chromatin c2
gi 312434031	Lrrc58	leucine rich repeat containing 58
gi 56605670	Lrrc59	Leucine-rich repeat-containing protein 59
gi 157819827	Lsm3	LSM3 homolog, U6 small nuclear RNA associated (<i>S. cerevisiae</i>) (Predicted)
gi 71795621	Lta4h	leukotriene A-4 hydrolase
gi 13786178	Lypla2	lysophospholipase II
gi 21326475	Macrocl1	MACRO domain containing 1
gi 270288740	Maoa	monoamine oxidase A
gi 158749620	Map1b	microtubule-associated protein 1B
gi 402744019	Marcks	myristoylated alanine-rich C-kinase substrate
gi 57528264	Mccc1	methylcrotonoyl-CoA carboxylase subunit alpha, mitochondrial
gi 15100179	Mdh1	malate dehydrogenase
gi 221316701	Me2	NAD-dependent malic enzyme, mitochondrial
gi 157818123	Mgarp	mitochondria-localized glutamic acid-rich protein
gi 19705453	Mgst1	microsomal glutathione S-transferase 1
gi 20304123	Mpst	3-mercaptopyruvate sulfurtransferase
gi 71361655	Mrpl12	mitochondrial 39S ribosomal protein L12
gi 81295383	Mrpl47	mitochondrial ribosomal protein L47
gi 157820897	Mthfd2	methylenetetrahydrofolate dehydrogenase (NADP+ dependent) 2
gi 125630382	Mtus1	microtubule-associated tumor suppressor 1 homolog
gi 392342260	Mut	methylmalonyl CoA Mutase
gi 282158051	Myh11	myosin-11
gi 203097140	Myl12a	myosin regulatory light chain RLC-A
gi 287328046	Myo18a	myosin 18a
gi 124107592	Myo1c	unconventional myosin-Ic
gi 300798598	Myof	myoferlin
gi 77404363	Nap111	nucleosome assembly protein 1-like 1
gi 161760644	Ncl	nucleolin
gi 114145517	Ndufa8	NADH dehydrogenase .CHCH, CHCH domain
gi 198278533	Ndufa9	NADH dehydrogenase .NDUFA9_like_SDR_a, NADH dehydrogenase (ubiquinone) 1 alpha

gi 282154799	Nfu1	subcomplex, ...Epimerase, NAD dependent epimerase/dehydratase family histone cell cycle regulation defective interacting protein 5 (Predicted), isoform CRA_a
gi 19924089	Nme1	nucleoside diphosphate kinase A
gi 55926145	Nme2	nucleoside diphosphate kinase B
gi 12408334	Nolc1	nucleolar and coiled-body phosphoprotein 1
gi 311771778	Npc1	Niemann-Pick disease, type C1
gi 109463944	Npm3	nucleophosmin/nucleoplasmin 3
gi 13489067	Nsf	N-ethylmaleimide-sensitive factor
gi 8394272	Nudc	nuclear migration protein nudC
gi 157820537	Nup205	Nucleoporin 205kDa
gi 148747459	Opa1	dynammin-like 120 kDa protein, mitochondrial precursor
gi 61889110	Ostf1	osteoclast-stimulating factor 1
gi 157821731	Otub1	ubiquitin thioesterase OTUB1
gi 11693154	Pafah1b2	platelet-activating factor acetylhydrolase IB subunit beta
gi 16924002	Park7	parkinson protein 7
gi 158303308	Pcca	propionyl-CoA carboxylase alpha chain, mitochondrial
gi 148747119	Pccb	propionyl coenzyme A carboxylase, beta polypeptide
gi 56961640	Pcmt1	protein-L-isoaspartate(D-aspartate) O-methyltransferase
gi 11693142	Pcna	proliferating cell nuclear antigen
gi 157818653	Pdcd6	Programmed cell death 6 (Predicted), isoform CRA_a
gi 210032180	Pdcd6ip	programmed cell death 6-interacting protein
gi 8393322	Pdia3	protein disulfide-isomerase A3 precursor
gi 61557370	Pea15	astrocytic phosphoprotein PEA-15
gi 8393910	Pebp1	phosphatidylethanolamine-binding protein 1
gi 57528238	Pepd	peptidase D
gi 13929002	Pfkm	6-phosphofructokinase, muscle type
gi 57977273	Pfkp	6-phosphofructokinase type C
gi 42476144	Pfn1	profilin-1
gi 77627971	Pgm1	phosphoglucomutase-1
gi 11120720	Pgrmc1	membrane-associated progesterone receptor component 1
gi 56605824	Pgrmc2	membrane-associated progesterone receptor component 2
gi 13937353	Phb	prohibitin
gi 61556754	Phb2	prohibitin-2
gi 164663846	Phpt1	phosphohistidine phosphatase 1
gi 25742825	Pi4ka	phosphatidylinositol 4-kinase alpha
gi 16758324	Picalm	phosphatidylinositol-binding clathrin assembly protein
gi 8393962	Pitpna	phosphatidylinositol transfer protein alpha

		isoform
gi 157819139	Pitrm1	pitrilysin metallepetidase 1
gi 16758216	Plg	plasminogen
gi 46485405	Plp2	proteolipid protein 2
gi 157821883	Plxnb2	plexin-B2 precursor
gi 54234052	Pmpca	mitochondrial-processing peptidase subunit alpha
gi 11693166	Pmpcb	mitochondrial-processing peptidase subunit beta
gi 157822819	Pnp	purine nucleoside phosphorylase
gi 293351610	POLR2A	polymerase (RNA) II (DNA directed)
gi 213972586	Ppa1	polypeptide A, 220kDa
gi 8394009	Ppia	inorganic pyrophosphatase
gi 11968062	Ppp1cc	peptidyl-prolyl cis-trans isomerase A
		serine/threonine-protein phosphatase PP1-gamma catalytic subunit isoform 1
gi 55926139	Ppp2r1a	serine/threonine-protein phosphatase 2A 65 kDa regulatory subunit A alpha isoform
gi 16923958	Prdx1	peroxiredoxin-1
gi 8394432	Prdx2	peroxiredoxin-2
gi 11968132	Prdx3	peroxiredoxin-3
gi 16758404	Prdx5	peroxiredoxin-5
gi 117647220	Prkacb	cAMP-dependent protein kinase catalytic subunit beta
gi 157818781	Prkesh	protein kinase C substrate 80K-H
gi 298231229	Psap	prosaposin
gi 8394072	Psma5	proteasome subunit alpha type-5
gi 71043724	Psmb10	proteasome subunit beta type-10
gi 160333293	Psmb5	proteasome subunit beta type-5
gi 54019419	Psmb6	proteasome subunit beta type-6
gi 258614009	Psmb9	proteasome subunit beta type-9
gi 14010879	Psmd1	26S proteasome non-ATPase regulatory subunit 1
gi 157821581	Psmd13	26S proteasome non-ATPase regulatory subunit 13
gi 38454206	Psmd6	26S proteasome non-ATPase regulatory subunit 6
gi 392334544	Psme2	proteasome activator complex subunit 2
gi 402765974	Ptbp1	polypyrimidine tract binding protein 1
gi 62078455	Ptrh2	peptidyl-tRNA hydrolase 2
gi 51948490	Pyroxd2	pyridine nucleotide-disulfide oxidoreductase .
gi 307746876	Pzp	alpha-1-macroglobulin precursor
gi 56090285	Qars	glutaminyl-tRNA synthetase
gi 13592037	Rab3b	ras-related protein Rab-3B
gi 121583768	Rab5b	ras-related protein Rab-5B
gi 347800697	Rab5c	ras-related protein Rab-5C
gi 13027392	Rab7a	ras-related protein Rab-7a
gi 349501086	Rangap1	ran GTPase activating protein 1
gi 52138628	Rap1b	ras-related protein Rap-1b precursor

gi 157817007	Rbbp4	chromatin Assembly Factor 1 Subunit C
gi 158187535	Rbp4	retinol-binding protein 4
gi 51948422	RGD1303003	ES1 protein homolog, mitochondrial precursor
gi 166157530	RGD1304982	quinone oxidoreductase-like protein 2
gi 62079139	RGD1309534	ester hydrolase C11orf54 homolog
gi 157819755	RGD1309586	uncharacterized protein LOC364073
gi 114145796	RGD1310507	LRRGT00161
gi 392356141	RGD1564597	similar to 40S ribosomal protein S25
gi 11968136	Rhob	rho-related GTP-binding protein RhoB precursor
gi 81295355	Rmdn2	regulator of microtubule dynamics protein 2
gi 62078823	Rmdn3	regulator of microtubule dynamics protein 3
gi 157822227	Rpl12	60S ribosomal protein L12
gi 77404207	Rpl13a	60S ribosomal protein L13a
gi 109461025	Rpl17l1	ribosomal protein L17-like 1
gi 14389297	Rpl19	60S ribosomal protein L19
gi 56090279	Rpl23	60S ribosomal protein L23
gi 11968096	Rpl24	60S ribosomal protein L24
gi 157786616	Rpl26	60S ribosomal protein L26
gi 38454246	Rpl3	60S ribosomal protein L3
gi 13592051	Rpl5	60S ribosomal protein L5
gi 109492566	Rpl5l1	ribosomal protein L5-like 1
gi 56090277	Rplp1	60S acidic ribosomal protein P1
gi 392344748	Rplp2	60S acidic ribosomal protein P2-like
gi 392345425	Rps15a12	40S ribosomal protein S15a-like
gi 13928986	Rps8	40S ribosomal protein S8
gi 13929188	Rtn4	reticulon-4
gi 25742657	Sardh	Sarcosine dehydrogenase
gi 158749626	Scamp1	secretory carrier-associated membrane protein 1
gi 50356003	Scp2	non-specific lipid-transfer protein
gi 19173736	Scpep1	retinoid-inducible serine carboxypeptidase
gi 18426858	Sdha	succinate dehydrogenase complex, subunit A,
gi 157786714	Sec23a	Sec23 homolog A
gi 40538882	Sec61a1	protein transport protein Sec61 subunit alpha isoform 1
gi 51036655	Serpina1	Alpha-1-antiproteinase
gi 56090431	Serpinb9	serpin peptidase inhibitor, clade B (ovalbumin), member 9
gi 310772258	Sf3b2	splicing factor 3B subunit 2
gi 12621120	Sfxn3	sideroflexin-3
gi 56090475	Skp1	S-phase kinase-associated protein 1
gi 19173788	Slc25a10	mitochondrial dicarboxylate carrier
gi 11693170	Slc25a11	mitochondrial 2-oxoglutarate/malate carrier protein
gi 189011598	Slc25a24	calcium-binding mitochondrial carrier protein SCaMC-1
gi 61557225	Slc25a30	solute carrier family 25, member 30
gi 32189355	Slc25a4	solute carrier family 25 (mitochondrial carrier;

gi 32189350	Slc25a5	adenine nucleotide translocator), member 4 solute carrier family 25 (mitochondrial carrier; adenine nucleotide translocator), member 5
gi 82734227	Slc41a3	solute carrier family 41 member 3
gi 77404395	Snd1	staphylococcal nuclease domain-containing protein 1
gi 157818069	Snrpd1	small nuclear ribonucleoprotein Sm D1
gi 157820925	Snrpd2	small nuclear ribonucleoprotein D2
gi 13592087	Soat1	sterol O-acyltransferase 1
gi 16758606	Sorbs2	sorbin and SH3 domain-containing protein 2
gi 300797282	Spcs3	signal peptidase complex subunit 3
gi 397529553	Spg20	spastic paraplegia 20
gi 158711683	Spr	sepiapterin reductase
gi 31543764	Sptan1	spectrin alpha chain 1, non-erythrocytic
gi 61557085	Sptbn1	spectrin beta chain, brain 1
gi 20302113	Stip1	stress-induced-phosphoprotein 1
gi 72255527	Stoml2	stomatin-like protein 2, mitochondrial
gi 13928908	STX8	syntaxin-8
gi 157821845	Supt16h	suppressor of Ty 16 homolog (S. cerevisiae)
gi 392348016	Svep1	sushi, von Willebrand factor type A, EGF and pentraxin domain containing 1
gi 157823001	Syne3	spectrin repeat containing, nuclear envelope family member 3
gi 61557028	Tagln2	transgelin-2
gi 42476292	Taldo1	transaldolase
gi 58865526	Tardbp	TAR DNA binding protein
gi 55741823	Tars	threonine--tRNA ligase
gi 62078811	Tars2	threonine--tRNA ligase 2
gi 13592105	Tceb2	transcription elongation factor B polypeptide 2
gi 19924091	Tecr	trans-2,3-enoyl-CoA reductase
gi 86129590	Tes	testin
gi 6981652	Th	tyrosine 3-monooxygenase
gi 392339355	Timm23	translocase of inner mitochondrial membrane 23 homolog (Yeast)
gi 8394449	Timm44	translocase of inner mitochondrial membrane 44 homolog (yeast)
gi 157823439	Tjp1	tight junction protein 1 (Predicted)
gi 12018252	Tkt	transketolase
gi 291045133	Top2b	DNA topoisomerase 2
gi 29336093	Tpm3	tropomyosin alpha-3 chain
gi 52353308 [†]	Tpm3	tropomyosin alpha-3 chain isoform 1
gi 13786206	Tpp1	tripeptidyl-peptidase 1 precursor
gi 158508582	Tpr	translocated promoter region
gi 16758734	Tpt1	translationally-controlled tumor protein
gi 84781723	Trap1	TNF receptor-associated protein 1
gi 209870077	Trim28	transcription intermediary factor 1-beta
gi 209571551	Ttll12	tubulin--tyrosine ligase-like protein 12
gi 40018568	Tubb4b	tubulin beta-4B chain

gi 27465535	Tubb5	tubulin beta-5 chain
gi 18266686	Txnl1	thioredoxin-like protein 1
gi 78191795	Txnrd1	thioredoxin reductase 1, cytoplasmic
gi 112983840	U2af1	uncharacterized protein LOC687575
gi 197384571	Uba2	SUMO-activating enzyme subunit 2
gi 82617581	Ube2d2	ubiquitin-conjugating enzyme E2 D2
gi 84781733	Ubr4	E3 ubiquitin-protein ligase UBR4
gi 61098212	Uchl1	ubiquitin carboxyl-terminal hydrolase isozyme L1
gi 51172600	Ufc1	ubiquitin-fold modifier-conjugating enzyme 1
gi 83320084	Unc45a	protein unc-45 homolog A
gi 77627996	UPF0587	UPF0587 protein C1orf123 homolog
gi 57164091	Uqcrh	ubiquinol-cytochrome c reductase hinge protein
gi 9507177	Uso1	general vesicular transport factor p115
gi 6981696	Utrn	utrophin
gi 11177880	Vapb	vesicle-associated membrane protein-associated protein B
gi 76096306	Vat1	vesicle amine transport 1
gi 392334392	Vat1l	vesicle amine transport 1-like
gi 157822133	Vcl	vinculin
gi 17865351	Vcp	valosin containing protein
gi 13786202	Vdac2	voltage-dependent anion-selective channel protein 2
gi 13786204	Vdac3	voltage-dependent anion-selective channel protein 3
gi 13591864	Vgf	neuroendocrine specific protein VGF precursor
gi 219275534	Vps13a	vacuolar protein sorting 13 homolog A
gi 205360969	Vps35	vacuolar protein sorting 35 homolog (S. cerevisiae)
gi 162287178	Vtn	vitronectin
gi 392353662	Vwa8	von Willebrand factor A domain-containing protein 8 isoform X1
gi 18777778	Xpnpep1	xaa-Pro aminopeptidase 1
gi 162138924	Ykt6	synaptobrevin homolog YKT6
gi 420837274	YPN	YPN putative esterase
gi 392348365	Zbtb8os	zinc finger and BTB domain containing 8 opposite strand
gi 8392999	Zfp361l	zinc finger protein 36, C3H1 type-like 1

* All 5 time points compared to 0min (p <0.05; unpaired Student's t-test)

† Different gene identifiers entered into BLAST, produced same protein match

Table A3. Proteins assessed by ANOVA as being changed between multiple time points

Gene	Symbol	Name	P value <0.05
------	--------	------	---------------

identifier			
<u>Differentially expressed*</u>			
gi 6978429	Acaa1a	3-ketoacyl-CoA thiolase A, peroxisomal	0.003542154
gi 8394162	Aco1	aconitate hydratase-like protein	0.021064429
gi 16758426	Acs14	long-chain-fatty-acid--CoA ligase 4	0.008561539
gi 70912366	Actr3	actin-related protein 3	0.011755327
gi 6978477	Ahsg	alpha-2-HS-glycoprotein precursor	0.043647188
gi 6978479	Ak3	GTP:AMP phosphotransferase, mitochondrial	0.025627986
gi 148540194	Akr1b7	Akr1b7, Aldose reductase-related protein 1	0.008317725
gi 27465603	Akr1b8	aldose reductase-related protein 2	0.010721839
gi 6978497	Ambp	alpha-1-microglobulin	0.043079069
gi 6978505	Anxa5	annexin A5	0.005729715
gi 6978515	Apoa1	apolipoprotein A-I preproprotein	0.002253944
gi 9506411	Atp5h	ATP synthase subunit d, mitochondrial	0.001005599
gi 48675371	C1qbp	complement component 1 Q subcomponent-binding protein, mitochondrial precursor	0.017021971
gi 392351269	Cenpv	centromere protein V-like isoform X1	0.048929965
gi 57529187	Ces1c	Carboxylesterase 1C	0.009882295
gi 259906405	Cyp21a1	Steroid 21-hydroxylase	0.030316368
gi 78365255	Dlat	dihydrolipoamide S-acetyltransferase	0.024008357
gi 61556967	Eef1d	elongation factor 1-delta	0.024503613
gi 51948418	Eef1g	elongation factor 1-gamma	0.046624464
gi 76096304	Eif5a	eukaryotic translation initiation factor 5A-1	0.007336715
gi 66793366	Eprs	bifunctional aminoacyl-tRNA synthetase	0.029767472
gi 75832132	Esyt1	extended synaptotagmin-1	0.031843901
gi 13162347	Fdxr	ferredoxin reductase	3.00E-05
gi 17865327	Fetub	fetuin-B	0.006411223
gi 392356055	Hprt1	PREDICTED: hypoxanthine-guanine phosphoribosyltransferase	0.027429858
gi 59797058	Hsd3b1	3 beta-hydroxysteroid dehydrogenase/Delta 5-->4-isomerase type 1	0.036957813
gi 25742763	Hspa5	heat shock 70kDa protein 5 (glucose-regulated protein, 78kDa)	0.002138432
gi 13242237	Hspa8	heat shock cognate 71 kDa protein	0.011716291
gi 206597443	Hspd1	60 kDa heat shock protein, mitochondrial	0.006281017
gi 77917546	Immt	mitochondrial inner membrane protein	0.041502233
gi 9845261	Lgals1	lectin, galactoside-binding, soluble, 1	0.016668527
gi 392348563	LOC100362830	PREDICTED: 40S ribosomal protein S7-like	0.003824874
gi 392346176	LOC100911966	PREDICTED: 60S ribosomal protein L7a-like	0.024369568
gi 392353337	LOC10091203	PREDICTED: ubiquitin-40S ribosomal	0.036121261

	2	protein S27a-like	
gi 71795621	Lta4h	leukotriene A-4 hydrolase	0.037693668
gi 57528264	Mccc1	methylcrotonoyl-CoA carboxylase subunit alpha, mitochondrial	0.041973952
gi 15100179	Mdh1	malate dehydrogenase, cytoplasmic	0.025817901
gi 157818123	Mgarp	mitochondria-localized glutamic acid-rich protein	0.030284734
gi 157820897	Mthfd2	methylenetetrahydrofolate dehydrogenase (NADP+ dependent) 2	0.020841939
gi 124107592	Myo1c	unconventional myosin-Ic	0.013222864
gi 161760644	Ncl	nucleolin	0.034241567
gi 19924089	Nme1	nucleoside diphosphate kinase A	0.000798643
gi 55926145	Nme2	nucleoside diphosphate kinase B	0.008385161
gi 13489067	Nsf	N-ethylmaleimide-sensitive factor	0.00207537
gi 11693154	Pafah1b2	platelet-activating factor acetylhydrolase IB subunit beta	0.019321398
gi 8393322	Pdia3	protein disulfide-isomerase A3 precursor	0.019347638
gi 8393910	Pebp1	phosphatidylethanolamine-binding protein 1	0.002457997
gi 11120720	Pgrmc1	membrane-associated progesterone receptor component 1	0.000193577
gi 61556754	Phb2	prohibitin-2	0.04976963
gi 157822819	Pnp	purine nucleoside phosphorylase	0.040534471
gi 55926139	Ppp2r1a	serine/threonine-protein phosphatase 2A 65 kDa regulatory subunit A alpha isoform	0.023062699
gi 16758404	Prdx5	peroxiredoxin-5, mitochondrial precursor	0.012187504
gi 157821581	Psmc13	26S proteasome non-ATPase regulatory subunit 13	0.036132183
gi 402765974	Ptbp1	Polypyrimidine tract binding protein 1, isoform CRA_a	0.005895011
gi 13592037	Rab3b	ras-related protein Rab-3B	0.021053256
gi 51948422	RGD1303003	ES1 protein homolog, mitochondrial precursor	0.007558092
gi 166157530	RGD1304982	quinone oxidoreductase-like protein 2	0.024365536
gi 81295355	Rmdn2	Regulator of microtubule dynamics protein 2	0.015530866
gi 14389297	Rpl19	60S ribosomal protein L19	0.009169421
gi 56090277	Rplp1	60S acidic ribosomal protein P1	0.005297645
gi 392344748	Rplp2	PREDICTED: 60S acidic ribosomal protein P2-like	0.004020254
gi 40538882	Sec61a1	protein transport protein Sec61 subunit alpha isoform 1	0.048557252
gi 11693170	Slc25a11	mitochondrial 2-oxoglutarate/malate carrier protein	0.004388521
gi 189011598	Slc25a24	calcium-binding mitochondrial carrier protein SCaMC-1	0.012350385

gi 61557085	Sptbn1	spectrin beta chain, brain 1	0.026336675
gi 42476292	Taldo1	transaldolase	0.010476413
gi 19924091	Tecr	very-long-chain enoyl-CoA reductase	0.027523842
gi 6981652	Th	Tyrosine 3-monooxygenase	0.031105255
gi 392339355	Timm23	translocase of inner mitochondrial membrane 23 homolog (Yeast)	0.003657176
gi 291045133	Top2b	DNA topoisomerase 2	0.024775698
gi 29336093	Tpm3	Tropomyosin alpha-3 chain	0.007847862
gi 158508582	Tpr	translocated promoter region	0.03507787
gi 112983840	U2af1	uncharacterized protein LOC687575	0.004020254
gi 9507177	Uso1	general vesicular transport factor p115	0.023177669
gi 76096306	Vat1	vesicle amine transport 1	0.045826316
gi 13786204	Vdac3	voltage-dependent anion-selective channel protein 3	0.009897678
gi 205360969	Vps35	vacuolar protein sorting-associated protein 35	0.015268099

Differentially expressed over time⁺

gi 75905479	Aldh9a1	4-trimethylaminobutyraldehyde dehydrogenase	0.013015
gi 61556832	Aprt	adenine phosphoribosyltransferase	0.043292
gi 19705465	Atp5f1	ATP synthase subunit b, mitochondrial precursor	0.009073
gi 11693172	Calr	calreticulin precursor	0.048331
gi 6978639	Cd81	CD81 antigen	0.018713
gi 9506497	Cltc	clathrin heavy chain 1	0.037211
gi 18158449	Copb1	coatamer subunit beta	0.035649
gi 8393180	Cox4i1	cytochrome c oxidase subunit 4 isoform 1, mitochondrial precursor	0.040437
gi 158749632	Dbt	Dihydrolipoamide Branched Chain Transacylase E2	0.011435
gi 13591940	Dpyd	Dihydropyrimidine Dehydrogenase	0.021143
gi 109491989	Eftud2	elongation factor Tu GTP binding domain containing 2	0.04992
gi 62945328	Gbas	glioblastoma amplified sequence	0.015737
gi 126723054	Gcsh	glycine cleavage system H protein, mitochondrial precursor	0.015689
gi 57527919	Gpd1	glycerol-3-phosphate dehydrogenase	0.048106
gi 300798457	Gpd11	glycerol-3-phosphate dehydrogenase 1-like protein	0.01859
gi 6981010	Hba1	hemoglobin subunit alpha-1/2	0.018136
gi 13928690	Idh1	isocitrate dehydrogenase	0.003826
gi 392343883	LOC684270	PREDICTED: isochorismatase domain-containing protein 2A, mitochondrial-like isoform 2	0.01575
gi 392337504	LOC687295	PREDICTED: mitochondrial import inner membrane translocase subunit TIM50-like isoform 2	0.048428
gi 13928780	Por	NADPH-cytochrome P450 reductase	0.024281

gi 8394069	Psma4	proteasome subunit alpha type-4	0.020433
gi 13929006	Rab2a	ras-related protein Rab-2A	0.042849
gi 6981486	Rpn1	ribophorin I	0.017499
gi 8394212	Rps15	ribosomal protein S15	0.046279
gi 13928754	Star	steroidogenic acute regulatory protein	0.011566
sp TRYP_PIG	Trypsin	EC 3.4.21.4; Flags: Precursor;	0.002015
gi 118142811	Vapa	vesicle-associated membrane protein-associated protein A	0.005943
gi 92373398	Ybx1	Y box binding protein 1	0.028874

*differentially expressed when compared to 0min

⁺only considered differentially expressed when compared to a time point other than 0min.

ANIMAL RESEARCH AUTHORITY (ARA)

AEC Reference No.: 2014/018

Date of Expiry: 30 March 2015

Full Approval Duration: 31 March 2014 to 31 March 2017 (36 Months)

This ARA remains in force until the Date of Expiry (unless suspended, cancelled or surrendered) **and will only be renewed upon receipt of a satisfactory Progress Report before expiry (see Approval email for submission details).**

Principal Investigator:

A/Prof Ann Goodchild
School of Advanced Medicine (ASAM)
Macquarie University, NSW 2109
0410 610 302
Ann.Goodchild@mq.edu.au

Associate Investigators:

Sarah Hassan 0410 357 056
Phillip Wisinski-Bokiniec 0448 297 545

Student:

Roshana Vander Wall 0401 500 680

In case of emergency, please contact:
the Principal Investigator / Associate Investigator
named above or Animal Welfare Officer - 9850 7758
/ 0439 497 383

The above-named are authorised by MACQUARIE UNIVERSITY ANIMAL ETHICS COMMITTEE to conduct the following research:

Title of the project: Time dependent protein changes in brain regions and the adrenal medulla after exposure to acute hypoglycaemia.

Purpose: 4 - Research: Human or Animal Biology

Aims: To understand how these brain regions and the adrenal gland are altered by hypoglycemia by identifying what proteins change in them and the timecourse of these changes.

Surgical Procedures category: 6 - Minor Physiological Challenge

All procedures must be performed as per the AEC-approved protocol, unless stated otherwise by the AEC and/or AWO.

Maximum numbers approved (for the Full Approval Duration):

Species	Strain	Age/Sex/Weight	Total	Supplier/Source
02-Rats	Sprague-Dawley	Any	72	ARC Perth
		TOTAL	72	

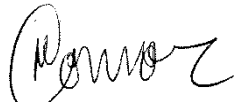
Location of research:

Location	Full street address
Central Animal Facility	Building F9A, Research Park Drive, Macquarie University, NSW 2109
ASAM	Level 1, F10A, 2 Technology Place, Macquarie University, NSW 2109

Amendments approved by the AEC since initial approval: N/A

Conditions of Approval: N/A

Being animal research carried out in accordance with the Code of Practice for a recognised research purpose and in connection with animals (other than exempt animals) that have been obtained from the holder of an animal suppliers licence.



Professor Mark Connor (**Chair, Animal Ethics Committee**)

Approval Date: 20 March 2014